Fatemeh Ahmadi

STUDY OF PROCESS-INDUCED STRESSES AND DEFORMATIONS IN THERMOPLASTIC MATRIX COMPOSITES

Master Dissertation
European Master Advanced Structural Analysis and Design using Composite Materials

Work developed under the supervision of
Professor Philippe Olivier

Funded by the European Union

July 2023

DECLARATION

Name: Fatemeh Ahmadi

Email: fatemeh.ahmadi2120@gmail.com **Phone number:** +33649096045

Citizen Card Number: XXXXXXXXXXXXXXXXXXXX

Title of the Thesis: STUDY OF PROCESS-INDUCED STRESSES AND DEFORMATIONS IN THERMOPLASTIC MATRIX COMPOSITES

Supervisors:

Professor Philippe Olivier

Year of Conclusion: 2023

Master Course in Advanced Structural Analysis and Design using Composite Materials

University of Toulouse III Paul Sabatier, XX/XX/XXXX

Signature:

ACKNOWLEDGEMENTS

I am deeply grateful to the individuals who have played a significant role in the completion of my master's thesis. Their unwavering support, guidance, and encouragement have been invaluable throughout this journey.

First and foremost, I would like to express my heartfelt thanks to my beloved parents, whose unconditional love, sacrifices, and unwavering belief in my abilities have been the driving force behind my accomplishments. Their constant encouragement and unwavering support have been my pillars of strength.

I would also like to extend my sincere appreciation to my supervisor, Professor Philippe Olivier, for his exceptional guidance, expertise, and patience. His insightful suggestions, constructive feedback, and continuous support have significantly shaped the quality and direction of my research. I am grateful for the opportunity to learn from his vast knowledge and experience.

Additionally, I would like to acknowledge the Erasmus Mundus Scholar award, which has provided me with an incredible opportunity to pursue my studies and engage in international academic experiences. I am deeply thankful for their generous support, which has been instrumental in my academic journey.

Finally, I want to express my gratitude to all those who have provided their valuable insights and assistance, including my colleagues, friends, and the participants of my research study. Their contributions have enriched my work in profound ways.

Fatemeh Ahmadi

ÉTUDE DES CONTRAINTES ET DÉFORMATIONS INDUITES PAR LE PROCESSUS DANS LES COMPOSITES À MATRICE THERMOPLASTIQUE.

RESUME

Ce mémoire de maîtrise porte sur l'étude des contraintes et des déformations induites par le processus dans les composites à matrice thermoplastique. Il étudie les différents facteurs influents qui contribuent à la formation de contraintes résiduelles, notamment la disparité du coefficient de dilatation thermique et le retrait de la résine au cours du traitement, qui peuvent introduire des fissures matricielles transversales et une défaillance prématurée dans les pièces composites. Il est essentiel de comprendre l'état des contraintes résiduelles pour garantir la performance et la fiabilité des composites. Ce projet passe en revue diverses techniques expérimentales utilisées pour évaluer les contraintes résiduelles thermiques à différents niveaux, y compris les contraintes micromécaniques, interlaminaires et stratifiées. Ces techniques englobent l'utilisation des propriétés intrinsèques des matériaux, des capteurs de déformation extrinsèques intégrés, des déformations dans le plan et hors du plan, des essais destructifs et de la modélisation numérique (F.E.A). Les défauts induits par les contraintes résiduelles et leurs effets sur les propriétés mécaniques des laminés composites sont également expliqués. En outre, des mécanismes proposés pour réduire les contraintes résiduelles dans les composites thermoplastiques sont présentés, dans le but d'améliorer la conception des composites et les processus de fabrication.

MOTS-CLES: Revue de littérature ; Composites à matrice thermoplastique ; Contraintes induites par le procédé ; Contraintes résiduelles ; Fabrication

STUDY OF PROCESS-INDUCED STRESSES AND DEFORMATIONS IN THERMOPLASTIC MATRIX COMPOSITES

ABSTRACT

This master thesis investigates the study of process-induced stresses and deformations in thermoplastic matrix composites. It delves into different influential factors that contribute to the formation of residual stresses, including mismatch in the coefficient of thermal expansion and resin shrinkage during processing, which can introduce transverse matrix cracks and premature failure in composite parts. Understanding the state of residual stress is crucial for ensuring composite performance and reliability. In this project, various experimental techniques are reviewed which are employed to assess thermal residual stresses at different levels, including micromechanical, interlaminar, and laminate stresses. These techniques encompass the utilization of intrinsic material properties, extrinsic embedded strain sensors, in-plane and out-of-plane deformations, destructive testing, and Numerical modelling (F.E.A). Residual stress-induced defects and their effects on the mechanical properties of composite laminates are also explained. Additionally, proposed mechanisms for reducing residual stresses in thermoplastic composites are presented, aiming to enhance composite design and manufacturing processes.

KEYWORDS: Literature Review; Thermoplastic Matrix Composites; Process-Induced Stresses; Residual Stresses; Manufacturing.

TABLE OF CONTENTS

CONTENTS

Acknowledgements III
Résumé IV
Abstract V
Table of Contents VI
List of Figures IX
List of Tables XII
List of Abbreviations and Symbols XIII
Chapter 1: Formation of Residual Stresses 1
1. 1. Introduction 1
1.2. The manufacturing process of thermoplastic composite structures 2
1.2.1. Autoclave or press; Flat plate _ Uniform Pressure and Temperature 2
1.2.2. Tape Laying; Flat Plate _ Nonuniform Pressure and Temperature 4
1.2.3. Filament Winding; Nonuniform Pressure and Temperature 6
1.2.4. The main advantages of the filament winding and tape placement over the autoclave and press molding 8
1.2.5. Tape Placement 8
1.3. Residual stress formation on three mechanical levels 11
1.4. Micromechanical residual stresses 15
1.4.1. Reinforcing fibers dominated properties 15
1.4.1.1. Fiber volume fraction 15
1.4.2. Thermoplastic matrix dominated properties 17
1.4.2.1. Shrinkage 17
1.4.2.2. Coefficients of thermal expansion 18
1.4.2.3. Temperature difference 19
1.4.2.4. Processing conditions 21
1.4.2.4.1. Cooling rate effects in amorphous matrix composites 21
1.4.2.4.2. Cooling rate effects in semi-crystalline polymer matrixes 23
1.4.2.4.2.1. Crystallization Kinetics 27

1.4.2.5. Elastic properties 27
1.4.3. Fiber–matrix interface 28
1.4.4. Composite general properties 30
1.4.4.1. Temperature gradient 30
1.4.4.2. Laminate thickness 32
1.5. Macro-mechanical residual stress formation 33
1.5.1. Lay-up of the laminate part 33
1.6. ‘‘Global’’ (skin-core) residual stresses 33
1.6.1. Annealing 34
1.6.2. Influence of processing mold material 36
1.7. parameters governing residual stresses 39
Chapter 2: Experimental Techniques for Measuring Residual Stress 41
2.1. Introduction 41
2.2 Techniques utilising intrinsic material properties of the composites’ constituents 41
2.2.1. Photo-elasticity 42
2.2.2. Micro-Raman spectroscopy 43
2.2.3. Electrical conductivity of carbon fiber reinforcement 44
2.3. Residual strain determination by means of extrinsic (foreign) embedded strain sensors 45
2.3.1. Embedded strain gauges 45
2.3.2. Embedded fiber optic sensors 46
2.3.3. Embedded metallic particles 49
2.4. Experimental techniques based on in-plane and out-of-plane deformations 50
2.4.1. Interferometry based methods 50
2.4.2. Warpage of non-symmetric laminates 51
2.4.3. Digital image correlation technique 56
2.5. Residual stress determination by means of destructive testing 57
2.5.1. Overview of destructive testing 57
2.5.2. First ply failure 58
2.5.3. Destructive/relaxation-based techniques 59
2.5.3.1. Layer removal of symmetrical laminates 59
2.5.3.1.1. CL-deformation technique 61

2.5.3.1.2. PSL-strain gage technique 63
2.5.3.2. Other stress relaxation-based techniques 64
2.6. Numerical modelling (F.E.A) of process-induced stresses 65
2.7. Review of techniques for estimating the magnitude of residual thermal stresses 66
2.8. Experimental determination of model parameters 67
2.9. Relaxation experiments 68
Chapter 3: Effects of Thermal Residual Stresses 70
3.1. Introduction 71
3.2. Residual stress effects and the matrix-dominated properties 71
3.3 Effects occurring at the fiber–matrix interface 73
3.4. Residual stress-induced defects 73
3.4.1 Fiber waviness 73
3.4.2 Transverse cracking 76
3.4.3 Delamination 79
3.4.4 Warpage of laminates 80
3.5. Residual stress effects on the mechanical properties of laminates 82
3.5.1. Tensile Loading 82
3.5.2. Flexural and Impact Resistance 84
3.5.3. Compression and shear 84
3.5.4. Modes I and II fracture toughness 85
3.5.5. Long-term mechanical properties: fatigue and creep 86
3.6. Residual stress effects in composite structures 90
3.6.1. Effect of residual stresses on composite structures according to their sources 91
3.6.2. Filament-wound cylinders 92
3.7. Proposed mechanisms for relief of residual stresses 92
General Conclusion 94
References: 95

LIST OF FIGURES

1.1 Illustration of the press ..... **Error! Bookmark not defined.**

1.2 Thermal boundary conditions for the press ..... **Error! Bookmark not defined.**

1.3 An autoclave machine, and its internal components and process schematic. .....**Error! Bookmark not defined.**

1.4 Illustration of the tape laying apparatus . ..... **Error! Bookmark not defined.**

1.5 Thermal boundary conditions for the tape laying process. **Error! Bookmark not defined.**

1.6 An AFP machine laying into a female mold ,and Automated fiber placement head. .**Error! Bookmark not defined.**

1.7 Local application of heat and pressure during the filament winding process . .....**Error! Bookmark not defined.**

1.8 Application of heat and pressure in the filament winding process.**Error! Bookmark not defined.**

1.9 Thermal boundary conditions for the filament winding process.**Error! Bookmark not defined.**

1.10 Laser-assisted thermoplastic tape winding of a pressure vessel.**Error! Bookmark not defined.**

1.11 The thermoplastic composite tape placement process ..... **Error! Bookmark not defined.**

1.12 The effect of preheat temperature on the maximum tensile stress.**Error! Bookmark not defined.**

1.13 The effect of roller velocity on the maximum tensile stress.**Error! Bookmark not defined.**

1.14 The effect of heated length on the maximum tensile stresses**Error! Bookmark not defined.**

1.15 Residual stress (σxx) distribution through the thickness of a sample laminate.. .....**Error! Bookmark not defined.**

1.16 Three different Internal stress levels in advanced composite materials are illustrated ..... **Error! Bookmark not defined.**

1.17 Schematic view of the effect of cooling on the matrix around a fiber.**Error! Bookmark not defined.**

1.18 Schematic view of residual stress formation..... **Error! Bookmark not defined.**

1.19 Laminate skin-core residual stress distribution. ..... **Error! Bookmark not defined.**

1.20 The origin of 'global' stresses in tape laying ..... **Error! Bookmark not defined.**

1.21 Composite configurations for testing contact resistivity as a function of temperature.. ..... **Error! Bookmark not defined.**
1.22 Specific volume of polysulfone and polyethyleneterephthalate**Error! Bookmark not defined.**
1.23 Correlation of experimental transverse residual stress for a unidirectional laminate. ..... **Error! Bookmark not defined.**
1.24 Comparison of model with experiment at different cooling rates..**Error! Bookmark not defined.**
1.25 Stress-free temperature vs constant cooling rate..... **Error! Bookmark not defined.**
1.26 Effect of cooling rate on free volume and glass transition temperature**Error! Bookmark not defined.**
1.27 Cooling cycles used in the experimental work of the reference.**Error! Bookmark not defined.**
1.28 Transverse crack densities after thermal cycling . ..... **Error! Bookmark not defined.**
1.29 Effect of cooling rate on crystallization onset temperature .**Error! Bookmark not defined.**
1.30 The transverse normal stress (σy) distribution in the y-z plane for a sample laminate ..... **Error! Bookmark not defined.**
1.31 The transverse normal stress (σy) distribution in the y-z plane for a sample laminate. ..... **Error! Bookmark not defined.**
1.32 The degree of crystallinity (XC) distribution in the y-z plane for a sample laminate. ..... **Error! Bookmark not defined.**
1.33 The degree of crystallinity (XC) distribution in the y-z plane for a sample laminate. ..... **Error! Bookmark not defined.**
1.34 Predicted influence of cooling rate on the transverse residual stress..**Error! Bookmark not defined.**
1.35 Model prediction of the matrix moduli at the laminate surface **Error! Bookmark not defined.**
1.36 Microstructure of polypropylene sample around a carbon fibre**Error! Bookmark not defined.**
1.37 Developments of parabolic residual stress distribution due to thermal skin-core effect...**Error! Bookmark not defined.**
1.38 Model prediction of the transient temperature profile for a sample laminate.....**Error! Bookmark not defined.**

1.39 The degree of crystallinity through the thickness of a laminate.**Error! Bookmark not defined.**
1.40 Predicted influence of thickness on the transverse residual stress of sample laminates ..... **Error! Bookmark not defined.**
1.41 Effect of dwell time and dwell temperature on curvature reduction.**Error! Bookmark not defined.**
1.42 The basic steps of a thermostamping process . ..... **Error! Bookmark not defined.**
1.43 Typical cooling profile of an unbalanced laminate during thermostamping. .....**Error! Bookmark not defined.**
1.44 Strain measurements of a unidirectional laminate by cure cycle**Error! Bookmark not defined.**
2.45 Schematic representation of the automated micropolariscope.**Error! Bookmark not defined.**
2.46 The photoelastic image of residual stresses present in the epoxy matrix.....**Error! Bookmark not defined.**
2.47 Thermal stress distribution in fibre ..... **Error! Bookmark not defined.**
2.48 Sketch of the experimental setup to measure the residual strains in an autoclave....**Error! Bookmark not defined.**
2.49 Schematic view of EFPI sensor..... **Error! Bookmark not defined.**
2.50 FBG response as a function of strain ..... **Error! Bookmark not defined.**
2.51 Wavelength response of a uniform FBG..... **Error! Bookmark not defined.**
2.52 Influence of unequal transverse strains on the spectral response of an FBG. .....**Error! Bookmark not defined.**
2.53 Transverse strain histories measured by middle-tail FBG sensor.**Error! Bookmark not defined.**
2.54 Curvature measurement experimental setup. ..... **Error! Bookmark not defined.**
2.55 Evolution of the curvature with temperature for sample unsymmetrical laminates.**Error! Bookmark not defined.**
2.56 Unsymmetrical cross-ply laminate; and saddle-shaped of unsymmetrical laminate . ..... **Error! Bookmark not defined.**
2.57 Measurement of radius of curvature..... **Error! Bookmark not defined.**
2.58 Curvature measurement ..... **Error! Bookmark not defined.**
2.59 A transverse crack in the outer ply of a balanced laminate**Error! Bookmark not defined.**

2.60 Schematic of the laminate abrading technique..... 60
2.61 Schematic of the process simulated laminate (PSL) with constitutive laminates (CL) ..... **Error! Bookmark not defined.**
2.62 Schematic of a process simulated laminate (PSL) configuration**Error! Bookmark not defined.**
2.63 Schematic showing the principal stress release of a constItutive laminate.....**Error! Bookmark not defined.**
2.64 Schematic of the setup for the PSL-strain gage measuring technique**Error! Bookmark not defined.**
2.65 Flow-chart for calculating thermal residual stress . ..... **Error! Bookmark not defined.**
3.66 Micrograph of a composite laminate showing fiber waviness .**Error! Bookmark not defined.**
3.67 Failure mechanisms in a unidirectional composite with graded waviness under axial compression..... **Error! Bookmark not defined.**
3.68 Failure progression in a unidirectional composites with graded waviness under axial compression ..... **Error! Bookmark not defined.**
3.69 Crack initiation along fiber–matrix interfaces . ..... **Error! Bookmark not defined.**
3.70 Transverse cracks in surface plies of a carbon fiber polyetherimide laminate . .....**Error! Bookmark not defined.**
3.71 Predicted failure strain (mixed-mode linear interaction) and experimental data .....**Error! Bookmark not defined.**
3.72 Photograph showing the warpage due to tool-part interaction**Error! Bookmark not defined.**
3.73 Typical defects of thermoplastic ATP laminates ..... **Error! Bookmark not defined.**
3.74 Measured mechanical properties on ±45 tensile coupons of sample composites .....**Error! Bookmark not defined.**
3.75 The deformation after creep loading. ..... **Error! Bookmark not defined.**
3.76 The deformation after creep loading. ..... **Error! Bookmark not defined.**
3.77 The deformation after creep loading ..... **Error! Bookmark not defined.**
3.78 Deformation after creep loading. ..... **Error! Bookmark not defined.**
3.79. Deformation after creep loading. ..... **Error! Bookmark not defined.**
3.80. Schematic of spring-in deformation and problems induced during assembly .....**Error! Bookmark not defined.**

3.81. Schematic of the relationship between various aspects of the residual stresses .....**Error! Bookmark not defined.**

LIST OF TABLES

1.1 Comparison between autoclave and compression molding for thermoplastic composites ..... **Error! Bookmark not defined.**
1.2 Activation energy for various composites..... **Error! Bookmark not defined.**

LIST OF ABBREVIATIONS AND SYMBOLS

Abbreviations

TPCs	Thermoplastic Composites
CTE	Coefficients of Thermal Expansion
SFT	Stress Free Temperature
CR	Cooling Rate
ATL	Automated Tape Laying
AFP	Automated Fiber Placement
PSLs	Process Simulated Laminates
FOS	Fiber optic sensors
FBG	Fiber Bragg Grating sensors
EFPI	Extrinsic Fabry-Perot Interferometric sensors
FEA	Finite Element Analysis
FEM	Finite Element Modelling
CLT	Classical Lamination Theory
CL	Constituent Laminate
DSC	Differential Scanning Calorimeter
WAXS	Wide Angle X-ray Spectroscopy
DMTA	Dynamic Mechanical Thermal Analyzer
UD	Unidirectional Laminates
CR	Cooling Rate
DCB	Double Cantilever Beam
UMAT	User Material Subroutine in ABAQUS
GF	Glass Fibers
CF	Carbon Fibers
PEEK	Polyetheretherketone - Thermoplastic Matrix
AS-4	A Specific Type of Carbon Fiber
APC-2	Composite Composed of PEEK Matrix and AS-4 Carbon Fiber
PP	Polypropylene - Thermoplastic Matrix
PEI	Polyetherimide - Thermoplastic Matrix
TPI	Polyimide - Thermoplastic Matrix
PES	Polyethersulfone - Thermoplastic Matrix

PSU	polysulfone - Thermoplastic Matrix
AS4/3501-6	Composite Made of AS-4 Carbon Fiber and 3501-6 Epoxy Resin
Polyamide 66 (PA66)	A Type of Thermoplastic Polymer
IM6G/3501-6	Composite Composed of IM6G Carbon Fiber and 3501-6 Epoxy Resin
T800H/3900-2	Composite Composed of T800H Carbon Fiber and 3900-2 Epoxy Resin
PA12	Polyamide 12 (PA12) Thermoplastic Polymer
PP/G	Composite Material Consists of Polypropylene (PP) Matrix and Glass Fiber (G)
T300	A Specific Type of Carbon Fiber
IM7	A Specific Type of Carbon Fiber

Symbols

n	Number of Laminate Layers (Plies)
H	Thickness of a Composite
L	Length of a Composite
W	Width of a Composite
T_{st}	Temperatures on the Composite Top Surfaces
T_{sb}	Temperatures on the Composite Bottom Surfaces
T_t	Temperatures on the Top Outer Surface of the Platens
T_b	Temperatures on the Bottom Outer Surface of the Platens
q_t	Heat Fluxes to the top Platen Surfaces
q_b	Heat Fluxes to the Bottom Platen Surfaces
P	Known Pressure to the Composite Plate
V	Tape Layer Device Head Moves at a Constant Speed of V
T_{se}	Temperature at the Edges of the Composite
q_{se}	Heat Flux at the Edges of the Composite
ω	Angular Speed of the Mandrel
φ_0	Layer Winding Angle
T_{so}	Composite Surface Temperature
q_{so}	Composite Surface Heat Flux
T_{sj}	Temperature of the Mandrel's Inner Surface
q_{sj}	Heat Flux of the Mandrel's Inner Surface
σ_{xx}	Residual Stress Distribution
a_f	Fiber's Coefficients of Thermal Expansion
a_m	Matrix's Coefficients of Thermal Expansion
T_g	Glass Transition Temperature
T_m	Melting Temperature
T_C	Crystallization Peak Temperature
T_{sf}	Stress Free Temperature
ε_x	Strain of Fibers
ε_y	Transverse Strains
Ts	Solidification Temperature
λ	X-ray Wavelength

d_{hkl}	Lattice Space
θ_{hkl}	Bragg angle
$T_{mandrel}$	Temperature of the Mandrel
E_{11}	Moduli of the Ply in the Longitudinal Direction
E_{22}	Moduli of the Ply in the Transverse Direction
b	Thicknesses of the Longitudinal Plies
d	Thicknesses of the Transverse Plies
h	Ply Thicknesses in the Symmetrical Lay up
k	Ply Thicknesses in the Symmetrical Lay up
ΔT	Temperature Difference Between the SFT and the Service Temperature
α_{11}	Coefficients of Thermal Expansion in the Longitudinal Directions of the Fiber
α_{22}	Coefficients of Thermal Expansion in the Transverse Directions of the Fiber
κ	Curvature
h	Deflection
L	Length of the Sample Measured (Distance Between Support Pins)
ε_x^o	Strains of the Laminate's Mid-Plane in X Direction
ε_y^o	Strains of the Laminate's Mid-Plane in Y Direction
ε_{xy}^o	Strains of the Laminate's Mid-Plane in XY Direction
k_x	Curvatures of the Laminate's Mid-Plane in X Direction
k_y	Curvatures of the Laminate's Mid-Plane in Y Direction
k_{xy}	Curvatures of the Laminate's Mid-Plane in XY Direction
A	Laminate's Extensional Stiffness Matrices
B	Laminate's Coupling Stiffness Matrices
D	Laminate's Bending Stiffness Matrices
N_x^T	Laminate's In-Plane Forces in X Direction
N_y^T	Laminate's In-Plane Forces in Y Direction
N_{xy}^T	Laminate's In-Plane Forces in XY Direction
M_x^T	Laminate's Thermal Moments in X Direction
M_y^T	Laminate's Thermal Moments in Y Direction
M_{xy}^T	Laminate's Thermal Moments in XY Direction
$[\bar{Q}]_k$	Stiffness Matrix of Ply K
a_x	Coefficients of Thermal Expansion of Ply K in the X Direction
a_y	Coefficients of Thermal Expansion of Ply K in the Y Direction

a_{xy}	Coefficients of Thermal Expansion of Ply K in the XY Direction
h_k	Height of Ply K Relative to the Mid-Plane of the Laminate
Q_{ij}^k	Stiffness Constants of the Kth Layer
α_x^k, α_y^k	Coefficient of Thermal Expansion in XY Direction of Lamina K
Z_k, Z_{k-1}	Coordinate of Upper and Lower Surfaces of Lamina Relative to the Midplane
ΔT	Temperature Interval Over Which Residual Stress Has Built Up
$\sigma_{0/90}^t$	Tensile Strength of Cross-Ply Laminates
$\sigma_{0/0}^t$	Tensile Strength of Unidirectional Laminates
σ_R	Residual Interlaminar Stresses
$\{\sigma\}_{\boldsymbol{k,n}}$	Stress Matrix for the Kth Layer in the Nth CL
$[\bar{Q}]_{\boldsymbol{k,n}}$	Reduced Stiffness Matrix for the Kth Layer in the Nth CL
$\{\boldsymbol{\epsilon}^{\circ}\}_{\boldsymbol{n}}$	Extensional Strain Matrix for the Nth CL
$Z_{\boldsymbol{n}}$	Distance from Geometric Midplane for the Nth CL
$\{\kappa\}_{\boldsymbol{n}}$	Curvature Matrix for the Nth CL
ϵ_n°	Midplane Strain of the Nth CL in Either 0° or 90° Direction
L_n	Length of the Nth CL after Separation
L_0	Length of the PSL Before Separation
κ	Curvature in the 0° or 90° Direction
d	Deflection at Center of the Laminate
L	Length of the CL
Δz	Thickness of Layer
d	Laminate Thickness
$\Delta\epsilon_s$	Strain Difference Upon Removal of Layer
z	Distance from Center of Mass
E	Elastic Modulus
ϵ_s	Absolute Strain at the Top Surface
E_m	Modulus of Elasticity of Matrix
E_f	Modulus of Elasticity of Fiber
E_{11}	Composite Stiffness Parallel to the Fibers
E_{22}	Composite Stiffness Transverse to the Fiber Direction
α	Coefficients of Thermal Expansion in Each of the Principal Directions
a/p	Delamination Depth
θ	Laminae Orientation

THIS PAGE WAS INTENTIONALLY LEFT BLANK

1. 1. INTRODUCTION

The high specific strength and specific stiffness make composites ideal replacements for conventional materials. Recently, considerable attention has been given to the use of high-strength, high-temperature thermoplastic resins as matrix materials for fiber-reinforced composites. Thermoplastic matrices have the potential to decrease manufacturing costs and improve the damage tolerance of composite structures. Additionally, thermoplastic prepregs have the advantages of infinite shelf life, ambient storage, and multiple forming processes [1]. Thermoplastics also offer a number of advantages over thermosets, such as greater toughness, higher performance temperature, impact and chemical resistance, greater resistance to environmental influences, and shorter processing time [2]. As thermoplastic composites are processed at much higher temperatures than epoxy systems, which are thermoset polymers, more expensive tools, and manufacturing methods are required. This fact, combined with high procurement costs, is hampering the more widespread use of fiber-reinforced thermoplastics in high-performance aerospace structures [3,4].

Residual stress[1] can be described as ‘‘a stress that persists in a material that is free of external forces or temperature gradients’’ [5]. Residual stress formation in high-performance thermoplastic composites (TPCs) is one of the essential issues that we need to consider. After processing composite laminates and subsequently cooling them from the relatively high processing temperature to the service temperature, residual stresses will rise due to the significantly higher shrinkage of the matrix compared with the fibers [5,6]. In other words, residual stresses are usually introduced into a composite part during processing due to the unmatched thermal expansion coefficients of the constituent materials and the chemical or crystallization shrinkage of the resin [5,6,7,8,9]. In all fiber-reinforced polymers, due to their inherent inhomogeneous nature, we will face this kind of residual stress formation [5]. In addition, when forming advanced thermoplastic composite structures, the stresses generated during cooling have a profound effect on the deformation and strength of the formed parts [10]. Sometimes, the residual stress is so severe that transverse matrix cracks are introduced within the parts after processing and parts fail earlier than expected. Thus, residual stresses are critical

[1] In current literature, the terms residual stress and residual strains are often utilized interchangeably.

to the performance of the composite, and the state of residual stress within a composite structure after processing must be known before being put into service. Furthermore, an optimum processing cycle must be detected which can both minimize residual stresses and production time and maximize structural mechanical properties [1].

In this section, three mechanical levels of residual stress formation will be explained, namely: micromechanical residual stresses (resulting from shrinkage mismatch between matrix and fiber), interlaminar residual stresses (resulting from ply anisotropy in angle-ply composites), and residual stress gradients through the thickness (resulting from cooling rate gradients, material density, thermal gradients, etc.). In this study, the stresses at these three levels will be referred to as intralaminar stresses, interlaminar stresses, and laminate stresses, respectively.

1.2. THE MANUFACTURING PROCESS OF THERMOPLASTIC COMPOSITE STRUCTURES

Three types of processes have commonly been used to produce thermoplastic composite structures. These include autoclave or press, strip laying, and filament winding.

Mantell and Springer used models and computer codes to calculate the thermal and mechanical behavior of thermoplastic composites during processing in an autoclave or press, by tape laying and filament winding. Specifically, the computer codes provided interply temperature, crystallinity, viscosity, degree of intimate contact, degree of bonding, and residual stresses and strains in the composite. With this information, the codes can be used to assess the usefulness of each manufacturing process for a given application and to establish appropriate processing conditions [11].

1.2.1. Autoclave or press; Flat plate _ Uniform Pressure and Temperature

A flat plate includes n layers (plies) of thermoplastic prepreg tape. Each layer can be made of a different material. The plate is “thin” so that its thickness H is small in relation to its length L and width W ($H/L << 1$; $H/W << 1$). The composite plate is placed between two platens Fig. 1.1. These platens can be those of a press or simulate the tool platen, bleeder, breather, and vacuum bag of an autoclave. Consequently, the process described below is applicable to processing in an autoclave or press [11].

Heating (or cooling) and pressure are applied to the composite by means of the platens. Thermal behavior is specified by prescribing either the temperatures on the composite surfaces (T_{st} and T_{sb}) or on the outer surfaces of the platens (T_t and T_b), or the heat fluxes (q_t and q_b) to the platen surfaces Fig. 1.2 [11].

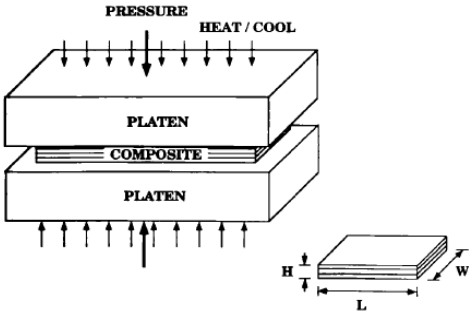

Fig. 1.1: Illustration of the press [11].

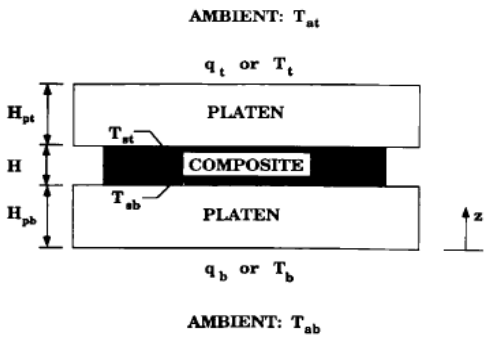

Fig. 1.2: Thermal boundary conditions for the press [11].

Temperatures or heat flows may be different on both sides and may vary over time, but they must be uniform on each surface. Temperatures or heat fluxes can be such that heat is transferred to or from the surface. Pressure P is also applied to the composite by the two platens Fig. 1.1. This pressure (which may be applied by a press or in an autoclave) may also vary over time, but it is uniform over the entire surface [11]. Regarding the autoclave molding method in detail, it is very similar to vacuum bagging, with a few changes. For example, for biocomposites, the heat and pressure required by biocomposites during the curing phase are provided by the autoclave machine (Fig. 1.3(a)). This process involves firmly stacking prepregs in a mold following a specific sequence. A release gel is applied to the mold surface to prevent sticking between the polymer and the mold surface. The process also allows the use of cores and inserts. This is followed by vacuum bagging to eliminate any air trapped between the layers (Fig. 1.3(b)). The assembly is then placed in the autoclave machine, where both heat and pressure are applied to promote uniform and efficient matrix distribution, as well as good interfacial adhesion between the fibers and matrix for a definite time interval. This stage is known as curing. The composite component is then demolded after the assembly has cooled and the vacuum bag has been removed, in sequence [12].

In addition, the principal advantages and disadvantages of autoclave and compression molding are presented in Table 1.1 [13].

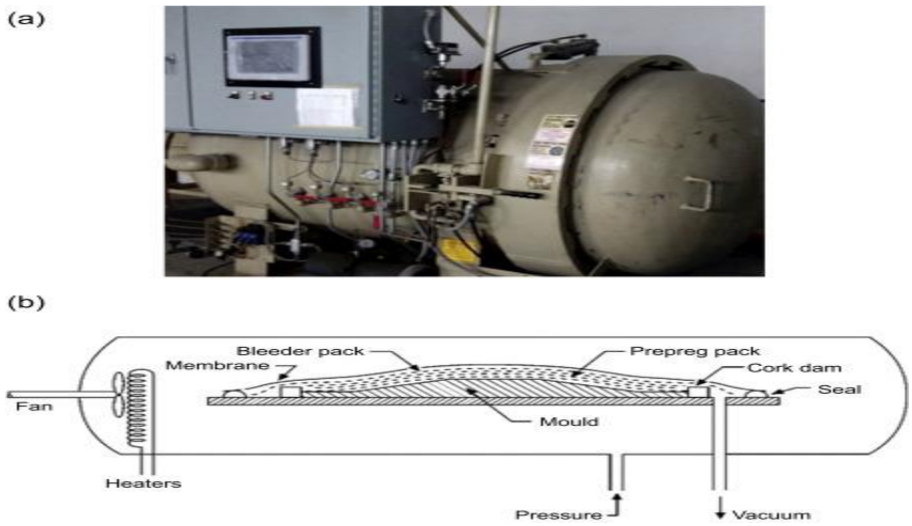

Fig. 1.3: (a) An autoclave machine, (b) its internal components and process schematic (Halley, 2012; Dixit et al., 2016) [12].

Table 1.1: Comparison of advantages and disadvantages between autoclave and compression molding for thermoplastic composites [13].

Process	Advantages	Disadvantages	
Autoclave	• Large and complex structures can be obtained • Consistency of components produced can be achieved	• Automation is difficult • Long consolidation time is necessary due to convection losses	[4]
Compression molding	• Short processing cycles • Automation is possible	• Process relate defects such as waviness and wrinkling are commonly observed	[5]-[6]

1.2.2. Tape Laying; Flat Plate _ Nonuniform Pressure and Temperature

As in the previous problem, we consider a thin flat plate (H/L<<1; H/W << 1) composed of n layers of thermoplastic prepreg tape. Each layer can be made of a different material. The composite plate is placed on a flat "tool plate" which can be either heated or cooled Fig. 1.4. Heating and cooling of the tool plate are described by specifying either the temperature T_b at or heat flux q_b on the bottom and side surfaces of the tooling plate Fig. 1.5. A moving head, consisting of heaters, coolers, and rollers, is mounted above the composite plate. The heating and cooling elements heat or cool the plate from above, while the rollers apply a known pressure P to the plate. The head moves at a constant speed of V, exposing parts of the composite plate to the head. The temperature T_{se} or heat flux q_{se} at the edges of the composite is assumed to be uniform and constant Fig. 1.5. The heating and cooling of the composite's top surface are

described by specifying either the composite's surface temperature T_{st} or the heat flux q_{st} to or from the surface. However, the temperature or heat flux specified for the top surface can vary arbitrarily along its length (i.e. in the direction in which the head moves). Temperature and pressure can therefore vary as a function of time and position along the length inside the composite (x direction). However, temperature and pressure distributions across the width are assumed to be uniform. The thickness of the composite H varies as successive layers are applied. Heat and pressure can be applied continuously during the tape laying application process, or after several plies have been applied [11].

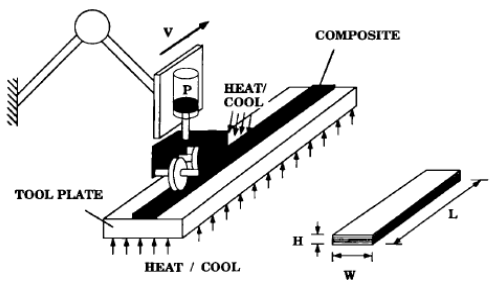

Fig. 1.4: Illustration of the tape laying apparatus [11].

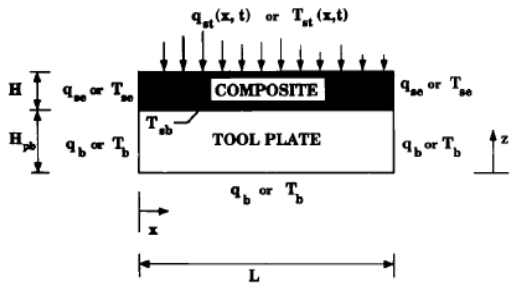

Fig. 1.5: Thermal boundary conditions for the tape laying process [11].

In addition, two of the main technologies for the automated deposition of prepreg materials are Automated Tape Laying (ATL) and Automated Fiber Placement (AFP). Both techniques use very similar machines, consisting of a computer-controlled poly-articulated robot with a placement head that lays bands of prepreg strips onto a mold to build up the layup (Fig. 1.6). The ATL is used to deliver wide prepreg tapes onto a surface while automatically removing the ply backing and is well suited to the manufacture of large parts of relatively simple geometry, such as the skin of an aircraft wing. The AFP is similar to the ATL but utilizes narrow prepreg strips (varying in width from 1/8 to 1/2), which are collimated on the head and then delivered together. Since narrower tapes can better steer sharply curved surfaces than wider tapes (which cannot be placed without buckling some fibers), AFP can be used to manufacture much more complex geometries, such as C-sections of wing spars [14].

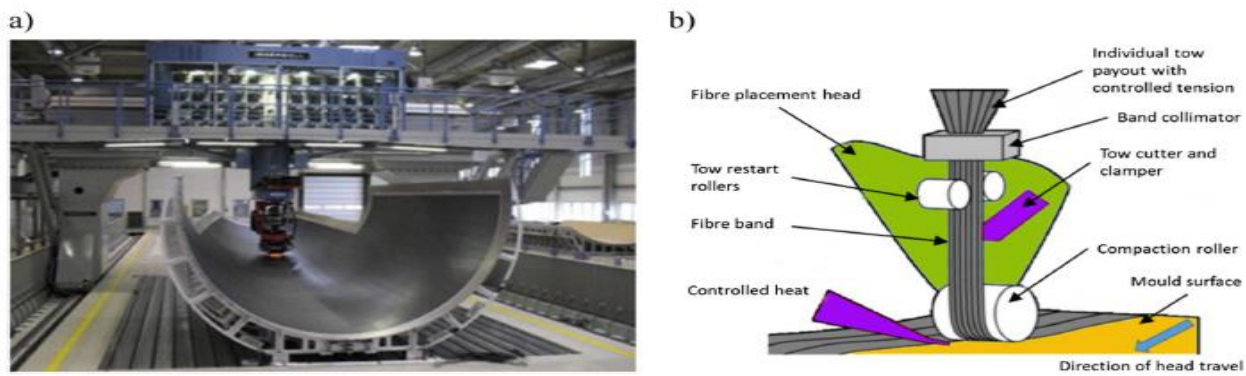

Fig. 1.6: (a) An AFP machine laying into a female mold – (b) Automated fiber placement head, redrawn from [14].

1.2.3. Filament Winding; Nonuniform Pressure and Temperature

A cylinder is made up of layers of thermoplastic prepreg tows by placing bands of tows on a rotating mandrel Fig. 1.7. The material of each layer can be different. The mandrel is demonstrated by a hollow cylinder with a uniform effective wall thickness [11].

The tows are deposited under tension (initial fiber tension F_o) by a crosshead moving at speed V parallel to the axis of the mandrel. The angular speed of the mandrel is ω. The orientation of the fibers in a layer (winding angle) is ϕ_o During winding, the outer surface of the composite can be either heated or cooled. In addition, pressure can be applied to this surface. Heat and pressure can be applied continuously at the location where the fiber bands are deposited Fig. 1.7, or after one or more layers have been wound Fig. 1.8. When heat and pressure are applied locally, the process is similar to the tape laying of strips described above [11].

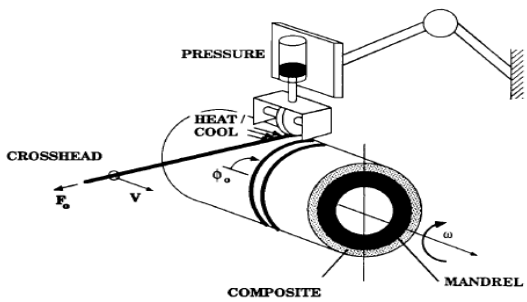

Fig. 1.7: Local application of heat and pressure during the filament winding process [11].

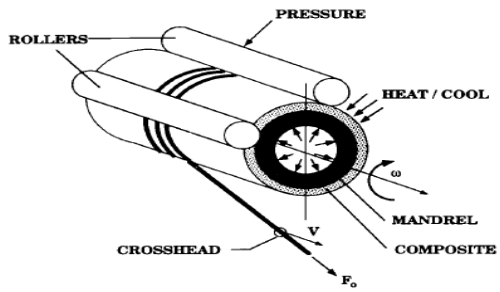

Fig. 1.8: Application of heat and pressure along the length of the cylinder in the filament winding process [11].

When heat and pressure are applied along the entire length of the cylinder, we assume that they vary along the circumference (but not in the axial direction) and that they can also vary with time. This latter condition implies that heating, cooling, and pressure can be applied at any time after the winding of one, two, or more layers. The pressure, heating, and cooling applied are known. Heating and cooling can be applied to the outer surface of the composite cylinder and to the inner surface of the mandrel. Heat transfer to the outer surface of the cylinder can be specified by prescribing either the composite surface temperature T_{so} or the heat flux q_{so}. These can vary in circumferential direction and over time Fig. 1.9. The conditions inside the mandrel can be specified by prescribing either the temperature of the mandrel's inner surface T_{si} or the heat flux q_{si}; to or from this surface. The temperature T_{si} and the heat flux q_{si}; may vary over time, but must be uniform over the entire inner surface of the mandrel. As in the case of tape laying, the thickness of the composite varies as successive layers are wound. Heat and pressure can be applied continuously or after the winding of one or more layers is complete [11].

Furthermore, an example of a filament winding application is pressure vessels, which are generally manufactured by filament winding. Pressure vessels made of carbon fiber composites are generally manufactured by thermosetting filament winding processes that are established for mass production purposes. Laser-assisted thermoplastic tape winding is an efficient manufacturing process for pressure vessels than thermoset filament winding. The two processes are similar in some respects but differ in the way the fiber-impregnated material is wound around the mandrel. In the thermoplastic winding process, pre-impregnated tapes are used which are in a solid state of aggregation when introduced into the process. When the current tape layer is placed on the previously laid layer of the mandrel, the thermoplastic is melted by a laser to enable subsequent consolidation. A schematic of the machinery and the process for the laser-assisted thermoplastic tape winding process is shown in Fig. 1.10 [15].

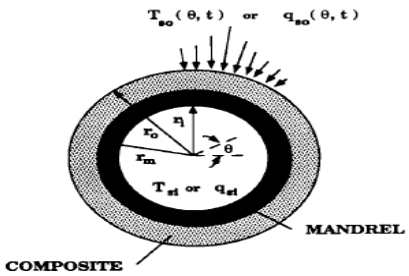

Fig. 1.9: Thermal boundary conditions for the filament winding process [11].

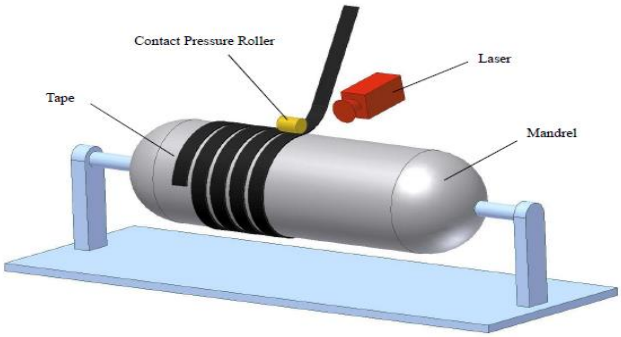

Fig. 1.10: Laser-assisted thermoplastic tape winding of a pressure vessel [15].

1.2.4. The main advantages of the filament winding and tape placement over the autoclave and press molding

Filament winding and tape placement offer a number of advantages over autoclave and press molding, including [13]:

- Fiber orientation accuracy is improved compared to autoclave and compression molding.
- Possibility of in-situ consolidation, reducing the entire process to a single task.
- Consistent product quality

For the automated filament winding process, there are two different winding technologies, depending on the material used:

- "Dry" winding, where prepregs are directly layed around the mandrel.
- "Wet" winding, where the fibers are impregnated in a resin bath before being placed on the mandrel.

The wet winding process is generally applied to thermoset materials; however, few studies have discussed the possibility of processing thermoplastic composites using this type of process [13].

1.2.5. Tape Placement

The tape placement for thermoplastic composites involves heating, melting, and cooling steps, just like other manufacturing processes. Thus, the development of residual stresses is inevitable due to the disparate thermal characteristics of matrix and fiber materials, as well as non-uniform cooling rates. From the point of view of product quality, such as interlaminar strength, dimensional accuracy, etc., these stresses must be kept within acceptable limits. The tape placement process is one of the few techniques that have the potential to continuous processing of thermoplastic composites in large-scale industrial production. In this process, an incoming composite tape is bonded to the previously laid and consolidated laminate by heat and pressure applied locally at the interface (Fig. 1.11) [10].

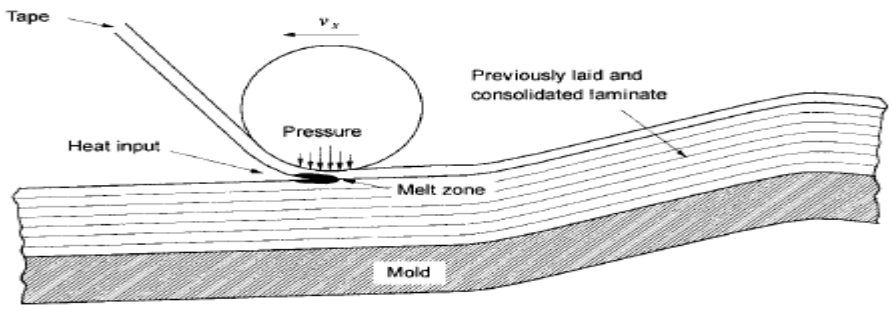

Fig 1.11: The thermoplastic composite tape placement process [10].

By laying additional layers in different directions, it is possible to manufacture a part with the desired thickness and properties. Since heat is mainly supplied to the region where the tape and laminate meet, the process is highly non-isothermal, and residual stresses can become critical. This process poses a very difficult problem for determining residual stresses, for the following reasons: The tape placement is a continuous process. When a new layer is placed, the previously laid and consolidated layers are heated again. If the temperature of these layers exceeds the glass transition temperature, annealing will ensue and the residual stresses developed during previous tape placement will relax [10].

Sonmez et al carried out a residual stress analysis on the tape placement process. In their research, it is noted that preheating the laminate to a certain temperature before placing the tape is a usual practice to help bonding. If the preheating temperature is increased, the temperature difference between the heated zone and the remaining region becomes smaller, and the material cools more slowly. As a result, residual stresses decrease, as shown in Fig. 1.12 [10]. In addition, Fig. 1.13 shows that increasing roller velocity results in a higher level of residual stress. This is due to the fact that, at high speeds, only regions close to the heated surface are heated to high temperatures. Localized heating leads to higher temperature gradients and therefore higher residual stresses [10].

The length of the heated surfaces on the tape and substrate was proved to have a considerable influence on temperature distribution. The effect of larger heated lengths is similar to the effect of preheating the substrate in slowing down the cooling rate. On the other hand, a small heated length results in a highly localized heated zone and therefore higher residual stresses, as suggested in Fig. 1.14 [10]. t's important to note that in the above results, both the tape and the substrate were heated equally. Fig. 1.15 illustrates the residual stress distribution (σ_{xx}) through the thickness of a cross-ply laminate, $[0_4/90_4]_S$ which was manufactured by the tape placement procedure. Ply numbers 1 and 16 indicate the top and bottom layers respectively. The distribution is uneven through the thickness of the laminate. Compressive stresses

develop in the top and bottom 4 plies, while tensile stresses develop in the middle 8 plies. These stresses are sufficiently high to cause undesirable deformations in the laminate. Tensile stresses in the middle plies are high enough to cause matrix cracking [10].

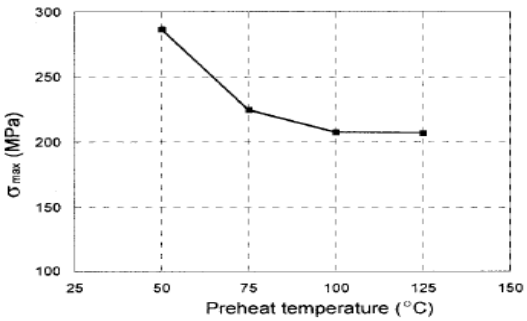

Fig. 1.12: The effect of preheat temperature on the maximum tensile stress, σx [10].

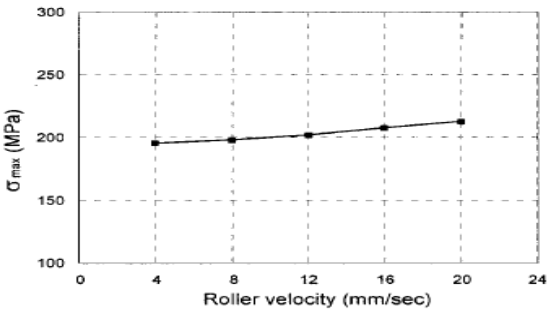

Fig. 1.13: The effect of roller velocity on the maximum tensile stress, σx [10].

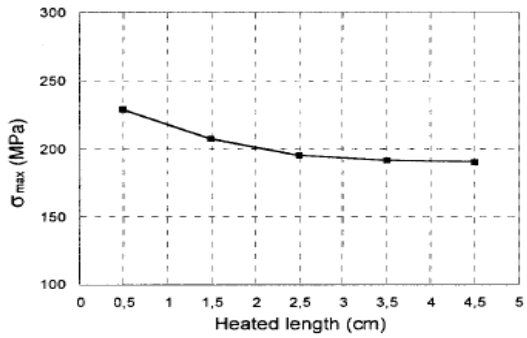

Fig. 1.14: The effect of heated length on the maximum tensile stresses [10].

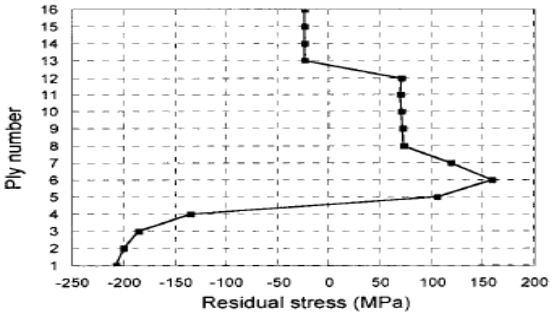

Fig. 1.15: Residual stress (σ_{xx}) distribution through the thickness of a 16-ply cross-ply laminate [10].

As a consequence, during tape placement, residual stresses build up gradually during successive lay-down of layers and can reach excessively high levels, particularly in thick laminates. Moreover, the unsymmetrical distribution of residual stresses can lead to the distortion of finished products. Process parameters, therefore, need to be optimized to minimize residual stresses and, at the same time, reduce their uneven distribution [10].

1.3. RESIDUAL STRESS FORMATION ON THREE MECHANICAL LEVELS

Depending on the origin of the stresses, they may act at different levels in the laminate and therefore have different levels of self-equilibration in the composite structure. Fig. 1.16 describes the generation of thermal stresses between skin and core during solidification under pronounced nonisothermal conditions of material with viscoelastic characteristics [4,16].

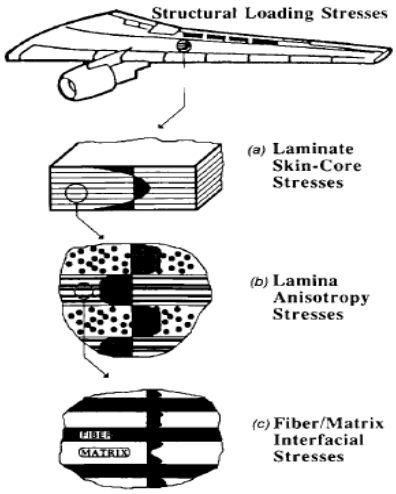

Fig. 1.16: Three different Internal stress levels in advanced composite materials are illustrated: (a) skin/core solidification governed by nonisothermal solidification over the thickness of the laminate; (b) lamina anisotropy governed by anisotropic coefficient of thermal expansion (CTE) longitudinal and transverse fiber direction, (c) fiber/matrix interface governed by heterogeneous expansivity of the constituents [4].

Fig. 1.16 (a) illustrates the global laminate level, (b) the macro-mechanical level, and (c) the micromechanical level. We will discuss these levels below. In general, the mismatch in thermal expansion between fiber and matrix can induce micro-stresses at a local level. Similarly, the mismatch in properties between constituent plies oriented in different directions can generate macro-stresses. In addition, skin-core effects resulting from differences in cooling rates through the thickness of the part can lead to the generation of high stresses within the laminate (global stresses) [17]. The first level of stresses is between individual fibers within a ply, which we can refer to as 'microstresses' [18]. On the micromechanical level, one of the governing parameters of residual stresses is the mismatch in the coefficient of thermal expansion between the fibers and the matrix [5,16]. Unlike a thermoset matrix, the thermoplastic matrix is heated to a processing temperature above its glass or melting temperature and then solidifies as it cools to service temperature (often ambient conditions), without any chemical reaction occurring.

Assuming that there is a fiber-matrix bond during cooling, Fig. 1.17 illustrates that this results in residual compressive stress in the fiber along the longitudinal axis as well as in the radial direction. Furthermore, there will be residual tensile stress in the matrix in the longitudinal and radial directions [5].

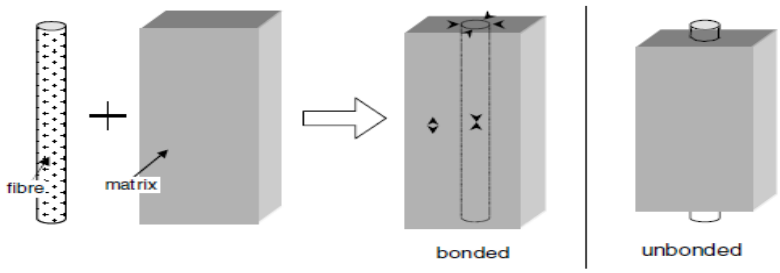

Fig. 1.17: Schematic view of the effect of cooling on the matrix around a fiber. The bonded (constrained) case represents the situation after processing, where ◄► and ►◄ represent tensile and compressive residual stresses, respectively [5].

For example, in one research continuous glass fiber-reinforced polypropylene composite PP/G is studied. It should be noticed that polypropylene is a semi-crystalline polymer. During the thermoforming process, PP matrix composites are heated above the melting point of the matrix, then cooled to room temperature. During cooling, residual stresses appear in the composites at various levels. In each ply, the crystallization shrinkage of the matrix and the mismatch in coefficients of thermal expansion between the fibers and the matrix ($a_m > a_f$) result in compressive stresses in the fibers and tensile stresses in the matrix. Since unidirectional composites have different coefficients of thermal expansion in the longitudinal and transverse directions, when a multi-layer laminate with different stacking angles is cooled down after consolidation, each ply is left with residual compressive residual stresses in the fiber direction and extensional stresses in the transverse direction. These thermal/residual stresses can considerably reduce composite strength and alter the final shape of molded parts. Controlling these stresses is therefore essential to improve the structural capability of thermoplastic matrix composites, and to ensure dimensional control and stability of manufactured parts [19].

On the macro-mechanical level, lamination residual stresses are present on a ply-to-ply scale because of lamina anisotropy (there is a variation between the transverse and longitudinal ply coefficients of thermal expansion) [5,18]. At this level, the residual stresses arise due to a difference in coefficients of thermal expansion in the transverse and longitudinal ply. For example, with cross-ply composites, as we have differences in thermal shrinkage directions, the 90° fibers impose a mechanical constraint on the 0° fibres upon cooling and vice versa Fig. 1.18 [5].

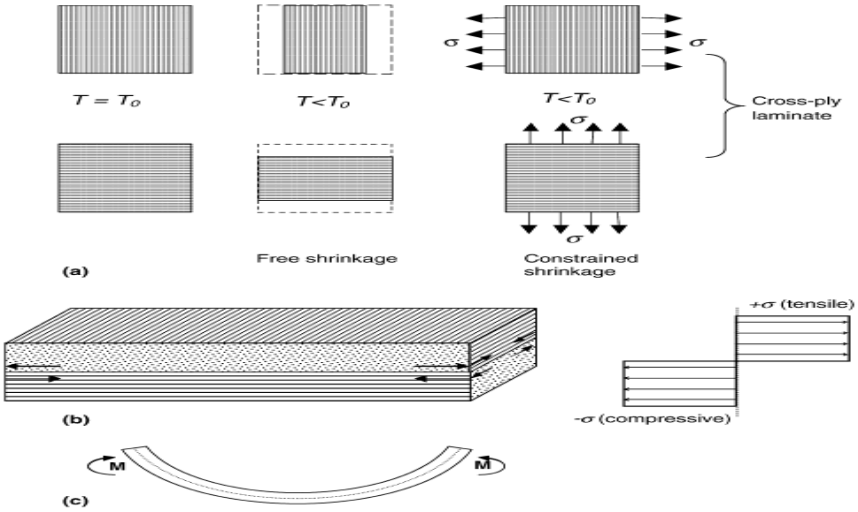

Fig. 1.18: Schematic view of residual stress formation in unbalanced cross-ply laminate (a), (b) residual thermal stresses when laminate is constrained, (c) front view of out-of-plane deformation when unconstrained [5].

On a global scale, there is a tertiary level of stress due to the differential thermal history of parts of a laminate during the cooling process. These stresses occur through the thickness of a laminate, and their distribution is generally parabolic [18]. In other words, on the global laminate level, a gradient in cooling rate, temperature conditions throughout the thickness of the composite laminate or structure may lead to a residual stress distribution through the thickness of the laminate. This can also be due to the interaction between the tool and the part. Generally, a thick laminate will experience a slower cooling rate in the center of the laminate than at the surface plies. At a certain temperature, the center plies might still require to solidify, whereas the surface plies have already become solid. During further cooling, the surface plies impose a constraint on the shrinkage of the center plies. Consequently, there will be a parabolic distribution of compressive residual stresses in the surface plies and tensile stresses in the center plies Fig. 1.19 [5]. In addition, Fig. 1.20 also shows a schematic of the origin of these stresses in tape-laying, where it is perhaps easiest to envisage the mechanism of generation. One important point of note concerning 'global' stresses is that they can be eliminated by raising the composite above the glass transition temperature (T_g) of the matrix and allowing relaxation processes to occur [18].

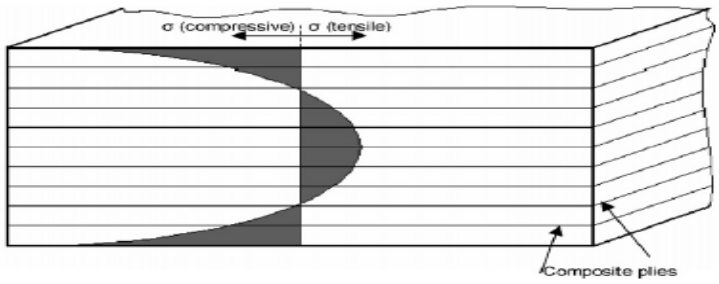

Fig. 1.19: Laminate skin-core residual stress distribution (grey area) [5].

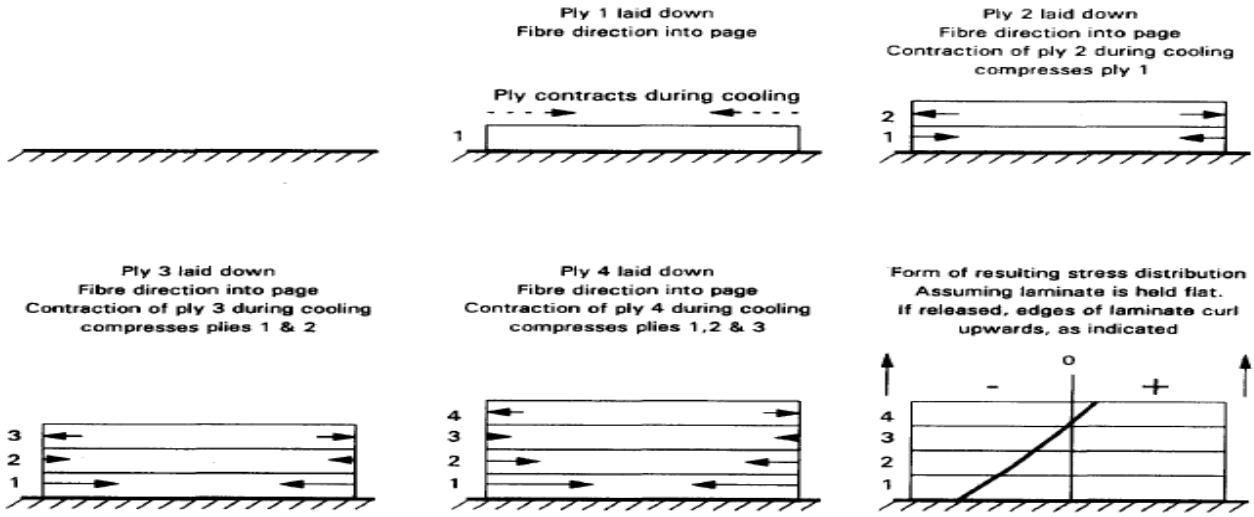

Fig. 1.20: The origin of 'global' stresses in tape laying [18].

The three different levels above would result in a complex three-dimensional residual stress state within a composite structure. To evaluate the parameters responsible for the formation of residual stresses, these levels will be considered separately. In a composite structure, however, the distinction between the three is not so clear [5].

If environmental and long-term parameters are omitted, the magnitude of residual stresses in composite structures will be dependent on four parameters: temperature difference, thermal expansion/shrinkage coefficients during cooling of the composite structures (or plies), elastic coefficients of these constituents (or plies), and fiber volume fraction. These parameters in turn depend largely on the morphology of the thermoplastic matrix (semi-crystalline or amorphous), the type of fibers, the morphology of the fibers (woven or unidirectional prepreg), the properties of the fiber- matrix interface, and the processing conditions [5]. These factors will be explained separately, starting with the micromechanical level and the fiber-dominated properties, followed by the matrix-dominated properties, and composite general properties.

1.4. MICROMECHANICAL RESIDUAL STRESSES

This section serves as a brief collection and summary of the works on micromechanical residual stresses in terms of reinforcing fibers-dominated properties and thermoplastic matrix-dominated properties.

1.4.1. Reinforcing fibers dominated properties

Studies on residual stresses in thermoplastic composites mainly concern carbon fibers (CF), with some studies on glass fibers (GF). Aramid fibers were studied only once. The coefficients of thermal expansion (CTE) of reinforcing fibers are generally much lower than those of thermoplastic matrixes, resulting in a large difference in expansion behavior between the matrix and reinforcing fibers [1,53,58]. However, perpendicular (radial) shrinkage of the fibers during cooling was found to be a relatively insignificant contribution to residual stress formation [5].

1.4.1.1. Fiber volume fraction

Fiber volume fraction has effect on the residual stresses. With regard to the fiber volume fraction, it was found that [5]:

-The model of the residual fiber stresses in carbon fiber/polypropylene (PP/CF) micro- and macro-composites showed that for higher fiber volume fractions, residual fiber strains were lower.

- For cross-ply composites, it has been reported that interlaminar residual stresses raise with increasing fiber volume fraction.

-For some composites, an optimal volume of fibers may exist.

In one study, two laminae of unidirectional carbon-fiber–epoxy-matrix prepregs in the form of strips, one strip on top of the other (Fig. 1.21), were fabricated into a composite at the overlapping region (6 mm×6 mm) of the two laminae by applying pressure and heat to the overlap region (without a mold). Each of the samples was put between the two heating platens of the hot press and heated linearly up to 175 ± 2 ◦C at the rate of 2.5 ◦C min−1. It was then cured at this temperature for 10 h and subsequently cooled linearly to 50 ± 2 ◦C at the rate of 0.18 ◦C min−1. Next, the sample was reheated up to 150 ± 2 ◦C, then cooled back to 50 ± 2 ◦C. Both the reheating and the subsequent cooling were linear and proceeded at the rate of 0.15 ◦C min−1. After reheating and cooling, the sample was heated linearly up to 150 ± 2 ◦C again at

the rate of 1 ◦C min−1 and then cooled linearly back to 50±2 ◦C at the rate of 0.15 ◦C min−1 [20].

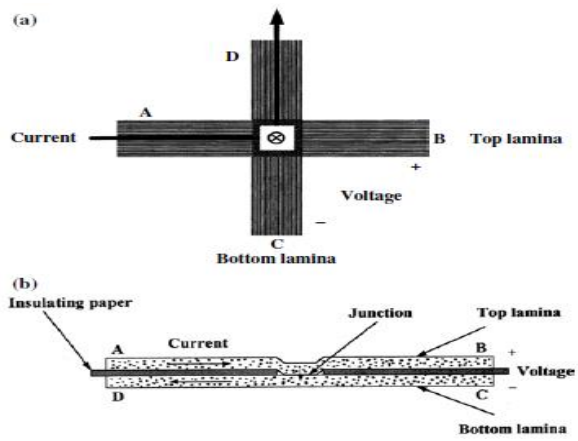

Fig. 1.21: Composite configurations for testing contact resistivity as a function of temperature. (a) Cross-ply, (b) unidirectional [20].

Activation energies (activation energy is the energy for an electron jumping from one lamina to another), thicknesses, and room temperature contact resistivities for samples fabricated at different curing pressures and composite configurations are shown in Table 1.2. All activation energies were calculated on the basis of data at 75–125 ◦C. In this temperature regime, the temperature change was highly linear and well-controlled. Table 1.2 illustrates that, for the same composite configuration (cross-ply), the higher the curing pressure, the lower the composite thickness (as more epoxy is squeezed out), the lower the contact resistivity, and the higher the activation energy. A smaller composite thickness corresponds to a higher fiber volume fraction in the composite [20].

Table 1.2: Activation energy for various composites. The standard deviations are shown in parentheses [20].

Composite configuration	Curing pressure (MPa)	Composite thickness (mm)	Contact resistivity ρ_{co} (Ω cm^2)	Activation energy (eV)		
				Heating at 0.15 °C min^{-1}	Heating at 1 °C min^{-1}	Cooling at 0.15 °C min^{-1}
Crossply	0	0.36	0.73	0.0131 (2×10^{-5})	0.0129 (3×10^{-5})	0.0125 (8×10^{-6})
Crossply	0.062	0.32	0.14	0.0131 (4×10^{-5})	0.0127 (7×10^{-5})	0.0127 (4×10^{-5})
Crossply	0.13	0.31	0.18	0.0168 (3×10^{-5})	0.0163 (4×10^{-5})	0.0161 (2×10^{-5})
Crossply	0.19	0.29	0.054	0.0222 (3×10^{-5})	0.0223 (3×10^{-5})	0.0221 (1×10^{-5})
Crossply	0.33	0.26	0.0040	0.118 (4×10^{-4})	0.129 (8×10^{-4})	0.117 (3×10^{-4})
Unidirectional	0.42	0.23	0.29	0.0106 (3×10^{-5})	0.0085 (4×10^{-5})	0.0081 (2×10^{-5})

Consequently, the activation energy for electrical conduction in the through-thickness direction was found to increase with increasing curing pressure and to be lower for unidirectional than

crossply composites. The reason is that the residual interlaminar stress increases with increasing fiber volume fraction, which increases with increasing curing pressure, and the residual interlaminar stress is higher for crossply than unidirectional composites. The higher the activation energy, the greater the interlaminar stress [20].

1.4.2. Thermoplastic matrix dominated properties

1.4.2.1. Shrinkage

The shrinkage of thermoplastic polymers is related to the morphology of the matrix, i.e., amorphous or semi-crystalline. In semi-crystalline thermoplastics, volumetric shrinkage results from densification during crystallization (crystals having a higher density than the amorphous phase) in addition to shrinkage due to temperature reduction. In amorphous polymers, the shrinkage is only because of the latter. The total shrinkage of semi-crystalline matrixes is ten times higher than that of amorphous matrixes, as shown in Fig. 1.22, where T_g is the glass transition temperature, T_m is the melting temperature, and T_c is the crystallization temperature upon slow cooling from the melt. The part of the curve that includes Tc is a representative plot during cooling. For the range of temperatures to which the thermoplastic matrix is subjected, the expansion and shrinkage behavior is not linear, i.e., the CTE is likely to change at different temperatures [5].

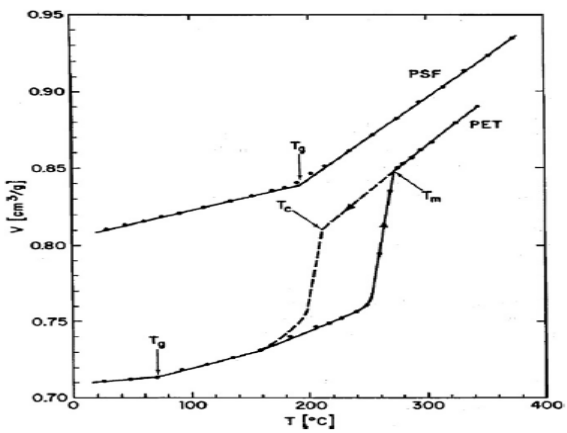

Fig. 1.22: Specific volume of polysulfone (PSF, amorphous) and polyethyleneterephthalate (PET, semi-crystalline) as a function of temperature atatmospheric pressure [5].

In addition, the problem of residual thermal stress is particularly important for thermoplastic matrix composites. The thermoplastic matrix may have a slightly higher coefficient of thermal expansion than thermoset matrices, and thermoplastic matrix composites are typically

manufactured at higher temperatures than thermoset matrix composites [21]. These differences can result in greater differential shrinkage of the matrix with respect to the fiber for the thermoplastic matrix composite, and this higher differential shrinkage will result in higher residual thermal stresses in the laminated composite [21,7]. Differential shrinkage and thermal decrement are much greater in thermoplastic-based composites than in thermoset-based composites (as mentioned), and if combined with high-modulus fibers such as Kevlar 49 or high-modulus graphite, this can lead to extremely high axial residual thermal stresses in the fiber, sometimes of the order of 100,000 atm (10 GPa) [7].

1.4.2.2. Coefficients of thermal expansion

Thermal properties can play an important role in the design and manufacture of composite structures in their industrial applications. Most often, with heterogeneous materials, we are concerned with the internal stresses that develop due to microstructural variations in the coefficient of thermal expansion (CTE). In elastic structures, these stresses are superimposed on those due to mechanical loads and thus influence load-carrying capacity. Deformations resulting from thermal expansion are sometimes a matter of concern. In fact, in some applications, precise dimensional control is required [22].

The magnitude and gradients of residual stresses are significantly affected by thermal expansion [23]. As previously mentioned, residual stresses are typically introduced into a composite part during processing because of the unmatched thermal expansion coefficients of the constituent materials [1,5,41,53,58,60]. On a macro level, the anisotropy in the ply coefficient of thermal expansion (CTE), which results from the anisotropy of fiber stiffness and CTE, is manifested itself in the residual ply stresses in multidirectional laminates [6]. It was also noted that the coefficients of thermal expansion (CTE) of reinforcing fibers are mainly much lower than those of thermoplastic matrices, resulting in a large difference in the expansion behavior between the matrix and reinforcing fibers [5].

The model predictions and the experimental residual stress profiles for the unidirectional 40-ply APC-2 laminate, which was a PEEK/AS-4 (APC-2) thermoplastic composite, and cooled at 35 °C/s are illustrated in Fig. 1.23. The model predicts a parabolic stress profile similar to the experimental data, although the absolute values differ. This difference can be attributed to the extreme sensitivity of the residual stresses to the thermal expansion coefficients [23].

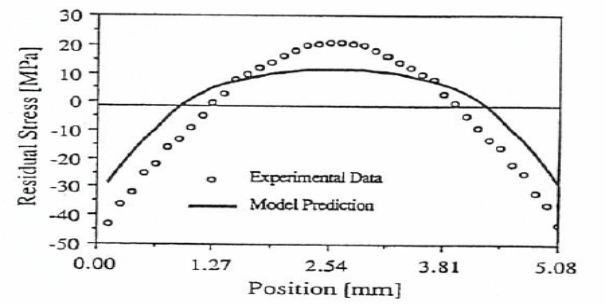

Fig. 1.23: Correlation of experimental transverse residual stress with the model prediction for a 40 ply APC-2 unidirectional laminate cooled at a constant surface cooling rate of 35 °C/s [23].

1.4.2.3. Temperature difference

Thermoplastic composites are processed at much higher temperatures than epoxy systems, which are thermosetting polymers. Consolidation temperatures are typically 300°C. These high consolidation temperatures have a significant effect on the residual thermal stresses that develop as the material cools down to its service temperature. These stresses can be very significant, leading to a considerable reduction in the material's apparent strength. Residual thermal stresses must therefore be taken into account in the design process [3,8,24].

The viscoelasticity of the polymer matrix is another important aspect when considering the effect of the cooling rate on thermal residual strains. For a viscoelastic matrix, increasing temperature favors stress relaxation and affects the evolution of thermal residual strains in the fiber during cooling. For a viscoelastic matrix, increasing the cooling rate will result in less relaxation and therefore higher residual stresses in the fibers [2]. Thus, when amorphous thermoplastic composites are cooled between the processing temperature and the glass transition temperature (T_g), the amorphous matrix is in a viscoelastic state. This means that any stress build-up due to thermal shrinkage can still be released, as the molecular chains possess sufficient energy to move freely at high temperatures, especially at low cooling rates. When T_g is reached, the amorphous polymer becomes glassy (thermoelastic state) and residual stresses will be formed during further cooling of the composite. As a consequence, for amorphous matrix composites such as polyetherimide (PEI), thermoplastic polyimide (TPI), polyethersulfone (PES), and polysulfone (PSU) which were reinforced with carbon fibers, the temperature at which thermal stresses begin to build up (also defined as the "stress-free" temperature) is around the glass transition temperature [5]. In a study to determine the stress-free temperature, a sample of graphite/thermoplastic composite with an amorphous matrix was heated in an oven until it became flat. It was found that the stress-free temperature, determined

from this sample, was slightly higher than its glass transition temperature. This is in agreement with previous results, as noted above, that residual stresses begin to build up from the glass transition temperature in amorphous polymer composites [21].

It is stated that stress-free temperature (SFT) is the initial temperature before cooling, and above which thermal stresses no longer exist [25]. For semicrystalline matrixes such as polyetheretherketone (PEEK), the stress-free temperature (SFT) can be found close to the peak crystallization temperature, due to the load-bearing capability of the crystalline phases below this temperature. The cooling rate affects the maximum crystallization temperature, which in turn has an influence on the stress-free temperature [5].

For all polymer matrix composites, the further the cooling or service temperature is from the SFT, the greater the residual stresses in the composite due to the difference in the coefficient of thermal expansion (CTE) between the polymer matrix and the fibers [5,7]. The SFT has often been determined by heating the composite until the residual stresses are zero [5]. It has been suggested that with thermosetting resins, the temperature at which stress begins to build up in a laminate may be lower than the curing temperature. If this is not taken into account, residual stress will be overestimated. These considerations do not apply to thermoplastic matrix materials; however, stress build-up will not necessarily begin during cooling, but can occur at the onset of crystallization or at the glass transition. The precise value of the stress-free temperature may vary depending on the material and the cooling rate. In addition, it was found that around 75% of the residual stress level in laminates builds up between T_g and room temperature [8].

Parambil et al. indicated that the onset and cessation of crystallization temperatures are predicted to decrease with an increasing cooling rate, as shown in Fig. 1.24. In their study, they considered the crystallization cessation temperature as the stress-free temperature (T_{sf}) for residual stress calculations. Furthermore, it was found that crystallinity at the termination of the crystallization process is 50% for all cooling rates, as shown in Fig. 1.24 for experiments conducted over the range of 2 to 40◦C/min. The stress-free temperature is defined as the termination of crystal growth, in this case 50% crystallinity. The stress-free temperature reached at different cooling rates is shown in Fig. 1.25 [26].

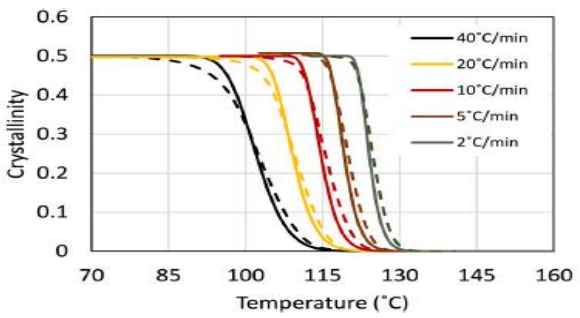

Fig. 1.24: Comparison of model with experiment at different cooling rates from 2 to 40 ◦C/min (dash lines – experiment, solid lines – model) [26].

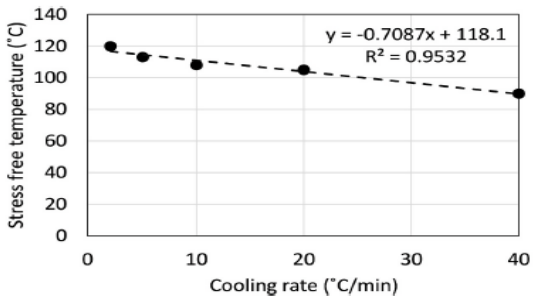

Fig. 1.25: Stress-free temperature vs constant cooling rate (50% crystallinity). (•) experiment; (—) fitting [26].

1.4.2.4. Processing conditions

The cooling rate is the most important processing condition that affects residual stress formation. The cooling rate proved to be a critical parameter in the molding process, as the matrix crystallization temperature, interfacial strength, and residual stress showed wide variations with different cooling rates [4,8,19]. We will discuss this parameter later in this section [4,5]. In addition, Pressure can affect the thermal properties of the polymer, which influences the formation of residual stresses. However, it has been concluded that pressure levels in composite processing are relatively low, so limited effects on matrix properties can be expected. The fibers are not affected by the pressure [5]. The processing environment is another factor that affects residual stress formation in thermoplastic composites [4,5]. Longer residence times and higher temperatures during processing have been shown to affect the glass transition temperature and thus the stress-free temperature, which in turn affects the formation of residual stress. This is different for each processing atmosphere [5].

1.4.2.4.1. Cooling rate effects in amorphous matrix composites

As mentioned in the temperature difference section, thermoplastic matrixes exhibit viscoelastic behavior and we have matrix relaxation during this time. The matrix relaxation is responsible for a significant reduction in residual stresses, especially at low cooling rates, as the polymer simply has more time to relax at higher temperatures. Moreover, the concept of “free volume” has been formulated to describe the response of the material to thermal expansion and shrinkage. This concept explains how the total volume of an amorphous polymer consists of the volume occupied by the polymer molecules and the free volume between the molecules.

When at a high rate the polymer is cooled, more free volume is "trapped" or "frozen" below T_g; therefore, the total volume of the polymer will be higher after cooling down Fig. 1.26. The figure illustrates when the glass transition temperature is lower with lower cooling rates (CR), there is a smaller temperature range at which stress can build up. It has been considered that the cooling rate in the glass transition region primarily controls the formation of residual stresses and at lower temperatures, the variation of residual stresses with temperature is generally independent of the cooling rate. As a result, for amorphous polymer matrixes, the faster the cooling rate in the glass transition region, the higher the residual stresses will be [5].

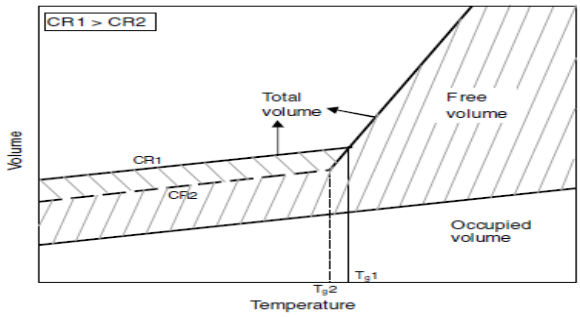

Fig. 1.26: Effect of cooling rate on free volume and glass transition temperature in an amorphous polymer (CR = cooling rate). The free volume is represented by the shaded area [5].

However, it was determined that being amorphous, the thermoplastic resin had only minimal sensitivity to the cooling rates employed. In other words, it was found that in amorphous resins, stress relaxation is the dominant mechanism for residual stress reduction compared to semi-crystalline resins. Hence, under fast cooling not much stress relaxation can take place. Rapid quenching will therefore result in higher curvature. In addition, it was reported that for an amorphous resin, there was a slight increase in residual stresses with increasing cooling rate, the change was rather small. Therefore, only a minimal amount of stress relaxation is expected to occur during the cool-down phase of processing [21].

In a research study, samples of AS-4 graphite/thermoplastic $[0_2/90_2]_T$ unsymmetric laminate with an amorphous polyimide resin were heated in a mold on a hot press to 305°C. The specimens were cooled down at three different cooling rates namely type I, type II, and type III Fig. 1.27. Type III cooling consisted of a rapid immersion of the copper mold containing the sample in ice water for a few minutes. The Type III specimen was then removed from the water and brought to room temperature. Fig. 1.28 shows the transverse crack density in 90° ply after cooling down from 305°C. To detect transverse cracks, three different samples were considered and also the crack density of the samples before going through a thermal cycle was examined.

After comparing crack density between the different thermal cycling, it was found that crack density values were higher when the sample was cooled in ice water Type III. As a result, the crack density increased slightly with the cooling rate. These higher values are probably due to the higher residual stress at 0°C, which is expected to be 10% higher than at room temperature. Therefore, the effect of the cooling rate on crack density is not very significant for this composite with an amorphous matrix [21].

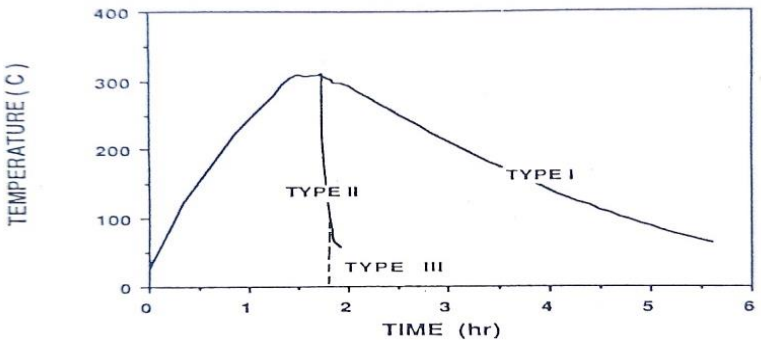

Fig. 1.27: Cooling cycles used in the experimental work of the reference [21].

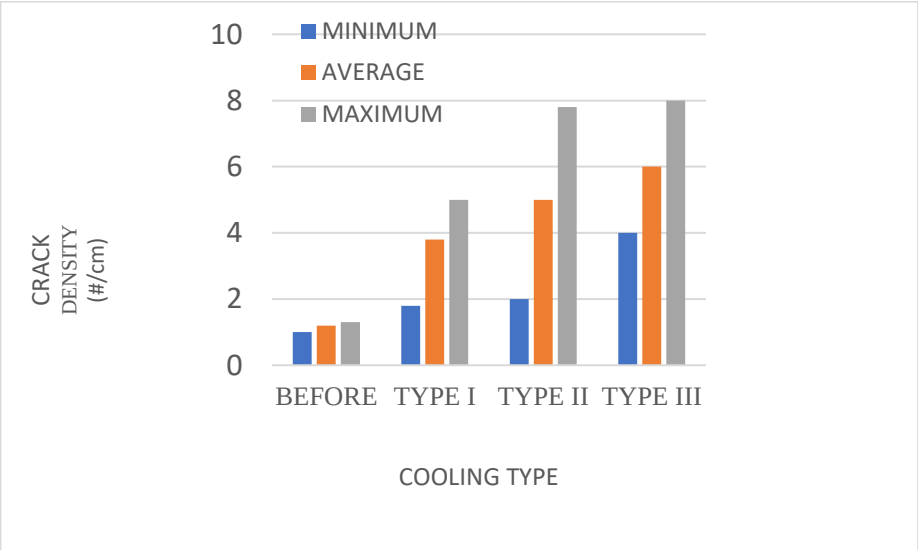

Fig. 1.28: Transverse crack densities after thermal cycling (annealing temperature is 305°C) [21].

1.4.2.4.2. Cooling rate effects in semi-crystalline polymer matrixes

It was found that the magnitude and gradients of residual stresses were significantly affected by variations in cooling rate for semicrystalline thermoplastic composites [23]. For semicrystalline thermoplastics, a higher cooling rate results in a lower peak crystallization temperature and lower levels of crystallinity. This will cause a lower stress-free temperature

and less shrinkage [5,21]. For example, it has been found that crystallinity is affected by the cooling rate, which typically increases from 25% at 1000°C/min to 50% at 3°C/min [8]. It was therefore concluded that residual stresses due to crystallization could be decreased by increasing the cooling rate [5]. Thus, rapid quenching will result in smaller curvature [21]. Although if the relaxation behavior of the amorphous content is considered, two competing mechanisms will exist in the semicrystalline matrixes upon rapid cooling: first, higher residual stresses will occur due to the rapid cooling of the amorphous phases. Second, lower residual stresses will be formed due to a lower stress-build-up temperature and less crystallization shrinkage in the crystal content. In this regard, it has been stated that a relationship must be determined between the viscoelastic behaviour and crystallinity kinetics of semicrystalline matrixes to fully understand residual stress development. Moreover, low crystallinity is generally undesirable due to poor solvent resistance [5].

Unger and Hansen experimentally investigated the effect of cooling rate from the molten state on the development of thermal and crystallization residual stresses in graphite-fiber-reinforced polyetheretherketone (APC-2) laminates by measuring the radius of curvature developed in non-symmetrical laminates (0/90). They found that the crystalline fraction achieved by PEEK depends strongly on its heat treatment history. In turn, the level of crystallinity controls the material's mechanical properties and environmental robustness. PEEK can be quench-cooled from the molten state to a purely amorphous state if cooling rates of around 5000°C/min or more are achieved. (The cooling rate required to reach the amorphous state varies considerably according to the study cited). At the other extreme, crystallinities in excess of 40% by weight can be achieved at extremely slow cooling rates, typically below 1°C/min. The effect of cooling rate on APC-2 crystallinity has been reported elsewhere. The rate of cooling from the molten state controls not only the degree of crystallinity finally achieved, but also the temperature at which crystallization begins. During cooling, crystallization is an almost discrete event rather than a continuous process. Based on measurements made with a differential scanning calorimeter (DSC), the researchers have shown that crystallization occurs over a very narrow temperature range of around 20°C, starting from a temperature determined by the cooling rate, as shown in Fig. 1.29 [24].

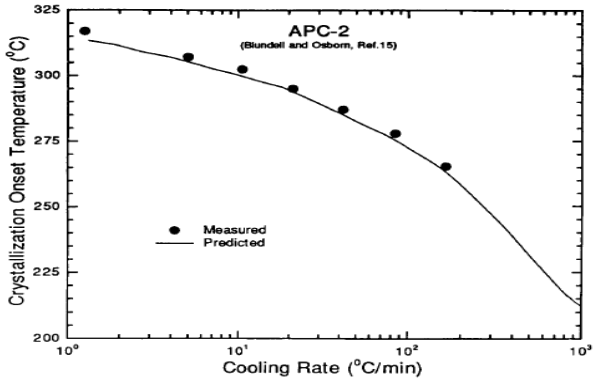

Fig. 1.29: Effect of cooling rate on crystallization onset temperature [24].

Furthermore, in one research, to analyse the residual stresses in graphite/PEEK composites, two different lay-ups of $[0_{40}]_T$ APC-2 unidirectional laminates and $[0_{10}/90_6]_T$ APC-2 non-symmetrical laminate were considered. The induced thermal residual stresses were measured using a shadow and moiré system. A model was also used to accurately estimate the out-of-plane displacement of these laminates. It was found that for unidirectional laminates, the magnitude of the transverse normal stress decreased as the surface cooling rate decreased. Fig. 1.30 and Fig. 1.31 clearly show that by decreasing the surface cooling rate of the $[0_{40}]_T$ APC-2 laminate from 35°C/s to 10°C/s, the magnitude of transverse normal stresses decreases [1].

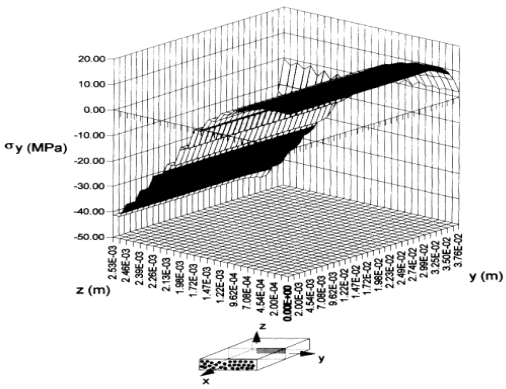

Fig. 1.30: The transverse normal stress (σ_y) distribution in the y-z plane for a $[0_{40}]_T$ APC-2 laminate processed at a surface cooling rate of 35°C/s [1].

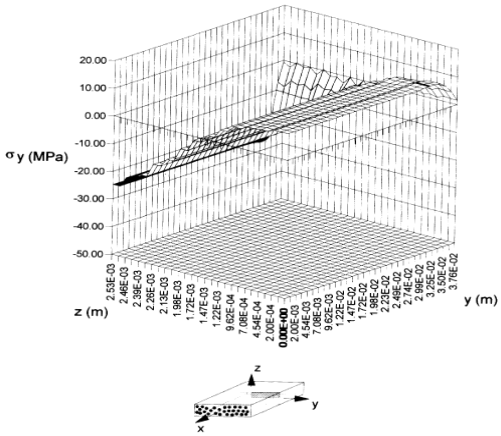

Fig. 1.31: The transverse normal stress (σ_y) distribution in the y-z plane for a $[0_{40}]_T$ APC-2 laminate processed at a 10°C/s surface cooling rate [1].

In addition, Fig. 1.32 and Fig. 1.33 display the distribution of the degree of crystallinity (X_C) for the $[0_{40}]_T$ APC-2 laminate processed at surface cooling rates of 35°C/s and 10°C/s. The comparison of the figures exhibits that as the surface cooling rate decreases, the degree of crystallinity distribution becomes more uniform and the magnitude of crystallinity becomes larger. The more uniform degree of crystallinity distribution decreased the magnitude of residual transverse normal stress for the laminate processed at a 10°C/s surface cooling rate [1].

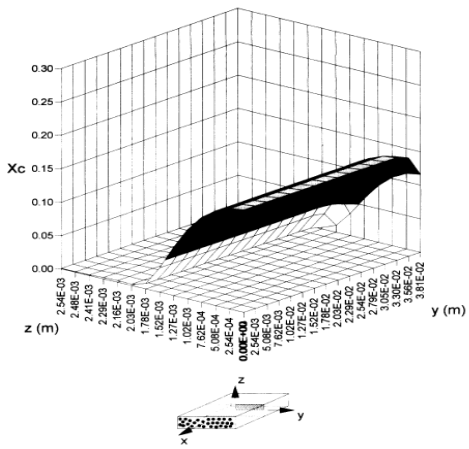

Fig. 1.32: The degree of crystallinity (X_C) distribution in the y-z plane for a $[0_{40}]_T$ APC-2 laminate processed at a 35°C/s surface cooling rate [1].

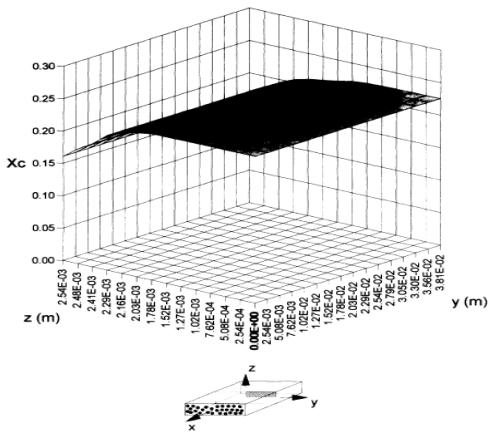

Fig. 1.33: The degree of crystallinity (X_C) distribution in the y-z plane for a $[0_{40}]_T$ APC-2 laminate processed at a 10°C/s surface cooling rate [1].

However, for the non-symmetrical $[0_{10}/90_6]_T$ APC-2 laminates, the magnitude of residual stress and the residual stress distribution for all stress components increased as the processing cooling rate decreased. This is believed to be because of differences in the lay-up and uniformity of the degree of crystallinity [1].

For a 40-ply PEEK/AS-4 thermoplastic composite laminate (APC-2), the effect of the cooling rate on the residual stress level at ambient temperature is shown in Fig. 1.34. As the cooling rate increased, the level of residual stress increased. At a cooling rate of 0.1 °C / s, the distribution of the residual stresses was uniform and essentially negligible throughout the thickness of the laminate. When the cooling rate was increased to 35 °C/s, the model predicted a parabolic residual stress distribution with compressive stresses of about 30 MPa at the surface and tensile stresses of 12 MPa at the center [23].

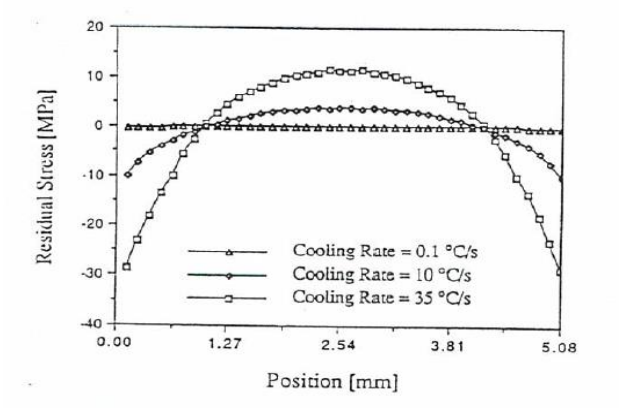

Fig. 1.34: Predicted influence of cooling rate on the transverse residual stress of 40 ply APC-2 unidirectional laminates at constant cooling rates of 0.1 °C/s, 10 °C/s and 35 °C/s [23].

1.4.2.4.2.1. Crystallization Kinetics

The cooling history has a strong influence on the final properties, especially for semi-crystalline polymers. In semicrystalline thermoplastics, the crystallization kinetics is related to the cooling rate, which in turn influences mechanical properties such as stiffness, fracture toughness, and solvent resistance. The crystallization kinetics are important for residual stress prediction because of the influence of the degree of crystallinity on mechanical properties and volumetric shrinkage [23].

1.4.2.5. Elastic properties

Young's modulus of the matrix is one of the physical properties of polymers that influences the formation of residual stresses in composites. Young's modulus is temperature-dependent and semi-crystalline materials are cooling rate dependent. A higher cooling rate generates a lower level of highly elastic crystals, and the resulting Young's modulus will therefore be lower [5].
For the PEEK/AS-4 thermoplastic composites (APC-2) the influence of the cooling rate on the transverse modulus of the resin is illustrated in Fig. 1.35 for a material point on the laminated surface. The surface of a 40-ply unidirectional laminate was assumed to be cooled at 35 °C/s and 10 °C/s. The cooling rate of 35 °C/s gives an amorphous PEEK material on the surface and corresponding lower mechanical properties are observed compared to the material with a higher crystallinity. It is observed that the transverse modulus strongly depends on the cooling rate of the process. It should be noted that the response of the material inside the laminate will be entirely different because the cooling rates vary considerably depending on the thickness [23].

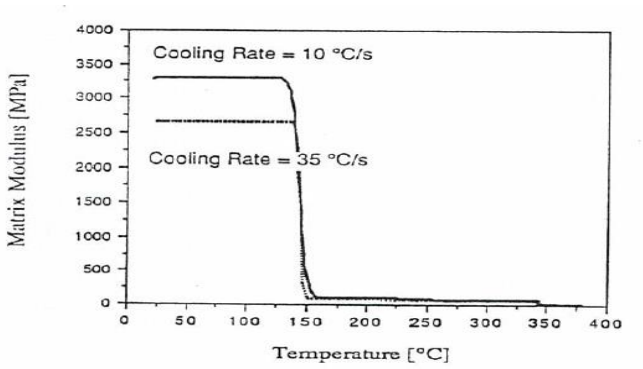

Fig. 1.35: Model prediction of the matrix moduli at the laminate surface as a function of temperature for constant surface cooling rates of 10 °C/s and 35 °C/s [23].

1.4.3. Fiber–matrix interface

The fiber-matrix interface plays a fundamental role in determining the properties of composites, which is why numerous efforts have been made to control the efficiency of the interface. In the case of thermosetting matrices, the degree of fiber-matrix interaction can be enhanced by chemical treatments, such as surface oxidation of carbon and graphite fibers, which modify the reactivity of the fiber surface with respect to the reacting polymer, and/or by the application of adhesion promoter sizings which improve wetting of the fiber surface and the formation of effective bonds. In the case of non-reactive matrices, such as most thermoplastics used in the composites industry, adhesion is mainly the result of physical interactions due to internal stresses between the polymer matrix and the fibers. These physical effects are also present in the case of thermoset matrices when network formation takes place at temperatures above room temperature [27].

In one investigation, residual stresses around fibers in composite systems were estimated on the basis of a linear elastic model that was adapted to take into account the viscoelastic behavior of polymer matrices. The results showed that a considerable effect of processing parameters, i.e., temperatures and cooling rates, on radial stresses at the fiber-matrix interface is to be expected in the case of thermoplastic and thermoset polymers. These residual stresses make a significant contribution to fiber-matrix adhesion as measured experimentally by the micro-fragmentation method. The results showed that in all cases, interface efficiency decreases sharply with decreasing radial stress. However, with thermoset matrices, a certain interface efficiency is maintained even when residual stresses are virtually zero, due to the possible presence of chemical bonds between the polymer matrix and the fiber surface. All the results imply that exposure of the composite to relatively high temperatures over a long period may lead to a

reduction in interface efficiency due to physical and mechanical effects, even if chemical adhesion remains effective [27].

As shown in Section 1.3, the considerable difference in shrinkage behavior between the fiber and matrix will result in longitudinal and radial residual compressive strains in the fiber (Fig. 1.17). Because of the thermal residual strains, fibers are loaded in compression along their length. As a consequence, the tendency of the fibers to buckle grows, and interfacial shear stresses will be produced. This can lead to interface debonding and ultimately microcracking. It is essential to have a strong bond between the matrix and the fiber to prevent this phenomenon [5]. There are treatments to improve the strength of the fiber-matrix bond and they are based on chemical bonding (at the molecular level). Greater fiber-matrix interfacial bond strength by chemical treatment will raise residual stresses because residual stresses can poorly be relieved by interfacial debonding. A weak chemical interface would allow fiber-matrix sliding in the longitudinal direction of the fiber which could lead to partial relieving of stress build-up. This decreases the residual stresses in the fiber and will prevent the fiber from buckling and interfacial debonding. Although this is not very desirable, it will result in a composite with lower mechanical properties. It is shown that for each fiber-matrix system, it is possible to reach an optimum in the fiber-matrix bond strength in relation to the residual stresses [5].

Another effect concerning the fiber-matrix interface is that in semi-crystalline composites, the fiber surface can act as nucleation points for crystalline spherulites. This can result in a trans-crystalline region around the fiber Fig. 1.36. This region has been shown to cause additional radial residual stresses. However, others believed that the trans-crystalline interface relieved residual thermal stresses due to the preferential orientation of the crystallites relative to the fiber. It appears that further research is needed to understand the exact mechanisms of the trans-crystalline layer and its effects on residual stress formation. Consistent with processing effects, the interfacial shear stress was higher for slowly cooled semicrystalline matrix composites due to additional matrix crystallization shrinkage and a thicker trans-crystalline region around the fiber. For amorphous thermoplastics, the interfacial shear stress raises with the cooling rate or lower end temperatures [5]. As research has shown, interface quality plays a considerable role in residual stress build-up. An effective residual stress prediction model must take into account the quality of the interface in addition to the relaxation mechanisms and the variation in matrix properties during the cooling down phase [19].

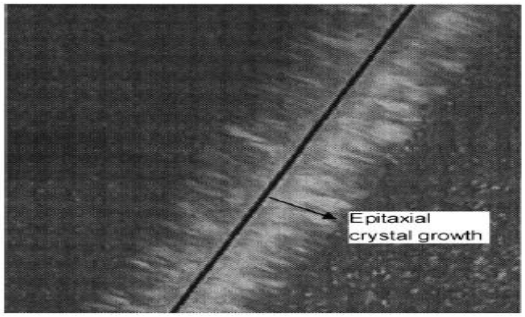

Fig. 1.36: Microstructure of polypropylene sample isothermally crystallised around a carbon fibre followed by quenching [5].

1.4.4. Composite general properties

1.4.4.1. Temperature gradient

The temperature gradient present in the thickness of the laminate, caused by a lower temperature at the surface layer than the inner layers of the composite during the curing of the resin, is another factor in increasing residual stress [5,38,60]. The temperature gradient resulting from the thermal lag and heat release during resin cure can intensify residual stresses and even produce distortions for the flat laminate with symmetrical and balanced layups after demolding [28]. As the thermoplastic resin gradually changes from a molten to a solid state during the cooling process, the time at which solidification begins is not uniform in the thickness direction. This situation gives rise to the so-called "thermal skin-core effect". It is known that the thermal skin-core effect induces a parabolic distribution of residual stress; the surface (inside) region has compressive (tensile) stress, as shown in Fig. 1.37 [29].

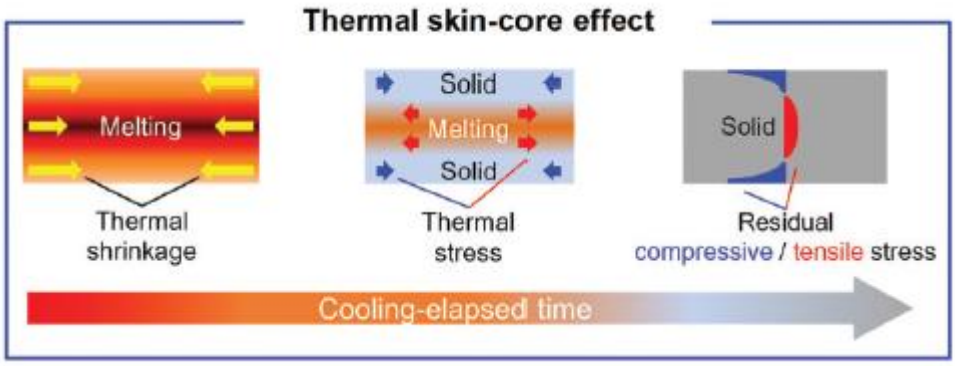

Fig. 1.37: Developments of parabolic residual stress distribution due to thermal skin-core effect; the surface (inside) region has residual compressive (tensile) stress [29].

A typical temperature profile for the surface and center of a 40-ply laminate, which was a PEEK/AS-4 (APC-2) thermoplastic composite, cooled to 35 °C/s in Fig. 1.38 shows that significant gradients are likely to develop during processing. These temperature gradients can lead to distributions in the degree of crystallinity and effective properties of the composite [23].

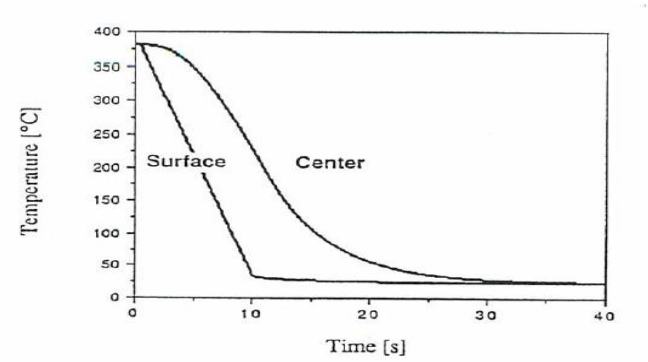

Fig. 1.38: Model prediction of the transient temperature profile for the surface and center of a 40 ply APC-2 unidirectional laminate during constant process cooling t 35 °C/s [23].

In one study, thermostamping, an advanced processing technique for thermoplastic composites, is considered. The composite studied was a carbon-fiber-reinforced polyetheretherketone (PEEK) composite (APC-2). For this study, 0 ° unidirectional 20-ply PSLs (process simulated laminates) were constructed. The study demonstrated that advanced thermostamping processing techniques for thermoplastic composites give rise to considerable skin-core phenomena that are reflected in the morphology, thermomechanical properties and residual stresses of a thermoplastic-reinforced composite laminate. The crystallinity profile of the balanced-cooling laminate was relatively constant, and there was a slight increase in crystallinity in the center of the laminate being attributed to the insulating effect of the surface layers. As can be seen in Fig. 1.39, the degree of crystallinity of the balanced-cooled laminate varies from around 14% by volume at the surface to 18% by volume at the center. The slight increase in crystallinity at the center is attributed to heat transfer considerations due to the insulating effect of the surface layers. The crystallinity distribution for the unbalanced cooled laminate varied from 15% by volume on the faster-cooled surface to 30% by volume on the slower-cooled surface. A significant difference was generated with only a small variation in surface cooling rates. Data for a conventional consolidated laminate processed under identical conditions are represented by the dashed line in Fig. 1.39, which indicates an average value for crystallinity. In addition, uneven stress build-up during the unbalanced cooling resulted in significant macroscopic deformations and stress distributions [30].

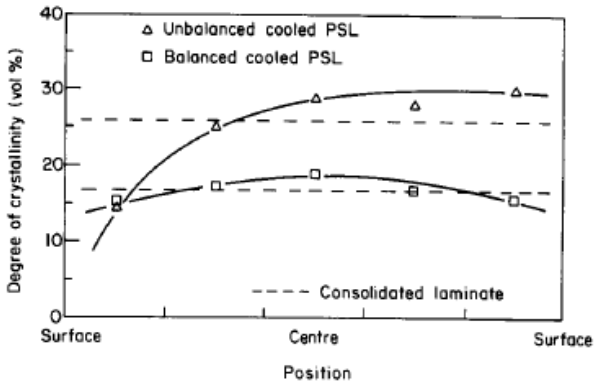

Fig. 1.39: The degree of crystallinity through the thickness of a balanced and unbalanced cooled laminate. The PSLs and consolidated laminates are represented by the solid and dashed lines respectively [30].

1.4.4.2. Laminate thickness

Laminate thickness was found to have a significant effect on the magnitude and gradients of residual stresses. For PEEK/AS-4 (APC-2) thermoplastic composites, the effect of laminate thickness on the residual stress level was studied by varying the number of plies. It was observed that the residual stress level was significantly influenced by the laminate thickness, as shown in Fig. 1.40. The effects of thickness were examined for 10, 20, and 40 plies. As expected, the increase in thickness increased the residual stress level due to the larger gradients observed in thicker laminates [23].

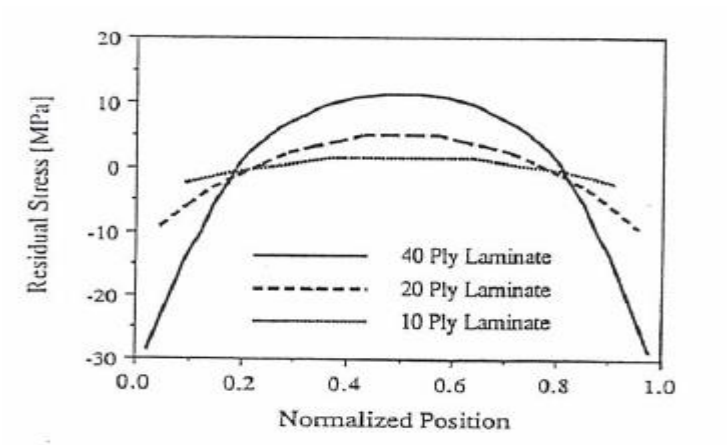

Fig. 1.40: Predicted influence of thickness on the transverse residual stress of constant 35 C/s surface cooled APC-2 unidirectional laminates. The position is normalized for 10, 20, and 40 ply laminates. The mid-plane corresponds to 0.5 on the x-axis [23].

1.5. MACRO-MECHANICAL RESIDUAL STRESS FORMATION

Most of the factors discussed in Section 2 are also responsible for the formation of macro-mechanical residual stresses in an angle-ply composite. The mechanism of this was described in Section 1.2. The parameters that further influence the magnitude of residual stresses in TPCs during lamination are briefly explained in this section. These consist of a lay-up of the laminate and fiber morphology, such as unidirectional prepregs, fabrics, fiber volume fraction, etc. In all cases, the residual fiber stresses were found to be compressive and higher for composites with a higher number of plies. For all levels of thermal residual stresses, the lamination residual stresses also increase as the final temperature moves away from the stress-free temperature [3,5,7,20,21,23,24].

1.5.1. Lay-up of the laminate part

Comparing the residual stresses of unidirectional laminates with those of non-symmetrical laminates, it is evident that the effect of the cooling rate is different for these two types of laminates. As discussed in the cooling rate part, in one research for analysing residual stresses in graphite/PEEK composites two different lay-ups of $[0_{40}]_T$ APC-2 unidirectional laminates and $[0_{10}/90_6]_T$ APC-2 non-symmetrical laminates were manufactured. The model accurately estimated the out-of-plane displacement of these laminates. The optimum processing cycles, which minimize the residual stresses and maximize the mechanical properties of composite materials, were found to be different for different lay-ups. Thus, in order to minimize the residual stresses and optimize the mechanical performance of the composite laminates, an appropriate processing cycle must be chosen for each specific lay-up [1].

In addition, it was found that the optimal processing cycle, which yields the lowest residual stresses and maximizes the mechanical properties of the composite, was different for each lay-up or for varying thickness ratios of 90°-0° plies in polyetheretherketone carbon fiber PEEK/CF and polyetherimide carbon fiber PEI/CF cross-ply laminates. In terms of fiber angles of ω±30°, the interlaminar shear stresses are maximal. It has also been stated that during consolidation, residual strains accumulate at different rates for each lay-up [5].

1.6. ‘‘GLOBAL’’ (SKIN-CORE) RESIDUAL STRESSES

As described earlier the cooling rate plays an important role in the formation of global residual stresses. High-performance thermoplastic composites are manufactured at high temperatures. Consequently, complex and high cooling rates in thick laminates are inevitable. According to Section 1.3, most of the initially induced stresses relax when temperatures are still high, while the stresses induced in the later stages of cooling remain when the matrix is partially crystallized or glassy. As a result, the process leaves the surface regions of a plate in a state of constant compression balanced by internal tension (skin-core thermal effects), see Fig. 1.19 [4,5]. It has been shown that with higher cooling rates, the residual stresses are greater and the distribution is more considerable. Most rapidly cooled or quenched composites, such as PEEK/CF and PET/CF, exhibit a nearly parabolic residual stress profile, with the surface plies subjected to a higher magnitude of compression than the tensile residual stresses in the central plies [5,23]. Annealing is typically performed on thick laminates to decrease skin-core residual stresses through stress relaxation [5,24]. The effects of annealing on residual stresses will be discussed in this section.

1.6.1. Annealing

Annealing can be achieved by increasing the temperature of the composites above the glass transition temperature of the matrix and allowing relaxation processes to occur. Therefore, the stress-free temperature can effectively be changed by annealing. For amorphous systems at the micromechanical ply scale, annealing does not considerably relax residual stresses. However, for semi-crystalline thermoplastics increasing the annealing time below the glass transition temperature (T_g) reduces the residual stresses through relaxation. The crystallinity level will be similar before and after annealing because annealing is performed below T_g. For annealing temperatures above the glass transition temperature and in the crystallization range, annealing will raise the crystallinity level of the (quenched) samples (accompanied by a growth in matrix modulus), and thus the degree of residual stresses due to enhanced shrinkage (crystallization) will also be increased. In other words, Under the effect of annealing, the density and crystallinity increase, resulting in increased shrinkage of the resin from the matrix and thus higher residual stresses. This effect was more Considerable for the surface plies where the microcracks were observed [5,31].

Unger and Hansen experimentally investigated the effect of annealing from the amorphous state on the development of thermal and crystallization residual stresses in graphite fiber-reinforced polyetheretherketone (AP-2) laminates by measuring the radius of curvature developed in non-

symmetrical laminates (0/90). Annealing, or "cold-crystallization" is another way besides the cooling rate by which the crystallinity of APC-2 may be altered. By heating amorphous APC-2 to a temperature above its minimum crystallization temperature (≈155°C) but below its melting temperature of 340°C, the crystalline fraction can be increased. The level of crystallinity thus achieved depends on the annealing temperature reached and the dwell time at this temperature. The dwell time is less important, as the majority of the crystallization process is rapid and occurs within the first few minutes of the annealing cycle. This is particularly true in the temperature range between 180°C and 260°C, where the crystallization rate is rapid and typically lasts from 2 to 20 seconds.

In another section, Unger and Hansen first measured the specimen's room-temperature curvature. The specimens were then placed in an oven preheated to the specified dwell temperature, allowed to reach thermal equilibrium, and then clamped to flatten state. The samples were held in this clamped state for a specified time, then unclamped and cooled to room temperature. Finally, the curvature of the sample was measured again. Six holding temperatures were studied: 25°C, 100°C, 125°C, 150°C, 175°C and 200°C. Fig. 1.41 shows the measured reduction in original curvature at room temperature as a function of both temperature and time. It can be seen that the temperature range where significant changes in curvature occur is narrow and lies in the vicinity of T_g. On either side of T_g, the change in curvature is less than 10% over the range of dwell times investigated. The maximum curvature changes measured, 18.2%, occurs at a test temperature of 125°C after a dwell time of 146 minutes. At first sight, these results seem a little surprising, as stress relaxation effects are generally expected to increase with temperature. Here, a maximum effect occurs near the glass transition temperature, then decreases to a very small effect at a temperature of 200°C. Considering the behavior of both matrix modulus and thermal strains, these results are consistent. The degree of stress relaxation depends on the magnitude of the stresses developed. Since both modulus and thermal strain decrease significantly with increasing temperature above T_g, it follows that those stresses, which are themselves a function of modulus and strain, must also decrease just as rapidly [24].

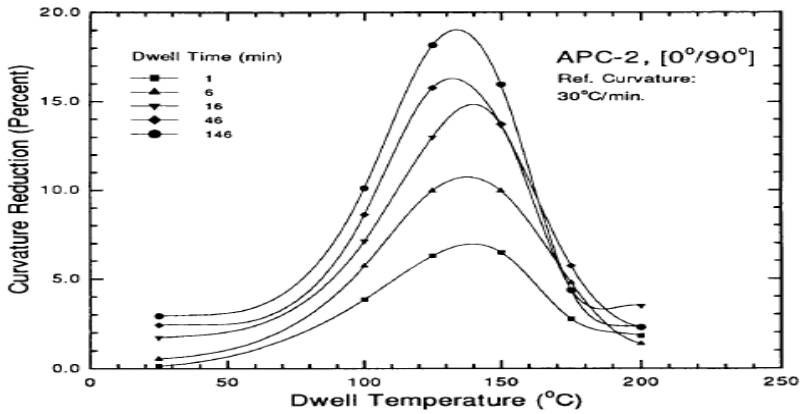

Fig. 1.41: Effect of dwell time and dwell temperature on curvature reduction [24].

1.6.2. Influence of processing mold material

Another processing parameter that affects residual stress formation and has been studied by a few researchers is the use of various mold materials during processing, such as a rubber mold on one half and a metal mold on the other, as in the case of rubber press forming. Two types of interaction between the tools and the composite part can be determined: thermal interaction and mechanical interaction. Both of which can influence the development of stresses in the composite [5]. With respect to the mechanical interaction, it was found that there is a mismatch in CTE between the tool and the composite, and mostly the CTE of the tooling is higher than that of the composite. During cooling, this can induce compressive residual stresses in the surface plies of the composite part at the tool interface, which can result in stress distribution throughout the thickness of the composite part, depending on the condition of the interface between the composite and the tool [5]. eventually, CTE mismatch can lead to laminate warpage or fiber waviness [5,9]. In addition, regarding the friction of the mold with the polymer matrix in the solidified state, it induces additional residual stresses in the surface ply due to forced shrinkage. In some processes, such as rubber forming, a deformable tool is utilized in combination with a rigid tool. The deformation of the deformable tool can be imposed on the composite part, the effectiveness of which is related to the frictional behavior in the contact interface. Because of this, the composite part experiences different loading on the two surfaces, which can lead to global residual stresses [5].

The thermal interaction was distinguished to have a significant influence on the formation and distribution of the global residual stresses (thermal residual stresses between the skin and the core) because of the differences in cooling rates on the two laminate surfaces. This difference comes from the difference in heat transfer properties of the mold materials and thus the cooling

rates. Residual stress profiles for unbalanced cooling rates were modeled, using two mold halves under various cooling conditions, which led to much higher residual stresses in the unidirectional laminate, in comparison with balanced cooling rates [5,30].

One study focused on thermostamping which is an advanced processing technique for thermoplastic composites. In general, these techniques use pre-consolidated laminates that are preheated in an oven, then transferred to a "cold" mold to be formed and solidified, as shown in Fig. 1.42. The composite studied was a carbon fiber-reinforced polyetheretherketone (PEEK) composite (APC-2). For this study, 0 ° unidirectional 20-ply PSLs (process simulated laminates) were fabricated. The transfer from oven to mold, as well as the initial cooling in contact with the mold surface, can result in high and often unbalanced cooling on both sides of the part. These conditions can result in stresses and corresponding morphological features at the macroscopic and/or microscopic levels. For unevenly cooled laminates, a thick silicone rubber membrane was placed on the bottom surface of the mold for insulation. A typical temperature profile for the bottom surface and center of a sample during unbalanced processing is illustrated in Fig. 1.43. The cooling profile has therefore been extrapolated from higher temperatures, as indicated by the dashed line in the figure. The thermostamping process used involves three stages during cooling. The first stage is the cooling of both laminate surfaces in the air during the transfer from oven to mold. The second stage is the initial contact of the bottom of the laminate with the mold surface during the charging of the mold. The final stage involves flow and solidification with the application of pressure by the closing mold. As a result, it has been shown that uneven stress build-up during unbalanced cooling, due to different cooling rates or cooling time lag between surfaces, induces significant macroscopic deformations and stress distributions. This effect should be more significant in complex laminates. This has been observed with curvature measurements for both balanced and unbalanced cooled laminates after demolding [30].

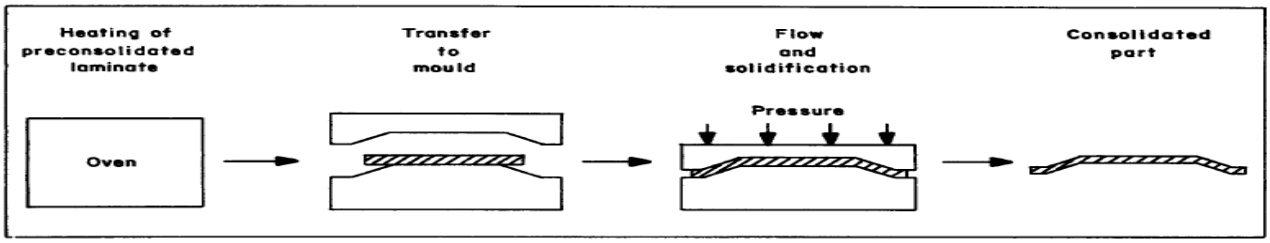

Fig. 1.42: The basic steps of a thermostamping process [30].

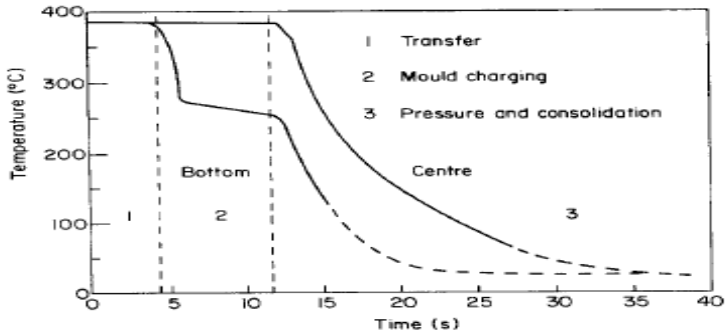

Fig. 1.43: Typical cooling profile for the surface (bottom) and centre of an unbalanced cooled 20-ply PSL showing three distinct steps during thermostamping [30].

Another experimental study was carried out on the effect of the curing cycle on the evolution of material properties, residual strains, and stresses of asymmetrical cross-ply laminates that were manufactured by the curing cycle with a peak curing temperature of 160°C. According to the cure kinetic model, full polymerization was achieved at this temperature in 10 min. Fig. 1.44 shows the strain measurements for this cure cycle. During the heating phase, the resistance strain gauge readings were almost identical to the mold strains. This means that the composite structure was fully constrained in both directions. The coefficient of thermal expansion (CTE) of the mold during the heat-up phase was 23.5 με/°C, a typical value for aluminum. This result shows that hot press clamping did not affect the mold's thermal expansion. As the temperature approached the peak curing temperature, the transverse strain (90°) increased more than the longitudinal strain (0°). During cooling, longitudinal and transverse strain rates differed. When the laminate was demolded at room temperature, sudden changes in strain were observed due to the release of stress from the mold structure. The results show that the composite laminate was under tension in the transverse direction and compression in the longitudinal direction during the cooling phase [32].

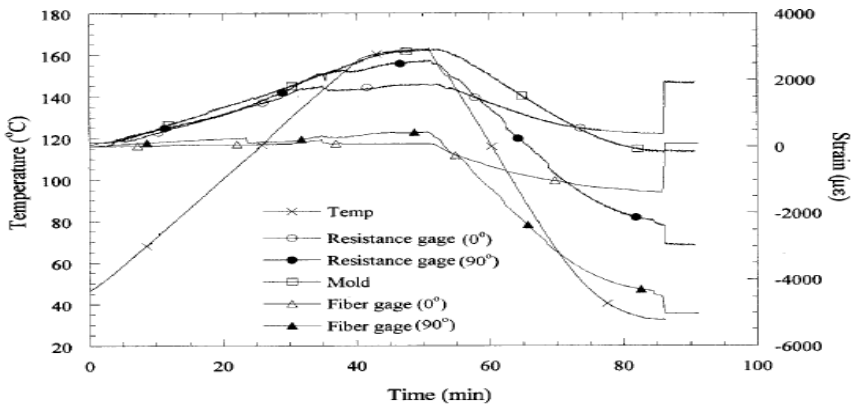

Fig. 1.44: Strain measurements during cure of unidirectional laminate by cure cycle with a peak curing temperature of 160°C [32].

1.7. PARAMETERS GOVERNING RESIDUAL STRESSES

Diagram of all the parameters identified in this project that govern residual stresses.

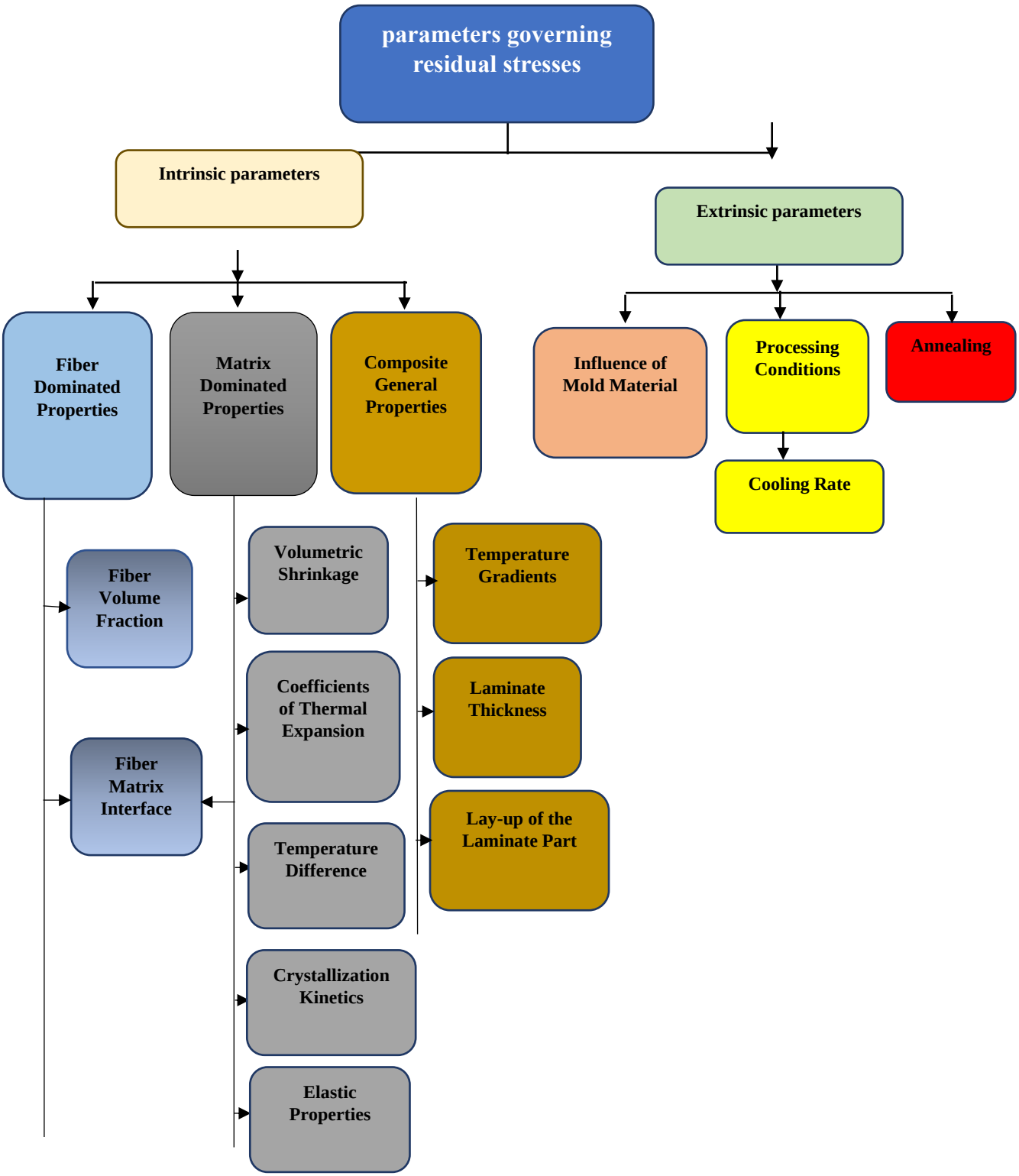

THIS PAGE WAS INTENTIONALLY LEFT BLANK

2.1. INTRODUCTION

As residual stresses are naturally present in almost all composite materials and remarkably influence the properties of composite structures, it is important to consider the thermal residual stresses in the design and analytical modelling of composite structures [3,8,33]. The models of thermal residual stresses and strains in composite materials must be verified and validated with experimental results. Thus, we require experimental techniques for the determination of thermal residual stresses. This review concentrates on experimental techniques that are applicable to continuous fiber-reinforced thermoplastic composites (TPCs), although they are recently applied to the thermoset composites or other materials. These techniques estimate the magnitude of thermal residual stresses at the three levels of residual stress origins, namely: the micromechanical level, the macro-mechanical level, and the global laminate level. These three levels were explained in the section 1.2. As we mentioned in part one, these three levels will be mentioned as intralaminar stresses, interlaminar stresses, and laminate stresses, respectively [33]. First, techniques using the intrinsic properties of the composites' constituent materials will be determined, followed by techniques using embedded "foreign" stress sensors. Afterward, techniques based on in-plane and out-of-plane deformations and also destructive techniques will be described. Subsequently, there will be a brief description of the techniques used to define the material properties required to calculate the residual stresses, such as the fiber modulus, the coefficient of thermal expansion of the laminate, etc. Additionally, stress-free temperature (the temperature at which stresses begin to build up) is the most important property to determine, and experimental techniques for its determination will also be discussed. Finally, the determination of the relaxation behavior will be expressed.

2.2 TECHNIQUES UTILISING INTRINSIC MATERIAL PROPERTIES OF THE COMPOSITES' CONSTITUENTS

Some material properties alter when exposed to strains or stresses, such as the electrical resistance of the metal wiring of a strain gauge [33]. This section illustrates experimental techniques to detect the change in the properties of the materials caused by thermal residual stresses in one of the components of the composite. These include changing the refraction of light, changing the position of the Raman peak of the crystalline phase, and changing the electrical conductivity. Applications so far include

only intraply and interply residual stresses that are at the micromechanical and macro-mechanical levels.

2.2.1. Photo-elasticity

Photo-elasticity is a classical optical technique for static stress analysis. To determine the stress fields in composites, a transparent or translucent matrix is needed. As a result, this method has been applied to transparent thermoset matrix composites and amorphous thermoplastic matrices [33]. In amorphous polymers, stress changes the molecular orientation distribution, and this influences the polarization and phases of light (photoelasticity) passing through the stressed material, in other words, stress causes anisotropic scattering of light, and intensity measurements provide orientation information [33,34]. To determine the magnitude of the residual stresses, measurement of retardation (phase difference between two light vectors moving at different speeds) must be measured, from which the constituents of the residual stresses can be calculated using the stress-optic law (or "Brewster's law"). Photo-elasticity can be utilized to distinguish the thermal residual stress distribution in the matrix when a unidirectional sample with fibers in the 0° direction is rotated between crossed polarizers. The maximum extinctions are found at 0° and 90°, indicating that the main stress directions are parallel and perpendicular to the fiber direction. One disadvantage of this method is that thin composite layers with low fiber volume fractions (i.e., <40%) are needed to detect the effects in the matrix [33].

In one study, Pawlak et al used the photoelastic method to investigate residual stresses in thermoset matrices. Changes in optical properties around inclusions were studied using the three-dimensional photoelastic method (Fig. 2.45). The micropolariscope based on a polarizing microscope was equipped with a sensitive CCD camera, frame grabber card, and a PC computer. A typical integrated photoelastic image of a short glass fiber embedded in DGEBA/amine epoxy resin is shown in Fig. 2.46. The maps of the characteristic directions and retardation clearly show that stresses are concentrated near the ends of the fiber. Much lower stresses were observed in the matrix along the fiber, away from the fiber ends. Their distance of influence (AB direction in Fig. 2.46) was around 70 μm from the fiber surface [35].

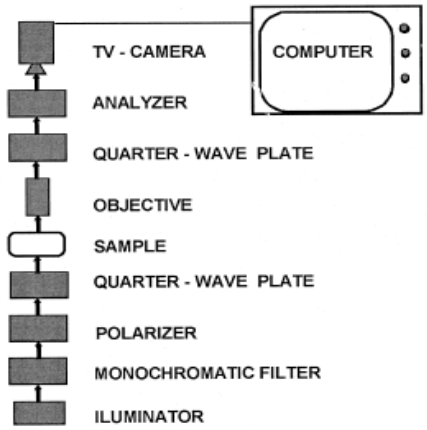

Fig. 2.45: Schematic representation of the automated micropolariscope [35].

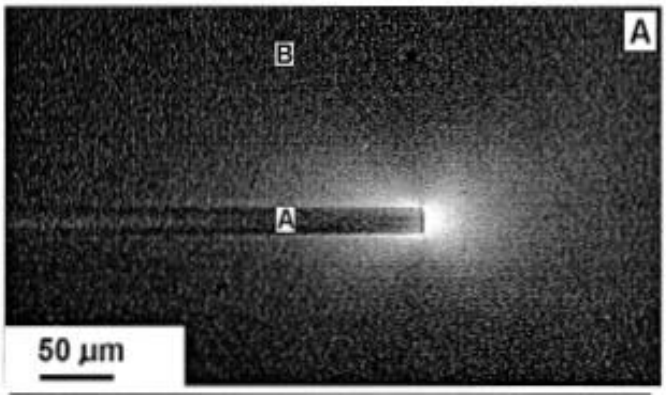

Fig. 2.46: The photoelastic image of residual stresses present in the epoxy matrix around a glass fiber: DGEBA/amine sample after curing [35].

2.2.2. Micro-Raman spectroscopy

Micro (laser) Raman spectroscopy is another technique for determining residual strain based on an intrinsic material property. This technique is on the basis of the stress (strain) sensitivity of most Raman vibrational modes in crystalline phases [33,34]. The energy difference between the incident photon and the Raman scattered photon is equal to the vibrational energy of the scattering molecule. The graphical representation of the intensity of the scattered light as a function of the energy difference is a Raman spectrum. Raman spectroscopy is a recognized technique for measuring the strain state of carbon fibers embedded in a translucent polymer matrix, as certain peak positions in the Raman spectrum of the fiber alter with applied strain. Furthermore, carbon fibers can be considered as in situ or intrinsic strain sensors when using Raman spectroscopy for the determination of the residual stress in carbon fiber reinforced composites. The Raman peaks of the fiber in, for instance, an unloaded polyetheretherketone (PEEK) prepreg display a shift to higher peak positions. This demonstrates the compressive fiber strain because of the thermal residual strains imposed by the surrounding matrix. First of all, a calibration curve on pure single fibers in the air must be established to relate the (change in the) position of the Raman peak to the magnitude of the residual thermal strain of the fiber in the composite [33].

In one study, Nilsen and Pyrz used polarized Raman microscopy to measure the local stress state in amorphous polymers. This work showed that strain in amorphous polymers can be measured by polarized Raman microscopy. In amorphous materials, strain affects molecular orientation. The method has also made it possible to measure interfacial shear stress distribution in a high-modulus carbon-polycarbonate single-fiber composite. The results were compared with the indirect assessment

of interfacial shear stress from fiber strain measurements. The indirect measurement of interfacial shear stress illustrated that the maximum interfacial shear stress of the fiber was 33 MPa, which is close to the 36 MPa of the matrix Fig. 2.47. As a result, yielding has taken place [34].

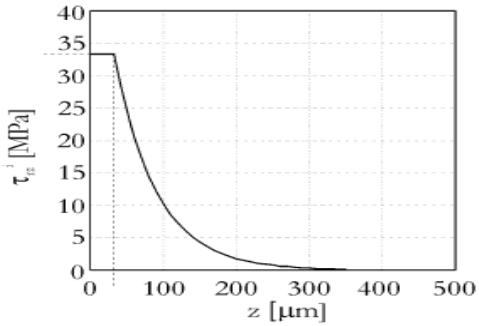

Fig. 2.47: Thermal stress distribution in fibre (room temperature) for HM-PC system: interfacial shear stress [34].

There are some problems related to the Raman spectroscopy technique. For example, one drawback of the Raman spectrum technique is that the Raman spectra are obtained from the surface of the laminate and fiber, and there may be differences in the behavior of the skin and core of the fiber and laminate under deformation. To solve this problem, remote laser Raman spectroscopy has been developed. It contains an optical fiber embedded into the mass of the composite, through which the excited laser light is transported. Another issue is that some amorphous fibers, such as glass fibers, have a very weak Raman response and, therefore, cannot be used as intrinsic stress/strain sensors. The solution is that a small number of aramid fibers, which represent very strong Raman responses since they are crystalline, can be placed in glass fiber-reinforced laminates to be as strain Raman sensors. These embedded aramid fibers act as Raman strain sensors in glass fiber reinforced composites [33].

Regarding the advantages of the micro (laser) Raman spectroscopy method, the residual stresses can be measured in steps as small as 1–2 μm, and analytical models are not required to predict the macroscopic residual stresses of the laminate. It should be noted that the contribution of the matrix peaks is considered, otherwise, it would give a too-high value of the residual stresses in the fiber [33,34].

2.2.3. Electrical conductivity of carbon fiber reinforcement

As carbon fibers are much more conductive than the polymer matrix, electrical behavior provides much information about the microstructure, such as the degree of fiber alignment, the number of

fiber-fiber contacts, the amount of delamination, and the extent of fiber breakage. This information is not only useful for the scientific understanding of the composite's properties, but it is also valuable for giving the composite the ability to detect its strain, damage, and temperature in real-time through electrical measurements. In other words, the strain, damage, and temperature affect the electrical behavior, such as electrical resistance, which therefore serves to indicate strain, damage, and temperature. In this way, the composite is self-sensing, i.e., intrinsically intelligent, without the need for attached or embedded sensors (such as optical fibers, acoustic sensors, and piezoelectric sensors), which increases cost, reduces durability and, in the case of embedded sensors, weakens the structure [33,36].

2.3. RESIDUAL STRAIN DETERMINATION BY MEANS OF EXTRINSIC (FOREIGN) EMBEDDED STRAIN SENSORS

In order to improve the curing process, increase product quality, and, above all, provide a repeatable product, smart sensors are used and are embedded into the composite to monitor the curing behavior of the composite and provide information on changes in physical properties. This information provides a better understanding of the relationship between composite constituents, processing, properties, and performance, and offers the possibility of controlling certain undesirable anomalies such as the release of volatiles which will lead to improved product quality [37]. An example has already been expressed in the previous section: aramid fibers embedded as Raman strain sensors in glass fiber reinforced composites. The sensors can be of any material or shape and the sensors currently in use are the following [33]:

1. Strain gauges.
2. Fiber optic sensors (FOS).
3. Embedded metallic particles in combination with X-ray diffraction.

These sensors present a measurable change in their properties when exposed to (residual thermal) stress. An explanation of the different sensors and techniques will be given in the next sections.

2.3.1. Embedded strain gauges

In one study researchers used strain gauges to directly measure the evolution of residual strain resulting from thermal and crystallization effects in PEEK/CF unidirectional laminates. A strain gauge was melt-embedded into the center of the surface plies for a short melting time, as strain gauges

that are highly resistant to high processing temperatures are not available [33]. In a research Crato et al. employed embedded strain gauges to monitor, in situ, the buildup of residual strains in carbon fiber-reinforced laminates during cure. The composites studied in this study were 16-ply AS4/3501-6 unidirectional lay-ups. Composites measuring 15.2 cm x 15.2 cm were laid down and strain gages were glued to the surface folds and/or embedded in the mid-plane. In all cases, the strain gauge element was located at least 1.3 cm from a free edge. Although the strain gauge itself is encapsulated. The prepreg stack was then vacuum-bagged and the composite was cured in an autoclave, using the set-up described in the sketch in Fig. 2.48. Using a gauge from the same production batch, the deformation resulted solely from the cure of the composite. Once the cure was complete, the same embedded gauges were used to measure the CTE of the composite between ambient and cure temperatures [6].

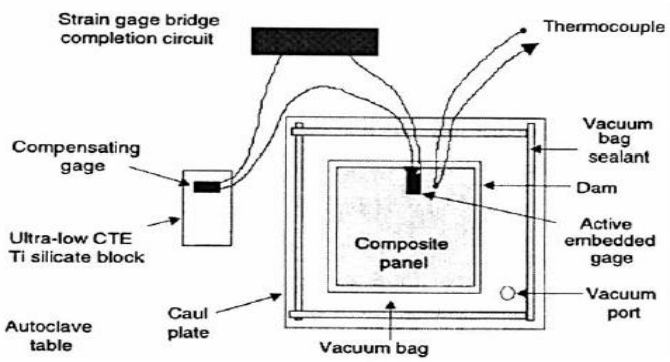

Fig. 2.48: Sketch of the experimental setup to measure the buildup of residual strains during composite cure in an autoclave [6].

2.3.2. Embedded fiber optic sensors

Recent studies show that fiber optic sensors (FOS) can be utilized as internal “strain gauges” to monitor the development of residual thermal stresses within a composite laminate, even during processing at the high temperatures required for thermoplastic composites. There are a number of fiber optic sensors, among which Fiber Bragg Grating (FBG) and extrinsic Fabry-Perot interferometric (EFPI) sensors have been most commonly used to track residual stress formation [33]. An EFPI sensor measures the strain by changing the length of the cavity, which is related to a phase change between the input and output signals and the reflection of the optical fibers Fig. 2.49. There are some drawbacks regarding the usage of the EFPI sensor. First of all, in the EFPI sensor, a cavity is included in the laminate and the diameter of the sensor is quite large, which can lead to stress concentrations. Moreover, the EFPI sensor was found to be vulnerable to failure due to residual

thermal stresses alone. It was also found that EFPI optical fibers did not measure any strain until the matrix was solidified [33].

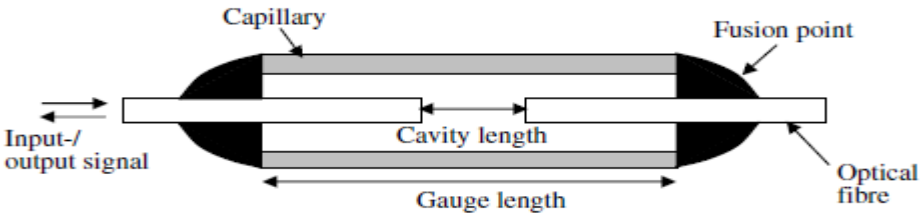

Fig. 2.49: Schematic view of EFPI sensor [33].

Regarding FBG sensors, the latest publications display a clear trend toward the application of FBG sensors, as they show great promise for monitoring the evolution of residual strain during treatment, due to their small diameter and accuracy. The principle of operation of FBG sensors is schematically shown in Fig. 2.50. The response to strain and temperature variations is characterized by a change in the Bragg wavelength λ.

FBG sensors are created by modulating the refractive index along the length of the core of an optical fiber. When illuminated by a broadband source, they strongly reflect light at the Bragg wavelength according to $\lambda_b = 2n_0\Lambda$, where λ_b is the Bragg wavelength, n_0 is the effective index of refraction and Λ the period of variation of the refractive index of the FBG (the grating period) [16,33].

The reflection spectra of optical sensors can be divided into one or two peaks. In the case of one peak, the transverse strains are equal in fibers with low birefringence ($\varepsilon_x = \varepsilon_y$), representing a single shift in Bragg wavelength. This is the case most often considered in sensor applications and is shown in Fig. 2.51. In terms of two peaks, there are unequal transverse strains. These strains deform the sensor so that its cross-section becomes non-circular (elliptical if the strains are symmetric), and birefringence is induced in the fiber. This causes the light to follow either the fast or slow axis, making the sensor response polarization dependent. For each polarization axis, a different wavelength will be reflected. If the polarized light is sent separately along each of the polarization axes, two distinct peaks can be distinguished (Fig. 2.52); however, if the light is sent along an arbitrary path, the resulting wavelength spectrum will be a mixture of the light reflected along both axes [16,33].

Wavelength changes can be used to determine thermal residual stresses with relationships based on photoelastic constants and the effective refractive index of the optical fiber [16,33]. The usage of integrated fiber optic sensors when integrated parallel to the reinforcing fibers has the advantage of minimal disturbance to the sensors. However, when a FOS is embedded perpendicular to the fiber direction, it results in an eye-shaped defect that causes high-stress concentration and decreased mechanical properties [33].

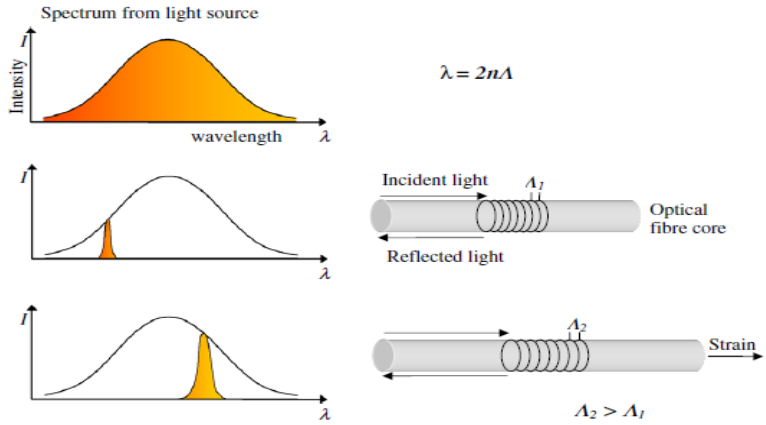

Fig. 2.50: FBG response as a function of strain [33].

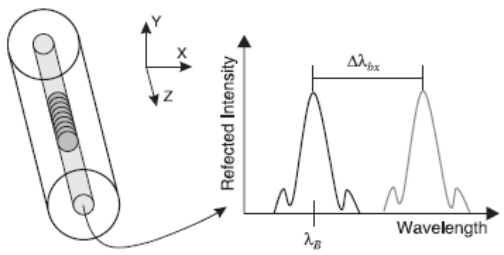

Fig. 2.51: Wavelength response of a uniform FBG to the application of a homogeneous strain field [16].

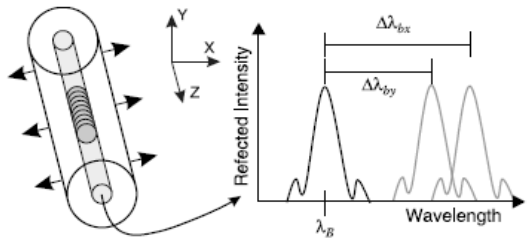

Fig. 2.52: Influence of unequal transverse strains on the spectral response of an FBG [16].

In one study, five different sensors are used to monitor the process parameters of a carbon-phenolic composite during cure: microelectric, ultrasonic, thermopile, thermocouple, and Extrinsic Fabry-Perot Interferometer (EFPI) sensors. Microelectric sensors are used to monitor changes in resin properties such as viscosity, permeability, and loss factor. Ultrasonic sensors are used to measure changes in stiffness and the development of porosity in the composite. Thermopiles and thermocouples are used to monitor temperature variations and reaction rate heat. EFPI's optical sensors are used to monitor local strain changes caused by temperature, pressure, or process-induced residual stresses. In addition to this optical measuring device, a modified EFPI thermal sensor is employed in this research to monitor temperature variation in laminates [37].

Another study has quantitatively clarified the mechanism of the skin-core thermal effect and identified the amount of residual stress/strain using fiber-optic-based internal strain measurement and process simulation. Firstly, the in-plane transverse strain of thin carbon fiber/polyphenylene sulfide laminates were measured using Bragg grating sensors, then Abaqus-based simulations were carried

out to calculate the stress/strain distribution in thick laminates. The transverse strain history under solidification temperature (Ts) is shown in Fig. 2.53. Intermediate shrinkage strain was measured by the middle-tail FBG sensor as expected, and the results of the finite element analysis (FEA) agree well with the experimental results; it was confirmed that residual stress developed over a relatively low-temperature range [29].

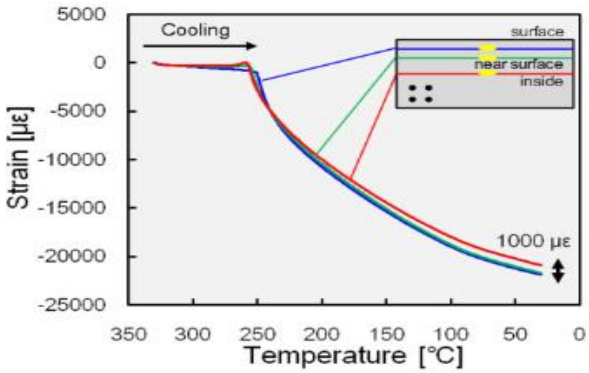

Fig. 2.53: Transverse strain histories measured by middle-tail FBG sensor [29].

2.3.3. Embedded metallic particles

The embedded metallic particles technique is one of the "embedded sensor" techniques that use X-ray diffraction on inclusions of metal particles in the matrix (also called "tracer") and thus measures their deformation imposed by residual strains in the polymer matrix [33]. X-ray diffraction is a powerful tool for studying interlaminar stresses in fiber-reinforced composites. Structural and as mentioned residual stresses in the material can be assessed by measuring the strain in embedded particles using X-ray diffraction. The measured state of strain in the detection particles is composed of the initial strain due to the manufacturing process and the structural strain due to the global traction applied to the composite sample. The relationship between the strain in the particles and the stress in the material is referred to as the X-ray elastic constants.

X-ray diffraction is a widely used method for the non-destructive analysis of the structure and residual stresses of polycrystalline materials. The method is based on determining the lattice space from the interference maximum of an X-ray beam. For an X-ray wavelength λ, the d_{hkl} lattice space of the (hkl) planes is calculated from the Bragg angle Θ_{hkl} of the diffraction spectrum using Bragg's law [38]:

$$\lambda = 2d_{hkl}sin(\Theta_{hkl}) \tag{2.1}$$

Embedded aluminium, copper, and silver particles exhibit a peak angle deflection when embedded in a composite. According to Bragg's law, this deflection is related to a change in the crystal lattice spacing induced by residual strain. The highest accuracy was for the regular-shaped aluminium particles. The metal must be chosen carefully because it should not fail when exposed to the residual thermal stresses of the composite. This type of experiment has been widely performed on thermoset matrix materials. However, thermosets need crystalline fillers because they do not have a crystal structure that changes in response to X-rays when exposed to stress. In the case of semi-crystalline thermoplastics, the lattice spacing between the crystals and the change in that place due to strain can be tracked by means of X-ray diffraction [33].

This method measures the complete three-dimensional stress state inside composite materials, unlike the classical strain gauge technique which is limited to the surface of the material. The separation of the state of stress into residual and structural stress provides an accurate way to study both the residual stress due to the manufacturing process and structural stress due to external loading [38].

2.4. EXPERIMENTAL TECHNIQUES BASED ON IN-PLANE AND OUT-OF-PLANE DEFORMATIONS

This section is a brief review and summary of works on experimental techniques for measuring residual stresses based on in-plane and out-of-plane deformations.

2.4.1. Interferometry based methods

There are a number of methods that use the phenomenon of interference of light waves reflected from a sample. This interference causes a visual fringe pattern that can be utilized to define deformations [33]. Some of these interference-based methods that are used to determine residual stress formation in composites will be explained here.

The Moire´ effect is one of the methods based on interferometry [33]. Moiré interferometry and microscopic moiré interferometry application (mainly for assessing thermal strains, but also for mechanical loading and material characterization) is introduced at the design and development, evaluation, and process control stages. The applications for the study of composite materials and components are numerous and growing but do not yet rival their use in the electronic packaging sector [39]. Moire´ effect is a well-known optical effect that is based on an interference pattern that develops when light passes through two gratings rotated at a small angle to each other. When one of the gratings

changes because of the deformation of the sample, the resulting interference pattern (Moire') will also change [33].

Moiré interferometry can be utilized to monitor in-plane and out-of-plane displacements. For in-plane measurements, a grating must be applied to the surface of the sample under study. To measure out-of-plane displacements, it is not necessary to apply a grid to the surface. The grating can be projected onto the surface at an angle to the direction of observation [33]. Moiré interferometry measures in-plane displacements with very high sensitivity. Data are received in the form of interference fringe patterns or contour maps of the displacement fields. Due to the high sensitivity and abundance of the data, reliable strain distributions (normal and shear strains) can be extracted from the patterns. The method differs from classical interferometry and holographic interferometry, which are most effective for measuring out-of-plane displacements [39].

2.4.2. Warpage of non-symmetric laminates

Common evidence of residual stresses is warping in structurally non-symmetrical laminates [9,33]. Therefore, the simplest way to assess the magnitude of residual stresses is to use non-symmetrical cross-ply or angle-ply laminates. This is because residual stresses can be partially relieved by out-of-plane deformations [8,19,33]. This is proved that this method is applicable to composites with any matrix. The out-of-plane deformations of an angle-ply or cross-ply laminate can be monitored during or after cooling from the processing temperature. The higher the curvature for a laminate of a certain thickness, the higher the residual stresses. A non-symmetrical laminate deforms under the effect of residual stresses occurring in the individual plies [33].

Curvature measurements can be performed with several methods and here we will discuss some of these techniques.

As part of an investigation to measure the curvatures of specimens at room temperature and their variations with temperature, the researcher used a curvature measurement system shown in Fig. 2.54. Six specimens were placed in a drying and heating oven. They were held on a metallic bar in the Binder using fold-back clips, as shown in Fig. 2.18, with their lateral side sections facing a digital camera under ambient room light. The fold-back clips are used to avoid the impact of gravity and friction on the evolution of curvature, which could have a significant impact if the samples were simply placed on a horizontal plate. This makes it possible to determine the curvature of the strips by analysing the images taken by the camera. The first series of measurements were carried out on laminates [($90_3/0_3$)] in the case of $T_{mandrel}$ = 25°C. Two heating and cooling cycles were applied with the following maximum temperatures: 120 and 150. After cooling from 120 °C, two out of six

samples were reheated to 150°C. The evolution of their curvature with temperature is shown in Fig. 2.55. It is evident that the curvature of the specimen decreases with reheating [13].

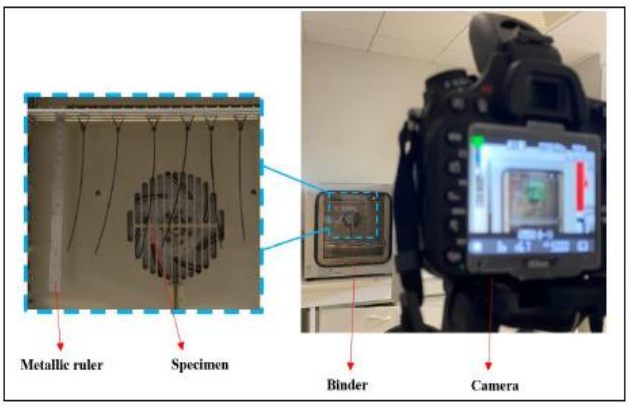

Fig. 2.54: Curvature measurement experimental setup [13].

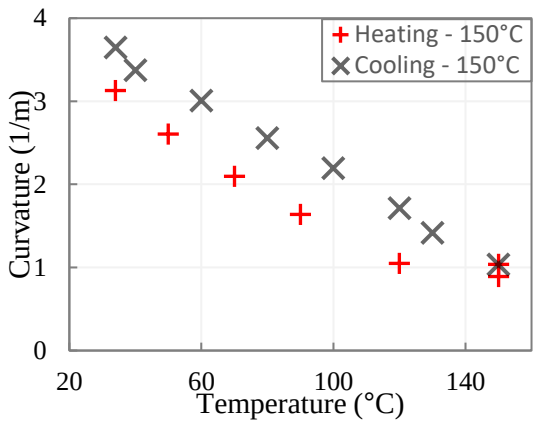

Fig. 2.55: Evolution of the curvature with temperature for unsymmetrical $[90_3/0_3]$ laminates fabricated using the un-heated mandrel during heating and cooling from 150°C [13].

To measure curvature, let's first consider a non-symmetrical laminate [Fig. 2.56(a)]. Significant contraction in the transverse direction results in curvature of the laminate due to out-of-plane coupling forces. The curvatures are produced simultaneously in both main directions and the resulting shape of the laminate is an anticlastic saddle [Fig. 2.56(b)] [40].

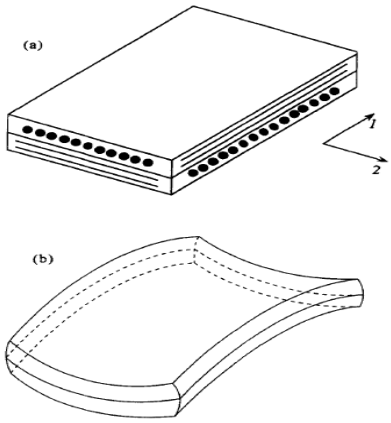

Fig. 2.56: (a) Unsymmetrical cross-ply laminate; (b) saddle-shaped distortion of unsymmetrical laminate [40].

At a certain temperature, the residual stress that would exist perpendicular to the fibers in a similar symmetric cross-ply laminate σ_{22}, is estimated from the curvature using equation (2.2), based on the linear lamination theory [18,33,40]:

$$\sigma_{22} = \frac{(E_{11} \times E_{22})}{(E_{11} + E_{22})} . \frac{t}{\rho} . \left(\frac{1}{2} + \frac{1}{24}\left(2 + \frac{E_{11}}{E_{12}} + \frac{E_{22}}{E_{21}}\right)\right) \tag{2.2}$$

where t is the thickness of the strip and ρ is the radius of curvature, E_{11} and E_{22} are the moduli of the ply in the longitudinal and transverse directions, respectively. The total thickness of the 0° ply is equal to the total thickness of the total 90° ply in this equation. The thickness of the longitudinal and transverse plies must be equal in other words the total thickness of the 0° ply should be equal to the total thickness of the total 90° ply in this equation. If not, the following equation can be used [33,40]:

$$\sigma_{22} = \frac{(E_{11} \times E_{22})h}{(E_{11}h + E_{22}k)} . \left(\frac{b+d}{2\rho} + \frac{E_{11}b^3 + E_{22}d^3}{6\rho(b+d)}\left(\frac{1}{E_{11}b} + \frac{1}{E_{22}d}\right)\right) \tag{2.3}$$

The thicknesses of the longitudinal and transverse plies in the unsymmetrical laminate are defined as b and d, respectively, while h and k are the corresponding ply thicknesses in the symmetrical lay-up. As a first approximation, instead of using the above equation, the maximum residual stress can be calculated from the cross-ply curvature using a linear elastic relationship [30,33]:

$$\sigma_{max} = E . \kappa . \frac{t}{2} \tag{2.4}$$

where

σ_{max} = maximum stress at the surface

E = modulus of the composite in the 90 ° direction

t = thickness of the composite; and

κ = curvature equal to ρ^{-1}.

Another approach is to compare the obtained curvatures with curvature predictions based on classical lamination theory (CLT) [8,33]. When the theory can accurately predict the curvatures, it can be assumed that the calculated residual stresses are also accurate and that the appropriate thermoelastic properties have been used. The curvature can also be predicted using a model similar to equations (2.2) and (2.3), where ΔT represents the temperature difference between the stress-free temperature and the operating temperature, and the coefficients of thermal expansion in the longitudinal and transverse directions of the fiber are α_{11} and α_{22}, respectively [33]:

$$(\alpha_{22} - \alpha_{11})\Delta T = \frac{b+d}{2\rho} + \frac{E_{11}b^3 + E_{22}d^3}{6\rho(b+d)}\left(\frac{1}{E_{11}b} + \frac{1}{E_{22}d}\right) \tag{2.5}$$

Only a few dimensions have been shown to follow CLT predictions, and it has been concluded that the thickness-to-length ratio and width-to-length ratio determine the final shape of the laminate at

room temperature [33]. When the researcher was verifying his predictions on the curvature of non-symmetric laminates, found that the cured shapes of thin non-symmetric laminates do not conform to the predictions of classical lamination theory (CLT), which was later confirmed [33,41]. However, it was proved that the shapes of thicker laminate conform to the predictions of the classical theory. Instead of forming saddle shapes as expected in CLT, it has been shown that the thin, non-symmetrical laminates form part of a cylinder during curing [33,42]. The solution for relatively thin laminates of intermediate size undergoes bifurcation, which means that for a laminate of a certain side length, called the bifurcation point, the saddle-shaped solution becomes unstable and turns into one of two possible stable cylindrical formations [33,40].

One disadvantage of the curvature method is that curvature values can show large changes for equal laminates under similar conditions [33]. This can be explained by a multitude of reasons, such as limitations in the accuracy of curvature measurement, fiber alignment, ply disorientation, and non-symmetry of ply thickness [33,43]. In addition, in the curvature method it is not possible to obtain information about the (global) stress distribution through the thickness of the laminate, nor is it possible to obtain information about symmetric laminates, since they are flat [33].

Curvature measurements can be made in several ways as explained above, the most common technique is to cut the laminate into thin strips and measure the deflection at the center of the sample. here h is the height of the deflection in the center of the sample and 2L is the total length of the specimen, see Fig. 2.57 [33,40,43].

From the deflection measurements, curvature was calculated using the following expression, with positive or + referring to deflection in the positive z-direction and negative or - referring to deflection in the negative z-direction. Thus, the radius of the curvature can then be calculated as [30,33]:

$$\kappa = \frac{8h}{L^2 + 4h^2} \tag{2.6}$$

where

κ = curvature (m^{-1});

h = deflection (m); and

L = length of the sample measured (distance between support pins).

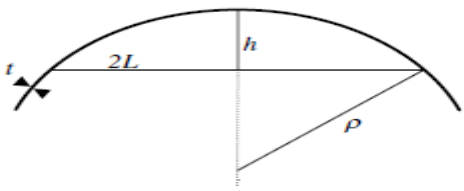

Fig. 2.57: Measurement of radius of curvature, after [33].

Some measurements which were used for measuring the deflection of the strip include a traveling microscope, measuring microscope, cathetometer, or dial micrometer fixed between two pins. The length of the specimen was measured with a (steel) ruler. Curvature measurements can also be made from digital scans or curvature plots on a sheet of paper, as well as from photographs taken from the side of the deformed laminate. In addition, it is necessary to ensure that no anomalies, such as fiber flow or ridges, are present in the laminates. Hence, curvature measurements were performed after the sides were trimmed to remove material from affected edges [33].

As mentioned above, numerous studies have been carried out to validate predictive models of residual/thermal stresses in thermoplastic and thermoset matrix composites. The methodology involves measuring the curvatures of unsymmetric cross-ply laminates and comparing them with model predictions for this laminate. A panel with an unsymmetric cross-ply stacking sequence takes on either a cylindrical or saddle shape at room temperature, depending on the ratio of its thickness and its in-plane dimensions. If one dimension of the panel is dominant (strip), only one curvature is measurable [19].

A study has shown that the simplest and most widespread model is to determine the strains $(\varepsilon_x^o, \varepsilon_y^o, \varepsilon_{xy}^o)$ and curvatures (k_x, k_y, k_{xy}) of the laminate's mid-plane using the equation of classical lamination theory [8,9,19,43]:

$$\begin{Bmatrix} N_x^T \\ N_y^T \\ N_{xy}^T \\ \hline M_x^T \\ M_y^T \\ M_{xy}^T \end{Bmatrix} = \begin{bmatrix} A & \vdots & B \\ \cdots & \vdots & \cdots \\ B & \vdots & D \end{bmatrix} \begin{Bmatrix} \varepsilon_x^0 \\ \varepsilon_y^0 \\ \gamma_{xy}^0 \\ \hline \kappa_x \\ \kappa_y \\ \kappa_{xy} \end{Bmatrix} \tag{2.7}$$

where A, B, and D are the laminate's extensional, coupling, and bending stiffness matrices, respectively. $\left(N_x^T, N_y^T, N_{xy}^T\right)$ and $\left(M_x^T, M_y^T, M_{xy}^T\right)$ are the in-plane forces and thermal moments given by [8,19,43]:

$$\begin{Bmatrix} N_x^T \\ N_y^T \\ N_{xy}^T \end{Bmatrix} = \Delta T \sum_{k=1}^{n} \left\{ \int_{h_{k-1}}^{h_k} |\bar{Q}|_k \begin{Bmatrix} \alpha_x \\ \alpha_y \\ \alpha_{xy} \end{Bmatrix}_k dz \right\} \tag{2.8}$$

And [45]:

$$\begin{Bmatrix} M_x^T \\ M_y^T \\ M_{xy}^T \end{Bmatrix} = \Delta T \sum_{k=1}^{n} \left\{ \int_{h_{k-1}}^{h_k} [\bar{Q}]_k \begin{Bmatrix} \alpha_x \\ \alpha_y \\ \alpha_{xy} \end{Bmatrix}_k z dz \right\} \tag{2.9}$$

where ΔT is the temperature differential for the residual stress build-up, $[\bar{Q}]_k$ is the stiffness matrix of ply k, a_x, a_y, a_{xy} are the coefficients of thermal expansion of ply k in the reference directions, and h_k is the height of ply k relative to the mid-plane of the laminate. Application of this model requires knowledge of the composite's stiffness characteristics, its thermal expansion coefficients, and the temperature at which residual stresses begin to build-up. Once the strains and curvatures of the laminate's mid-plane have been determined, the strains and stresses of the single plies can be calculated using the equations of classical lamination theory and the appropriate stiffness characteristics of the material. Classical lamination theory predicts saddle-shaped curvatures for unsymmetrical rectangular laminates, but cannot predict the cylindrical curvatures that are experimentally possible. Extended theories have been proposed to overcome this problem when plate dimensions are comparable [19]. In addition, for cross-ply laminates the thermal forces and moments are given by [8]:

$$\left.\begin{aligned} N_x^T &= \sum\left(Q_{11}^k\alpha_x^k + Q_{12}^k\alpha_y^k\right)(Z_k - Z_{k-1})\Delta T \\ N_y^T &= \sum\left(Q_{12}^k\alpha_x^k + Q_{22}^k\alpha_y^k\right)(Z_k - Z_{k-1})\Delta T \\ M_x^T &= \sum\left(Q_{11}^k\alpha_x^k + Q_{12}^k\alpha_y^k\right)(Z_k^2 - Z_{k-1}^2)\Delta T \\ M_y^T &= \sum\left(Q_{12}^k\alpha_x^k + Q_{22}^k\alpha_y^k\right)(Z_k^2 - Z_{k-1}^2)\Delta T \end{aligned}\right\} \tag{2.10}$$

with

$$N_{xy}^T = M_{xy}^T = 0$$

where

Q_{ij}^k = stiffness constants of the kth layer

α_x^k, α_y^k = coefficient of expansion in x,y direction of lamina k

Z_k, Z_{k-1} = coordinate of upper and lower surfaces of lamina relative to the midplane (z = 0)

ΔT = temperature interval over which residual stress has built up

The residual stresses within each lamina are calculated from [8]:

$$\left.\begin{aligned} \sigma_x^k &= Q_{11}^k(\epsilon_x^k - \alpha_x^k\Delta T) + Q_{12}^k\left(\epsilon_y^k - \alpha_y^k\Delta T\right) \\ \sigma_y^k &= Q_{12}^k(\epsilon_x^k - \alpha_x^k\Delta T) + Q_{22}^k\left(\epsilon_y^k - \alpha_y^k\Delta T\right) \end{aligned}\right\} \tag{2.11}$$

where for each layer

$$\left.\begin{aligned} \epsilon_x^k &= \epsilon_x^\circ + zk_x^\circ \\ \epsilon_y^k &= \epsilon_y^\circ + zk_{xy}^\circ \end{aligned}\right\} \tag{2.12}$$

2.4.3. Digital image correlation technique

The digital image correlation technique is used to record the curvature of laminates and their evolution with temperature. In one study Pérona et al. developed an experimental method for tracking the curvature of four asymmetrical laminated square plates of $[90_4/0_4]$ made from a polyamide 66 (PA66) matrix reinforced with continuous glass fibers. A speckle pattern was painted on the top of these plates. They were then hanged in a climate chamber, as previously described, using thin wires, and their out-of-plane shape was monitored during heating in the same temperature range. A VIC-3D image correlation system from Correlated Solutions was used to measure the top surface of the plate (Fig. 2.58a) [44].

For the stacking sequence under study, the shape of the plate is expected to be either cylindrical or saddle-like along its principal x and y directions. Analysis of the surfaces obtained by digital image correlation can therefore be reduced to the study of the main curvatures along the principal axes, which were designated as a and b along the x and y directions, respectively. These were obtained by extracting the surface deflection in the x and y directions along the X and Y lines shown in Fig. 2.58b. For both directions, the point cloud corresponding to the extracted lines was interpolated using a quadratic function in MATLAB 2017a software, thus leading directly to the curvatures a and b [44].

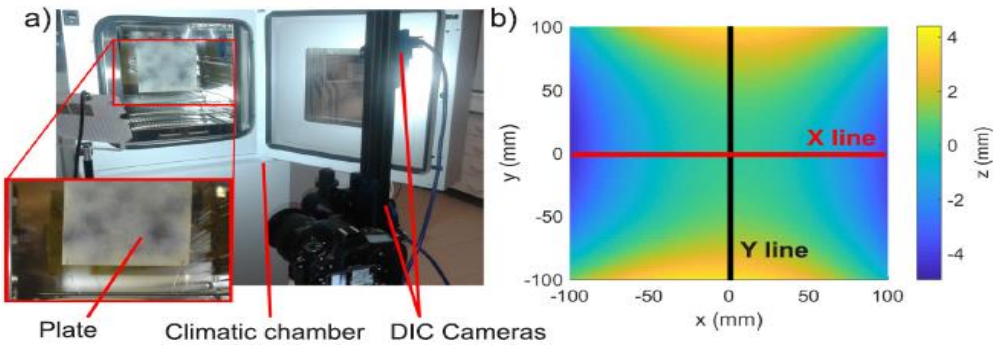

Fig. 2.58: Curvature measurement a) Experimental set up and b) Analysis of the surface deflection of the plate. (For interpretation of the references to colour in this figure legend, the reader is referred to the web version of this article.) [44].

2.5. RESIDUAL STRESS DETERMINATION BY MEANS OF DESTRUCTIVE TESTING

This section briefly reviews works on determining residual stresses by using destructive testing.

2.5.1. Overview of destructive testing

The early experimental techniques developed are mainly based on the destructive evaluation of residual stresses in composites [33]. These techniques include first-ply failure, stress-relaxation based techniques, and curvature methods for lamination stress levels to determine residual skin core stresses, which will be explained in the following sections.

2.5.2. First ply failure

Thermal shrinkage in a cross-ply (symmetrical) laminate creates a state of residual tensile stress in the transverse 90° plies. When the cross-ply is loaded in the transverse direction, the tensile strength of the laminate $\sigma_{0/90}^{t}$, where the superscript t denotes the transverse direction, is measured as being less than the transverse tensile strength of unidirectional laminates, $\sigma_{0/0}^{t}$. This tensile strength is recorded at the first audible crack (often determined by acoustic emission), hence the term is named "first ply failure". The difference between these values provides the estimation of the residual interlaminar stresses σ_R: $\sigma_R = \sigma_{0/0}^{t} - \sigma_{0/90}^{t}$ [2].

In one work residual stresses in cross-ply laminates made of APC-2 (carbon fibre-PEEK) prepregs have been investigated. The first ply failure method was used to measure the residual stresses in a $[90_2/0_4/90_2]$ laminate. It has been shown that, in tension, detecting failure of the first ply by a change in slope in the load-extension curve does not work, since the longitudinal plies carry most of the load and failure of the transverse ply has little effect on the laminate's stiffness or load-bearing capacity. However, audible emissions occurring during the test gave an indication of when a crack appeared in the transverse ply. As soon as a crack was heard during a test, the sample was unloaded and examined under the microscope; in all cases, there was an excellent one-to-one correlation between the audible emission and crack formation. Fig. 2.59 shows a typical first-ply failure on the outer 90° ply of the $[90_2/0_4/90_2]$ laminate [8].

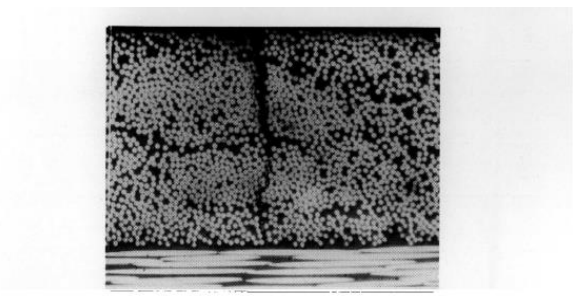

Fig. 2.59: A transverse crack in the outer ply of a balanced laminate (outer ply thickness = 0.25 mm) [8].

2.5.3. Destructive/relaxation-based techniques

Techniques to determine the distribution of residual stresses in the thickness are often based on destructive techniques. Destructive methods involve releasing internal stresses by removing material. The release of these stresses causes deformations in the sample, which can be measured and compared to the deformed state before removal [8,19,33]. The creation of additional free surface in the composite, i.e., damage to the composite, relaxes residual stresses and if this occurs in a controlled manner and the released stresses are measured, it is possible to calculate the residual stresses that were originally present in the laminate. As discussed earlier, the curvature method does not provide information about the (global) stress distribution in the laminate thickness [33]. However, these destructive methods are often used to determine the distribution of global residual stresses in the thickness (skin-core stresses), although they have also been applied to determine the lamination stresses [33,40]. Techniques that are used for determining residual stresses by relaxation include removing symmetrical laminate layers, drilling blind holes, and grooving [8,9,33].

2.5.3.1. Layer removal of symmetrical laminates

A variant of the bending technique is to obtain non-symmetrical laminates by removing one or more layers from a balanced (flat) laminate. The released strains can be detected by strain gauges and the resulting deformations monitored, for example, by Moire interferometry. The combination of these parameters can be used to calculate residual stresses in the laminate before layer removal, often calculated using the classical lamination theory (CLT) [8,9,33]. Layer removal was frequently performed by abrasion/milling to remove successive outer layers of the laminate. This method has been found not to be very accurate because it is sensitive to heat generation and the initiation of microcracks due to abrasion, both of which can release the internal stresses under investigation [4,33,40]. In addition, any irregularities in the layer thickness due to abrasion will affect the resulting curvatures [33,41]. The laminate abrading technique, illustrated schematically in Fig. 2.60, involves successive grinding of the surface using an end mill. As with the PSL strain gage technique, a strain gage was attached to the opposite side of the layer removal side, and the stress after each layer removal increment was monitored and calculated [4,9].

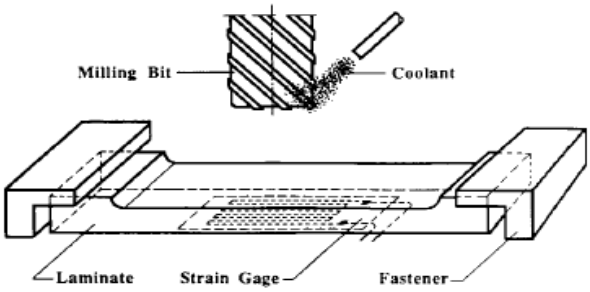

Fig. 2.60: Schematic of the laminate abrading technique. The laminate is held flat during abrading by the milling or grinding bit and simultaneously sprayed with a water coolant [4].

In order to avoid damage to the composite such as during abrasive layer removal, the concept of process simulation laminate (PSL) has been described. The PSL technique consists of several composite prepreg plies separated by thin separating plies, such as polyimide sheets. The composite plies between two separation films form a constituent laminate (CL), see Fig. 2.61, and these CLs can be separated after processing and analysis [4,33]. A summary of the process simulated laminate (PSL) methodology is also displayed in Fig. 2.62, involving building up a certain number of plies separated by a release ply (separation film) that allows the laminate to be separated into specific layers after processing. As mentioned, the unit of plies between the separating films is defined as the constitutive laminate (CL) [4].

The analysis can be performed in two ways [4,33]:

- The constitutive laminate deformation (CL-DEFORMATION) technique, where the residual stress distribution is determined by measuring the dimensional changes (curvature) of CL before and after separation.
- The PSL strain gauge technique (PSL-STRAIN GAGE), in which strain gauges are applied after processing to one surface of the laminate to monitor changes in strain during the removal of the constituent laminates on the other side of the laminate.

Both methods were compared to the layer abrasion method and the measured stress profiles were nearly identical, with the PSL strain gauge technique providing the greatest accuracy. The separation film is the critical component of the PSL technique, as it must allow "perfect" adhesion to the composite for load transfer and it must allow separation of the composite after the processing step. Furthermore, it must not interfere in any way with the formation of residual stresses, for example, by crystallinity effects, initiation of additional forces, etc [33].

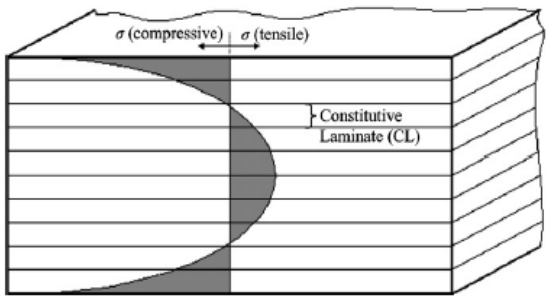

Fig. 2.61: Schematic view of the process simulated laminate (PSL) configuration with constitutive laminates (CL) for determination of laminate skin-core residual stress distribution (grey area) [33].

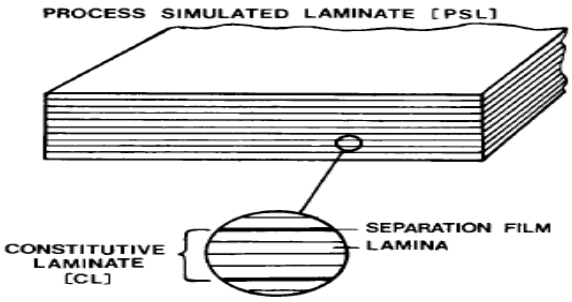

Fig. 2.62: Schematic of a 40/4 process simulated laminate (PSL) configuration. The illustrated PSL consists of 10 constitutive laminates (CL), each containing 4 lamina and separated by a separation film [4].

The CL-deformation technique and the PSL-strain gage technique will be explained in more detail below. Jeronimidis et al. used the milling method to measure residual stresses in APC-2 cross-ply laminates [$90_2/0_4/90_2$]. The milling method is an indirect method of measuring the stresses present in balanced laminates; it involves milling part of the laminate surface to produce an unbalanced laminate whose curvature can be predicted. The top 90° layer of a [$90_2/0_4/90_2$] laminate was removed by milling, leaving a [$0_2/90_4$] laminate. The radius of curvature measured after milling was compared with the predicted radius [8].

2.5.3.1.1. CL-deformation technique

As mentioned, using the CL-deformation technique, the residual stress distribution is defined by measuring the dimensional changes of PSL and CLs before and after separation. The dimensional change upon release of residual stresses during separation can be monitored by its linear and bending components, as shown schematically in Fig. 2.63. According to well-established constitutive relations for a transverse orthotropic laminate, the residual stress of an individual constitutive laminate can be calculated by the measured dimensional changes of the CL as follows [4]:

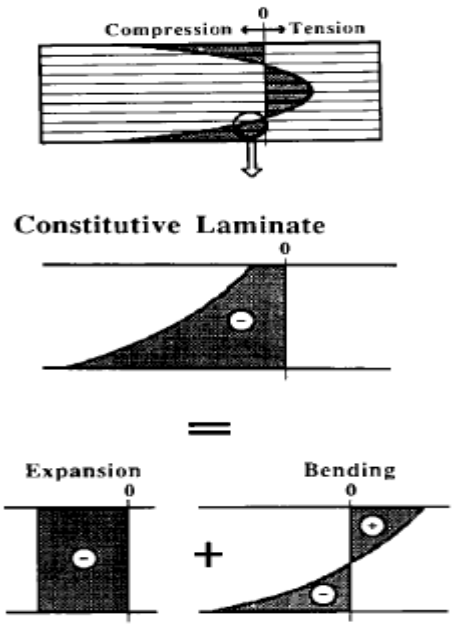

Fig. 2.63: Schematic showing the principal stress release of a constItutive laminate upon separation from the process simulated laminate [4].

$$\begin{Bmatrix} \sigma_x \\ \sigma_y \\ \tau_{xy} \end{Bmatrix}_{k,n} = \begin{bmatrix} \bar{Q}_{11} & \bar{Q}_{12} & \bar{Q}_{16} \\ \bar{Q}_{12} & \bar{Q}_{22} & \bar{Q}_{26} \\ \bar{Q}_{16} & \bar{Q}_{26} & \bar{Q}_{66} \end{bmatrix}_{k,n} \left\{ \begin{Bmatrix} \epsilon_x^{\circ} \\ \epsilon_y^{\circ} \\ \gamma_{xy}^{\circ} \end{Bmatrix} + z \begin{Bmatrix} \kappa_x \\ \kappa_y \\ \kappa_{xy} \end{Bmatrix} \right\}_n \tag{2.13}$$

where

$\{\sigma\}_{\boldsymbol{k,n}}$ = stress matrix for the kth layer in the nth CL

$[\bar{Q}]_{\boldsymbol{k,n}}$ = reduced stiffness matrix for the kth layer in the nth CL

$\{\boldsymbol{\epsilon}^{\circ}\}_{\boldsymbol{n}}$ = extensional strain matrix for the nth CL

$Z_{\boldsymbol{n}}$ = distance from geometric midplane for the nth CL

$\{\kappa\}_{\boldsymbol{n}}$ = curvature matrix for the nth CL

The strain and curvature for the CL laminate may be calculated according to Equations (2.14) and (2.15) as [4]:

$$\epsilon_n^{\circ} = (L_n - L_0)/L_0 \tag{2.14}$$

where

ϵ_n° = midplane strain of the nth CL in either 0° or 90° direction

L_n = length of the nth CL after separation

L_0 = length of the PSL before separation

And [50]:

$$\kappa = 8d/(L^2 + 4d^2) \tag{2.15}$$

where

$\kappa =$ curvature in the 0° or 90° direction

d = deflection at center of the laminate

L = length of the CL

Based on the PSL and CL dimensional measurements, the strain and curvature of each CL can be calculated from equations (2.14) and (2.15) and substituted into equation (2.13), giving the stress state in each CL. The total residual stress profile for the PSL is expressed by the combined values of the CLs [4].

2.5.3.1.2. PSL-strain gage technique

The CL-deformation and PSL-strain gage techniques, as illustrated schematically in Fig. 2.64, both use the PSL design of the laminate. However, for stress analysis, a strain gage was used to measure dimensional changes in the PSL. After processing, the strain gage was attached to the side opposite to that on which the layer was removed. The residual stress distribution was calculated from the deformation response of the PSL during the removal of each of the CL as follows [4]:

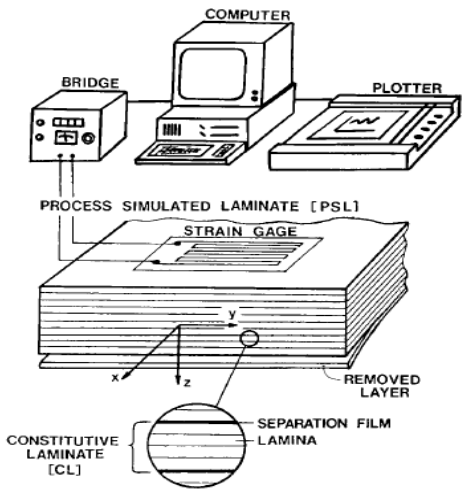

Fig. 2.64: Schematic of the setup for the PSL-strain gage measuring technique. The CLs are removed from the opposite side of the strain gage. The stream gage is connected to a PC computer through a conditioner and amplifier [4].

$$\sigma_r(z) = -\frac{E}{2}\left[\left(\frac{d}{2} - z\right)\frac{\Delta\epsilon_s(z)}{\Delta z} - 4\epsilon_s(z) + 6\left(\frac{d}{2} - z\right)\sum_{-d/2}^{z}\frac{\epsilon_s(\phi)}{\left(\frac{d}{2} - \phi\right)^2}\,\Delta\phi\right] \tag{2.16}$$

where:

$\sigma_r =$ residual stress

$\Delta z =$ thickness of layer

d = laminate thickness

$\Delta\epsilon_s$ = strain difference upon removal of layer

z = distance from center of mass

E= elastic modulus

ϵ_s = absolute strain at the top surface

The above expression is based on the strains induced in the beam and the non-uniform state of stress induced by layer removal. The strain gage was oriented in the direction transverse to the fibers, as the individual strains should be greater than in the longitudinal direction, due to the greater strains in this direction. In the longitudinal direction, the deformation will be significantly lower, but the stiffness is an order of magnitude higher than in the transverse direction, resulting in stress of the same order for both directions [4].

2.5.3.2. Other stress relaxation-based techniques

The blind-hole drilling technique is one of the most common techniques for determining residual stresses that depends on stress relaxation. This method is based on stress releasing by drilling a small hole. The dimensions and geometry of the hole change due to the stress release caused by the removal of the material. These changes result in the deformation of the material surrounding the hole. The deformities can be measured with for instance a strain gauge rosette. In this approach, a strain gauge rosette is attached to the area of the material, and a small hole is drilled through the material in the center of the rosette [33]. A hole is drilled in several stages at the geometric center of the strain gauge rosette. Residual stresses in the material surrounding the drilled hole are partially released as the hole is drilled. The associated released stresses are measured at a specified sequence of hole depth steps using a suitable strain-recording instrument. Moreover, the hole-drilling method identifies in-plane residual stresses close to the measured surface of the workpiece material. The method gives localized measurements that indicate residual stresses within the boundaries of the drilled hole. This test method applies in cases where the material's behavior is linear-elastic. In theory, it is possible for local yielding to occur as a result of stress concentration around the drilled hole [45].

Several drilling techniques have been investigated and found to be suitable for the hole-drilling method. The most common drilling technique, suitable for all but the hardest materials, involves the use of carbide or endmills driven by a high-speed air turbine or electric motor. For very hard materials, abrasive jet machining can also be useful. This drilling method involves directing a stream of high-velocity air containing fine abrasive particles through a small-diameter nozzle against the workpiece.

Abrasive jet machining may be less suitable for softer materials. It should not be used for non-uniform stress measurements, as hole geometry and depth cannot be controlled with sufficient precision [45]. One disadvantage of this method is that the size of a standard strain gauge rosette is two to four times the hole diameter, making the region covered by the rosette too larger compared to the released strain field. In addition, eccentric drilling error (i.e., the error which is caused when the hole is not drilled exactly in the center of the rosette) is a common problem with the strain-gauge rosette method. The hole-punching method has also been used in combination with other methods such as moiré interferometry, holographic interferometry, and speckle interferometry [33].

Another technique based on stress relaxation is known as the crack compliance method or successive grooving (slot drilling) technique in which one or more slots (also called grooves or slits) are gradually cut into a specimen. Strains due to stress relaxation are recorded with strain gauges to determine the residual stresses through the thickness. It was stated that these techniques offer a high degree of accuracy [9,33]. The compliance method consists of two elements: the forward solution and the inverse solution. In the forward solution, the strains resulting from incrementally introducing a slot into the sample with a known residual stress distribution are calculated. Forward solutions can also be identified as compliance calculations. Compliance calculations can be performed using fracture mechanics solutions, the finite element method, or the body force method. A slot is then progressively introduced into the sample, releasing stresses along the plane of the slot and causing deformation. At each increment, the strain or displacement is measured on an appropriate surface. In the inverse solution, the stress distribution that best matches the actually measured strain is determined [9].

2.6. NUMERICAL MODELLING (F.E.A) OF PROCESS-INDUCED STRESSES

Numerical modelling, in particular finite element analysis (FEA), has been used in some studies to predict the thermal residual stresses generated during a particular process. The results of these simulations are often compared with experimental data to assess their accuracy and reliability. For example, in one study Parambil et al. developed a finite element (FE) thermal residual stress model for carbon fiber/thermoplastic composites at the microscale and implemented it via the user material subroutine (UMAT) in ABAQUS. Their model took into account the effects of cooling rate on crystallinity and stress-free temperature, temperature-dependent elastic modulus, temperature-dependent coefficient of thermal expansion (CTE) of the matrix, and temperature-independent

transversely isotropic properties of the carbon fiber. Results were generated for a model composite consisting of a single carbon fiber embedded in a thin polypropylene film. Single filaments were pre-tensioned in the molten polymer to induce different levels of residual axial strain and maintain straight fibers during cooling down. Three different preload conditions (1g, 4g, and 8g) were experimentally fabricated and modeled. Residual strain along the length of the fiber was quantified and validated, including the region of shear lag that develops at the free edge of the sample. The experimentally measured residual strain showed a good correlation with FE predictions for applied fiber preload conditions [26]. Moreover, as previously mentioned, the residual stress state depends on the thermal history, crystallization kinetics, and temperature-dependent properties of the constituents. A computational finite element model of thermal residual stress has been developed and experimentally validated for AS4 carbon fiber/polypropylene composites and implemented via a user material subroutine (UMAT) in ABAQUS, as shown in Fig. 2.65 [26].

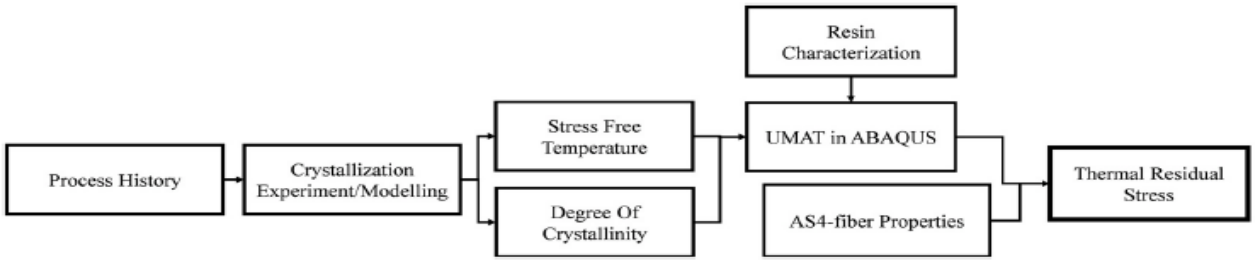

Fig. 2.65: Flow-chart for calculating thermal residual stress [26].

2.7. REVIEW OF TECHNIQUES FOR ESTIMATING THE MAGNITUDE OF RESIDUAL THERMAL STRESSES

The diagram illustrates the techniques reviewed in this project for estimating the magnitude of residual thermal stresses.

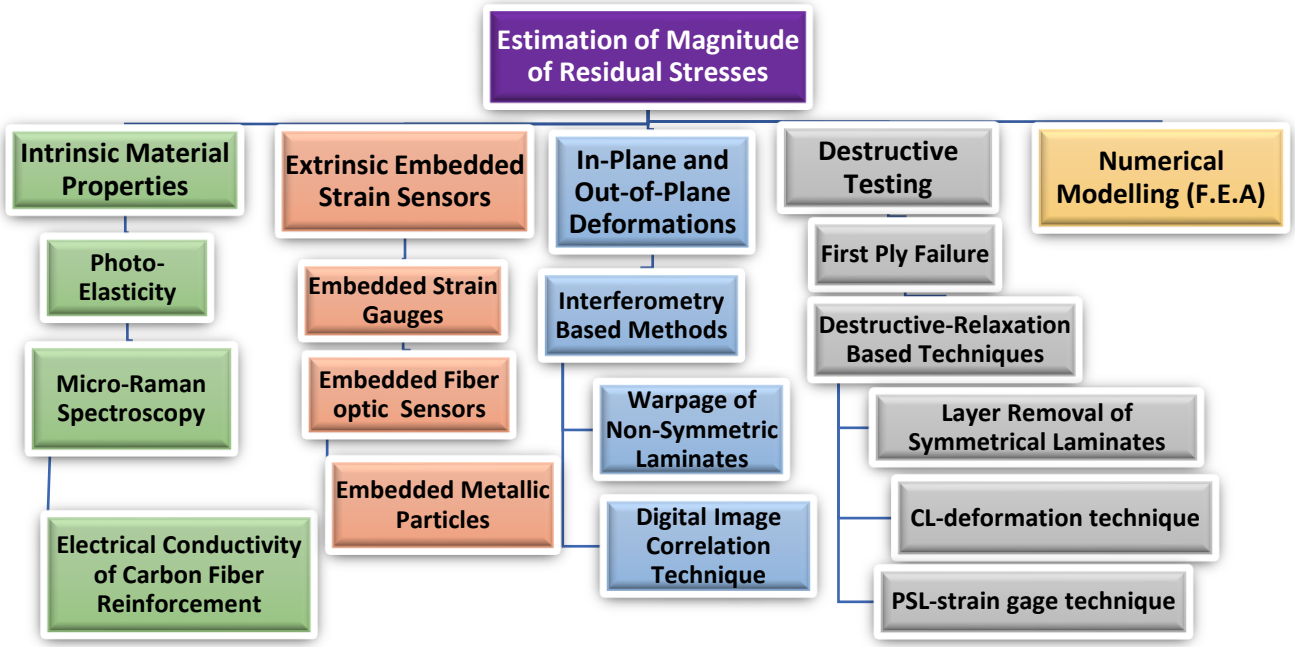

2.8. EXPERIMENTAL DETERMINATION OF MODEL PARAMETERS

It is essential to determine the composite properties because the distribution of the effective composite properties within a composite part can have a strong influence on the final properties obtained in the finished part, both for the short term and for long-term performance [23]. To determine residual stresses using the above experimental techniques, material properties must be determined in order to perform the necessary calculations. The following is a brief overview of the experimental techniques commonly used to measure some necessary parameters.

To calculate the magnitude of residual stresses in a composite, assuming sufficient fiber-matrix interaction, the essential parameters are as follows [18,33]:

- The shrinkage of the matrix and fiber during cooling (coefficients of thermal expansion α_m and α_f, respectively);
- The temperature difference ΔT between the stress-free temperature and the service temperature;
- The modulus of elasticity of the two components E_m and E_f at the service temperature.

For example, to calculate the interlaminar residual stresses in symmetric cross-ply laminates at service temperature, the values obtained for single composite plies in the transverse and longitudinal directions are required [1]. The magnitude of the resulting stresses can be approximately estimated by one-dimensional linear elastic analysis as below [18,33]:

$$\sigma_{22} = \frac{(E_{11} \times E_{22})}{(E_{11} + E_{22})} \times (\alpha_{22} - \alpha_{11})\Delta T \tag{2.17}$$

Where E_{11} is the composite stiffness parallel to the fibers, E_{22} is the composite stiffness transverse to the fiber direction, and the terms α denote the coefficients of thermal expansion in each of the principal directions. For simplicity, α_{11} can be assumed to be zero for carbon fiber composites [2,13]. For non-symmetrical cross-ply laminates, we use equation (2.2) and its parameters, which we mentioned in section 4.2 [18].

Shrinkage (of the matrix) upon cooling and moduli of semi-crystalline thermoplastics (composites) depend on the crystallinity level. The experimental work consisted of measuring the crystallinity levels for different cooling rates using a differential scanning calorimeter (DSC) and wide-angle X-ray spectroscopy (WAXS) and determining the modulus with temperature using a dynamic mechanical thermal analyzer (DMTA). The coefficients of thermal expansion (CTE) as a function of temperature must be measured as this is a temperature-dependent property. Techniques for measuring CTE include DMTA, the use of strain gauges in conjunction with a temperature-controlled chamber or during processing, and speckle interferometry. The stress-free temperature is often considered the glass transition temperature (T_g) for amorphous thermoplastics, and the crystallization peak temperature (T_c) for semi-crystalline thermoplastics. These values can be determined by DSC or DMTA. It is also possible to determine the stress-free temperature during cooling: the temperature at which the laminate starts to curve will be the temperature at which residual stresses appear. The photo-elasticity method combined with a hot stage was also used to determine the stress-free temperature. Coefficients of thermal expansion and moduli can also be calculated from the matrix and fiber parameters, for example, by using a rule of mixtures approach. Although it is known how to obtain values for material properties, there is still a fundamental lack of available material properties, especially for thermoplastic composites, which limits the validation of these techniques [33].

2.9. RELAXATION EXPERIMENTS

Residual stresses in thermoplastic composites can relax over time and temperature due to the pronounced viscoelastic behavior of the matrix [33]. This phenomenon has been expressed previously in this study and experimental techniques to track this behavior will be discussed here. One of the methods to determine the relaxation behavior is to follow the curvature of non-symmetric laminates [8,18,19,33]. In deformed laminates, there is no driving force to become flat, as some of the residual stress is relieved by the curvature itself due to the lack of a constraint [18,33,40]. However, when

curved specimens are clamped or restrained, such as during cooling in a mold, residual stresses relax by viscoelastic behavior over time and temperature and the curvature will be modified in this condition [33]. The relaxation behavior at room temperature was determined by storing non-symmetric laminates flat under a weight and tracking the curvature with time [33,40]. Relaxation tests at raised temperatures were also performed, by clamping the curved specimens to become flat at several temperatures and holding the specimens over several dwell times [33].

THIS PAGE WAS INTENTIONALLY LEFT BLANK

3.1. INTRODUCTION

Each property of composites depends on a matrix property that is affected by various stresses such as thermal residual stresses. These properties include solvent sensitivity, impact resistance, fatigue, and compression [31]. This study will begin with a discussion of the effects of residual stresses on the properties of dominant matrix composites, followed by a description of the effects that occur at the fiber-matrix interface. Residual stress-induced defects and their effects on the mechanical properties of composite laminates are explained, after which the effects on composite structures will be expressed and mechanisms for reducing residual stresses in TPC composites will be proposed.

3.2. RESIDUAL STRESS EFFECTS AND THE MATRIX-DOMINATED PROPERTIES

Because of the shrinkage mismatch between the fiber and the matrix, the matrix usually experiences thermal residual tensile stress [5,6,31]. Locally, the magnitude of this strain can vary due to variations in the volume fraction of the fibers [31]. It has proven difficult to experimentally determine the magnitude of residual thermal stresses experienced by the matrix in a composite laminate and thus it is difficult to attribute the effects of residual stresses to matrix properties [31,33]. However, it is possible to evaluate the effects of residual stresses on matrix-dominated properties of composites, such as moisture absorption and temperature resistance. These properties are considerably influenced by residual stresses [31].

T_g is one of the other matrix-dominated properties that is affected by the state of stress of the resin. Compressive load increases Tg and shear and tensile loads decrease it [31,46]. This may be important because the onset of the glass transition temperature (T_g) display the upper limit of the use temperature for polymers and their composites in structural applications. Differential scanning calorimetry (DSC) revealed that carbon fiber-reinforced polyetherimide (PEI) had a lower T_g than pure PEI, which was attributed to the presence of the carbon fibers and the accompanying residual stress. Moisture absorption by the matrix has also been found to significantly affect the residual stress state of the polymer composite. Several effects can occur, namely (a) swelling of the matrix, which leads to a change in the stress state; (b) plasticization of the polymer by moisture, which leads to a decrease in the glass transition temperature; (c) moisture can affect the fiber-matrix interphase; and (c) internal stresses influence the moisture uptake: the higher the residual stresses, the higher the moisture uptake [31].

An amorphous polymer (or the amorphous part of a semi-crystalline polymer) above its glass transition temperature is a viscoelastic rubber in thermodynamic equilibrium [46]. Because of the viscoelastic nature of the polymer matrix (and possibly the fiber-matrix interphase), the thermal residual stresses were found to be time-dependent, i.e., the matrix exhibits stress or strain relaxation over time [31,46]. When exposed to a certain constant load (stress), a polymer exhibits a decrease and relaxation in the strain of the polymer matrix. Or vice versa; it is found that the stress inside a polymer resulting from a certain strain decreases with time caused by the molecular relaxation that takes place inside the polymer. Higher residual stresses result in a higher relaxation rate. Environmental aspects, such as temperature and moisture, affect this relaxation behavior. For higher temperatures, the relaxation rate of residual stresses is higher as well as the total relaxation [31].

Experimental studies have exhibited that residual stresses in composites occurring during manufacturing can decrease significantly during storage under ambient hydrothermal conditions (ambient temperature of 23 °C and 50% relative humidity). Experimental observations have often been made by following the curvature of non-symmetric laminates, either forced flat or unrestrained. It has been reported that the room temperature curvature of unbalanced laminates decreased with time due to residual stress relaxation. It has been noted that when the residual stresses relax to limited values, the remaining residual stresses still have a considerable influence on the mechanical properties [31].

In addition to thermal stress relaxation, another time-dependent mechanism affects the properties of matrix-dominated composites: the effect of matrix aging [31,47]. The composite was found to age faster than the plain matrix [46]. When an amorphous polymer (or the amorphous phase of a semicrystalline polymer) is cooled below its glass transition temperature, a glassy solid is obtained whose polymer chains are in a state of thermodynamic nonequilibrium. Physical aging occurs when a polymer (matrix) is cooled below its T_g and the material evolves toward thermodynamic equilibrium. This evolution is characterized by changes in free volume and will produce measurable changes over time, namely an increase in modulus and yield strength and a decrease in fracture energy and toughness, thereby increasing the probability of failure initiation [31,46]. Temperature and processing have a strong influence on the physical aging rate, i.e., at higher temperatures (below Tg), the physical aging rate is higher. Consequently, for slow cooling rates, the effects of aging are more significant [31]. In addition, the environment plays an important role in the matrix-dominated properties. Isothermal aging (thermal aging) or hygrothermal aging (maintaining a certain temperature and relative humidity for a longer period of time) interacts with residual stresses [31]. Isothermal aging resulted in a growth in T_g or stress-free temperature, while relatively inert environments were found to degrade the properties of polymer composites to a lower extent.

Moreover, oxidation of the polymer matrix in an oxygen-rich environment can cause the matrix to become brittle, resulting in a decrease in the properties of the composite or the occurrence of damage [31,47].

3.3 EFFECTS OCCURRING AT THE FIBER–MATRIX INTERFACE

The fiber/matrix interface plays a critical role in the mechanical behavior of composites. The role of the interface is essential to the performance of composites, as their strength, stiffness, and fracture behavior depend on interfacial conditions [48]. In thermoset composites, the fiber-matrix interface is formed by chemical bonds, whereas in thermoplastic composites, the fiber-matrix adhesion is mainly due to the shrinkage of the matrix around the fiber, which increases the Van der Waals bonds between the fiber and the matrix. The strength of the fiber-matrix interfacial bond has an influence on the magnitude of the residual stresses. It was detected that with increasing radial residual stresses, the fiber-matrix interfacial bond became stronger, because of the mechanical locking. Although fiber-matrix interfacial debonding can occur parallel to the fiber axis caused by residual stresses if the fiber-matrix (chemical) bond strength is too low [31]. It has also been shown that processing-induced residual stresses considerably affect the initiation and propagation of interface cracks [48].

For reinforcing fibers, they are generally of such strength that residual stresses do not cause significant problems. However, in most cases, the fibers experience compressive thermal residual strain, a load case for which the fibers were not designed [31]. The fibers may be subjected to such a high load in their direction that they may fragment due to residual stresses [2,31].

3.4. RESIDUAL STRESS-INDUCED DEFECTS

Residual stresses can cause various defects in laminates and composite structures and they can significantly affect the performance of a composite system. Internal stresses can be released during processing through fiber buckling, warping of non-symmetrical laminates, void formation, macroscopic deformation as well as initiation of matrix cracking; or internal stresses can remain in the material after processing as residual stresses. The defects considered here are fiber waviness, transverse cracking, delamination, and warpage of laminates [23,31,40].

3.4.1 Fiber waviness

Fiber waviness, as a type of defect in composite materials, can result from a variety of manufacturing-induced phenomena. For example, during filament winding, the winding pressure can influence the linearity of the fibers in the underlying layers [31,49]. In detail, fiber waviness results from the local buckling of prepreg or wet hoop-wound filament strands under the pressure exerted by the overwrapped layers. Inspection of cylinder microstructures often reveals localized regions of layer waviness in the hoop direction, which results from post-consolidation and cure shrinkage. Layer waviness also occurs in thick cross-ply or multidirectional laminates, due to residual lamination stresses build up during curing [49]. Fiber waviness can be classified as in-plane or out-of-plane. In-plane waviness involves the cooperative undulation of fibers in the plane of the laminate. Out-of-plane waviness generally involves the cooperative undulation of multiple plies in the laminate thickness. In-plane waviness is generally more severe than out-of-plane crimping [31]. When fiber waviness occurs, the average fiber orientation generally remains parallel to the desired fiber direction but exhibits some periodic curvature, often modeled as sinusoidal. Neglecting fiber waviness by assuming straight fibers is a source of error in the structural analysis [22].

When, during the processing phase of composite products, the fibers experience axial loads, such as residual thermal stresses, while the matrix is not able to provide a certain level of transverse support to the fibers, the fibers become deformed (micro buckle) and there will be waviness. Fiber waviness in unidirectional laminates can be described as fibers deviating from the average direction of the laminate and forming a pattern that is mostly represented mathematically as a sine wave Fig. 3.66 [31].

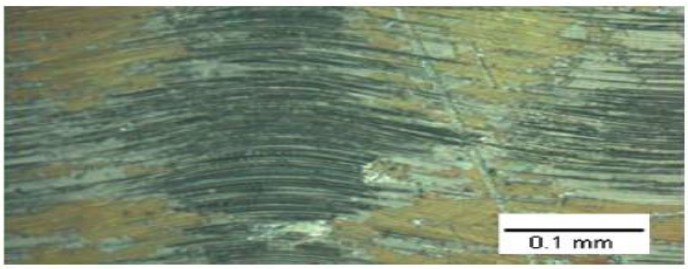

Fig. 3.66: Micrograph of a composite laminate showing fiber waviness [31].

It has been shown that the development of fiber waviness in carbon fiber/polysulfone composites is primarily affected by the tool plate material (specifically the difference in CTE between the tool and the composite part), as well as the cooling rate and length of the part. As shown previously, the cooling rate and the interaction between the tool and the workpiece play an important role in the formation of residual stresses. Therefore, it can be concluded that one of the effects of residual stresses is fiber waviness [5,31]. In addition to the CTE mismatch between the tool and part, sufficiently high-

temperature gradients present in the thickness of the laminate can cause fiber waviness [31]. With the increasing use of thick composite structures subjected to compressive loads, the effect of fiber waviness is becoming an important issue [49].

A systematic study has been carried out into the effects of fiber waviness on the stiffness and strength of unidirectional composites under compressive loading. Analytical models have been developed to predict the elastic properties and compressive strength of different types of waviness. It has been shown that in unidirectional composites, the principal Young's modulus and compressive strength degrade severely as fiber waviness increases [31,49]. Material anisotropy also influences the reduction in stiffness and strength, with carbon/epoxy material being much more sensitive to fiber waviness than S-glass/epoxy material. The reason is that carbon composite has a higher degree of anisotropy in the fiber direction than glass composite [49].

For unidirectional samples with gradual waviness, interlaminar shear failure was found to be the dominant mode of failure. These interlaminar shear stresses can cause local delamination in a composite with a low-strength matrix and, consequently, reduce the local transverse support of the fibers. Following the onset and propagation of delamination, the layers - particularly those with the highest degree of waviness are more susceptible to global buckling than the original laminate, due to their lower thickness. Global buckling of the layers leads to final failure [31,49]. Fig. 3.67 shows the observed sequence of events leading to the final failure of unidirectional specimens with gradual fiber waviness. The complete failure progression is illustrated schematically in Fig. 3.68 [49].

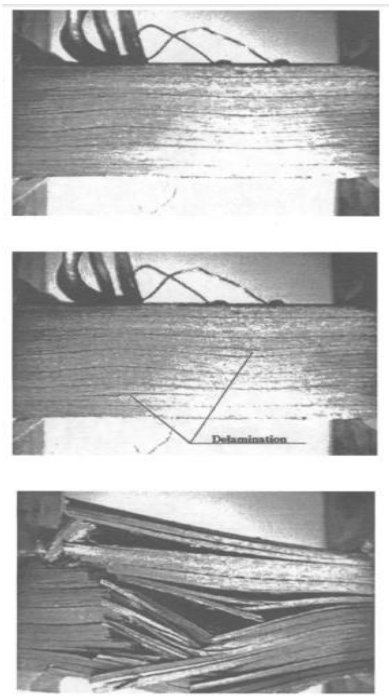

Fig. 3.67. Failure mechanisms in IM6G/3501-6 unidirectional composite with graded waviness under axial compression: (a) before test; (b) failure initiation; (c) ultimate failure [49].

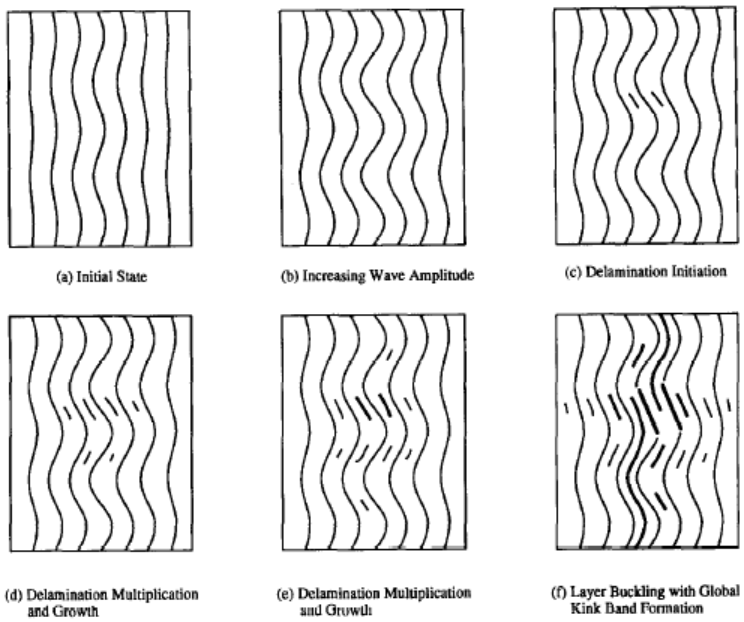

Fig. 3.68. Failure progression in IM6G/3501-6 unidirectional composites with graded waviness under axial compression [49].

3.4.2 Transverse cracking

Residual thermal stresses can cause transverse cracks (often called microcracks) in a composite laminate. It is believed that transverse cracking results from residual stresses caused by differences in coefficients of thermal expansion (CTE) between the polymer matrix and the reinforcement [6,31,50,51]. For example, the current state of high-temperature composites is limited to graphite-fiber-reinforced polyimides (such as PMR-IS) materials. These materials are acceptable for usage in engines at 288°C for up to 5,000 hours. Polyimide composites are processed at 316°C, and this temperature level poses problems due to the residual stresses created during room-temperature cooling after the forming and curing stage in laminate processing. This type of behavior can be more serious with composites at 427°C. The mismatch between the coefficients of thermal expansion of the graphite fiber (-1.0 to 10.0×10^{-6} °C^{-1}) and the polyimide matrix (56×10^{-6} °C^{-1}) creates a considerable amount of residual stress in the composite when cooled from curing temperature to room temperature (a range of 290°C). Depending on the ply layup, these residual stresses may be high enough to cause intralaminar cracks to appear during the cooling phase of the processing. This type

of damage is commonly referred to as microcracking. These microcracks can lead to the degradation of matrix-dominated mechanical properties and reduce the service life of the structure at elevated temperatures [50].

One of the damage initiation mechanisms is that when the residual thermal stress in the matrix exceeds the yield strength of the resin and/or the strength of the fiber-matrix bond, it leads to matrix cracking or fiber-matrix debonding. As the bond of the fiber-matrix interface is weak, cracks can propagate along the interface. In the presence of a strong interface, cracks can propagate into the matrix. The fiber and matrix debonds can join, through matrix cracking between the debonds, and in this way a microcrack can form, see Fig. 3.69. Microcracks are particularly important during cyclic loading (fatigue) [31]. Moreover, at the mesoscale (ply scale), one of the most important mechanisms for failure initiation is transverse cracking, i.e., the appearance of transverse cracks in off-axis plies. Initially, these cracks do not significantly affect the global stiffness of the laminate. However, they generally give rise to more dangerous failure mechanisms, such as delamination. In addition, they considerably reduce the impermeability of the laminate, which can be very important in certain applications such as vessels [51]. In summary, several stages of transverse cracking can be described as [31]:

1. Fiber matrix debonding/matrix cracking.
2. Matrix crack growth/debonding of fiber-matrix to form microcracks.
3. Microcracks may develop into transverse ply cracks.
4. Transverse ply cracks cause delamination and subsequent failure of the laminate.

These steps can occur over time, during the service life. Nevertheless, thermal residual stresses can reach values of the same order as the ply transverse strength, which can cause premature and almost instantaneous ply cracking during processing. For example, you can see an example of transverse crack initiation in surface plies in Fig. 3.70 [31].

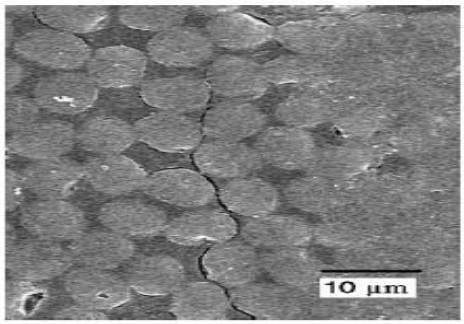

Fig. 3.69: Crack initiation along fiber–matrix interfaces in a carbon fiber polyphenylenesulfide laminate [31].

Fig. 3.70: Transverse cracks in surface plies of $0_3/90_9/0_3$ carbon fiber polyetherimide laminate [31].

Cracks usually appear near the free edges where residual stresses can be very high locally [31,50]. Cracks can be perpendicular or parallel to the plane of the composite, although perpendicular cracks are most often observed. Matrix strength and toughness, as well as fiber-matrix interfacial shear strength, must be sufficient to prevent crack formation. Most brittle matrices (often thermosets) exhibit transverse cracks during curing [31]. Overall, higher interlaminar residual stresses result in a higher density of microcracks in the composite [31,50]. Other environmental factors also contribute to the formation of cracks in relation to residual stresses. As mentioned previously, hygrothermal treatment and thermal cycling can affect the properties of the polymer, i.e., the toughness, so that microcracks can form under the effect of residual stresses [6,31,50]. The following environmental treatments were found to raise the crack density of thermoplastic composites: thermal cycling, hygrothermal treatment, hygrothermal cycling, aging, UV radiation [31].

In a research study, the effect of ply cracks on the warpage of an amorphous matrix graphite/thermoplastic composite specimen was investigated. It was found that the discrepancy between the measured and predicted curvature was mainly caused by the transverse cracks [21].

The effects of transverse cracking are as follows:

Laminate cracking provides an irreversible means of thermal residual stress relief/relaxation through stress redistribution. One of the effects of this redistribution caused by crack formation is a change (decrease) in the effective coefficient of thermal expansion of the composite. Additionally, transverse cracks have been reported to affect several properties of composites [31]:

- Decreases in composite stiffness and elastic moduli were observed.
- The flexural modulus was detected to reduce with increasing microcrack density.
- A reduction in in-plane shear strength and modulus.
- Lower transverse mechanical properties: strengths are reduced due to matrix cracking in off-axis plies.

- Lower values for interlaminar fracture toughness for modes I and II have been observed.
- Transverse cracks can serve as delamination initiation sites during fatigue loading.
- Increased deformation during creep loading.
- Growth of moisture absorption by creating diffusion pathways.
- Lower environmental (chemical) resistance; this allows the entry of corrosive liquids.
- Moreover, matrix cracking decreases the transverse electrical conductivity of carbon fiber reinforced laminates.

3.4.3 Delamination

The discontinuity in the level of residual stress between the 0° and 90° plies of a cross-ply laminate is evident, which could lead to premature delamination (interlaminar delamination) in service. As a consequence, the consolidation of the cross-ply laminate must be adequate. Progressive delamination can cause the interlaminar failure of the plies of a composite laminate, resulting in a loss of stiffness and strength of the structure [31].

The free-edge effect is one of the mechanisms responsible for interlaminar failure characterized by delamination of the plies, which can also lead to matrix cracking [3,31]. Delamination at the free-edge is related to high interlaminar stresses developed because of property discontinuities (such as discontinuity in residual stress level between plies) through the thickness at a free edge [31]. Interlaminar free-edge failure leads to a loss of stiffness and strength of the structure and, after impact damage, is one of the most serious failure modes in fiber-reinforced composite structures [3]. It can occur around any concentration of geometric stresses, including holes, cut-outs, or cross-sectional changes, which significantly limits the load capacities of the entire structure [31].

Unger and Hansen studied the delamination of the free edge of a graphite/PEEK $(+35_2/-35_2/0_2/90_2)_S$ laminate. Predictions of the applied critical strain for the onset of unstable crack growth obtained from its model are compared with experimentally measured values. In Fig. 3.71, the 0/90 ply interface failure loci are considered. It is clear that for crack depths greater than a/p=3 which is delamination depth, the failure strain becomes almost independent of crack depth and, consequently, the prediction of axial fracture strain is not sensitive to the assumed critical crack size. The range of experimental strains compares well with the predicted range when thermal residual stresses have been included. However, when thermal stresses were not included, the failure strain was considerably over-predicted. The mean predicted failure strain is 0.839% for the range of crack depths a/p=3 to a/p=16 when thermal residual stresses are included. The average measured failure strain is 0.912%. The mean failure strain for the same crack depth range, without thermal residual stresses taken into account, is

1.204%. This value is 32% higher than the experimentally measured mean. These results indicate the significant effect that thermal residual stresses can have on delamination failure in fiber-reinforced thermoplastics. Given the 32% over-prediction of failure strain when residual stresses are neglected, it is obvious that these stresses must be taken into account when designing with graphite/PEEK or any comparable thermoplastic material. Another interpretation of these results is to consider the increase in material strength that could be achieved if thermal residual stresses could be reduced or even eliminated [3].

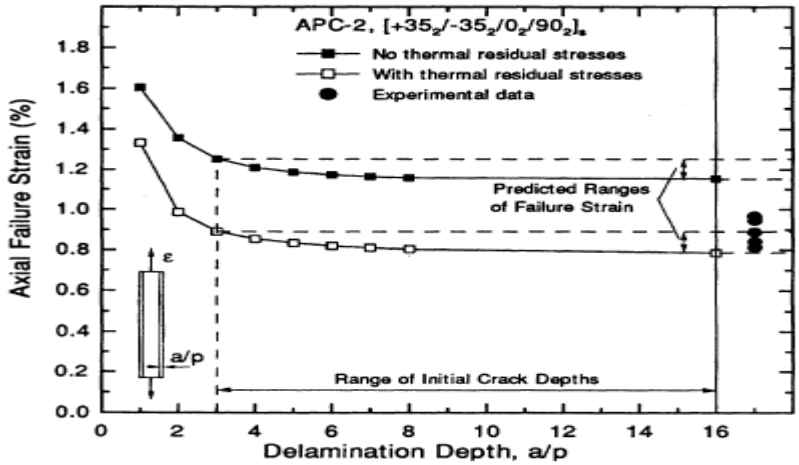

Fig. 3.71: Predicted failure strain (mixed-mode linear interaction) and experimental data, (0/90) delamination [3].

3.4.4 Warpage of laminates

One of the effects of interlaminar residual stresses is that, for relatively thin non-symmetrical laminates, a variation of curved shapes may result (warpage) [31]. Warpage is defined here as a deviation from flatness in initially flat laminates, due to process-induced stress or strain. In symmetrical, balanced laminates, warpage is generally due to non-uniform properties through the thickness, such as fiber volume fraction gradients, or to mechanical interaction between tool and workpiece [51]. In addition, non-symmetrical thermal residual stress gradients through the thickness of a composite can also lead to the deformation of a laminate (warpage) or dimensional instability of a composite structure [9]. When parts are processed on a tool material with a high coefficient of thermal expansion, the plies close to the tool-part interface can be stretched, causing a stress gradient through the thickness that locks in when the part cures. As a result, these parts warp away from the tool after machining, as shown in Fig. 3.72. The plates in the figure are made of T800H/3900-2 UD prepreg laminates processed under non-bleed conditions on aluminium tooling coated with a release agent and a fluorinated ethylene propylene release sheet under an autoclave pressure of 586 kPa. The

properties were uniform throughout the thickness, so the warpage was due to the mechanical interaction between the tool and the part. Fig. 5 shows an example of a warpage because of the tool-workpiece interaction on nominally flat 4-ply, unidirectional carbon/epoxy parts of different lengths [52]. Fig. 3.73 also illustrates a schematic of the warpage defect in the production of composites using the ATP (Automated Tape Placement) process with CF/PA12 materials. The figure demonstrates that component deflections occur easily due to the complex heat-pressure coupling field of the laminates during the cooling process, and the higher shrinkage rate of the semi-crystalline matrix compared to that of the fiber, such as lateral or longitudinal warping, as shown in Fig. 73 [53]. Curvature measurements are widely used to determine differences in residual stress levels caused by varying processing conditions [8,13,18,19,31,33,40]. A steady decrease in warpage was noticed with increasing temperature because of a reduction in thermal residual stresses. Furthermore, micro-cracking reduces curvature even in thin non-symmetrical laminates [31,21]. This can result from two mechanisms: unbalanced cooling and tool–part interaction [5,31]. The interaction between the tool and the part has been shown to contribute significantly to Warpage, especially for thin products. For the rubber press forming process, the difference in mold materials (steel/rubber) has been shown to cause significant warpage caused by a residual stress distribution. Nevertheless, the deformability (tool-part interaction) of the rubber mold was shown to have a greater effect on the warpage of plates than residual stresses due to thermal gradients induced by the relatively rapid cooling of the surface plies. In addition, a non-uniform temperature distribution in the press plates or molds can also induce warping [31].

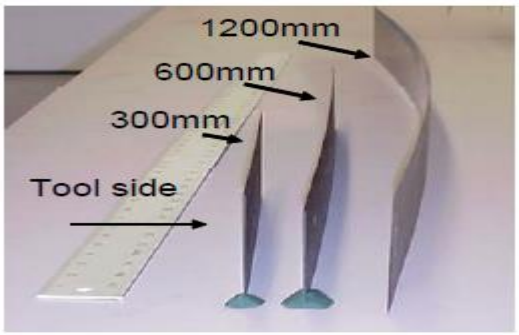

Fig. 3.72: Photograph showing the warpage due to tool-part interaction of nominally flat 4-ply unidirectional carbon/epoxy parts of various lengths. Parts were processed on aluminium tooling coated with release agent and a Fluorinated Ethylene Propylene sheet under 586 kPa (85 psi) autoclave pressure [52].

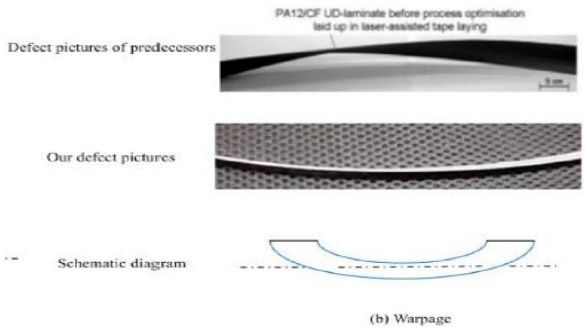

Fig. 3.73: Typical defects of thermoplastic ATP laminates [53].

3.5. RESIDUAL STRESS EFFECTS ON THE MECHANICAL PROPERTIES OF LAMINATES

When the residual stresses and the stresses resulting from external loads are of the same sign, the maximum allowable external stress reduces [31]. Thus, it is important that thermal residual stresses be considered in the design of composite structures [8,31,54]. For instance, residual stress distribution can influence fatigue behavior as well as impact and fracture resistance [31].

3.5.1. Tensile Loading

In unidirectional laminates (UD), residual thermal stresses generally leave the matrix in a state of tension in the direction parallel to the fibers (0° direction) and the reinforcing fibers under compressive loading [1,3]. In the radial or transverse direction (90°), depending on the fiber volume fraction, the fiber and matrix undergo similar states of stress (compression and tension, respectively) as in the 0° direction. In addition, it has been found that residual stresses can be damaging or beneficial for transverse tensile loading in UD composites. This depends on the magnitude of the residual stress and the strength of the matrix material. One experimental study on UD composites showed that when loaded in tension parallel to the fiber direction, a considerable variation in fiber strain was observed in the composites compared to bare fibers loaded in air, which was associated with the internal (residual) stress field [31].

In a cross-ply laminate, thermal shrinkage of the plies perpendicular to the fiber direction creates a state of residual tensile stresses in the plies, the magnitude of which depends on the thickness of the plies [3,7]. Furthermore, differences in residual stresses due to various cooling rates were shown to affect the tensile properties of cross-ply composites. A study on fiber-reinforced polymer matrix cross-ply laminates exhibited that even after relaxation, the remaining residual stresses still have a considerable effect on the damage progression of the cross- ply laminates during the next tensile loading [31].

A comparative study between thermoset and thermoplastic cross-plied laminates was carried out. It was concluded that, under monotonic tensile loading, the behavior of the thermoplastic composite was slightly higher than that of the thermoset composite, but that the trend was reversed under tensile fatigue loading [73].

In addition, in a study, Youssef and Denault carried out tensile tests on $[\pm 45]_{3S}$ laminates of PP/G and m-PP/s-G composites. The former, called PP/G, consists of a pure PP matrix reinforced with 52 wt%

of E-glass fibers, and the latter, called m-PP/s-G, consists of a blend of chemically modified PP and pure PP reinforced with 60 wt% of E-glass fibers coated with a specific thermoplastic sizing agent. The results of tensile tests on these two laminates are shown in Fig. 3.74, in terms of moduli, strains, and stresses. In general, the tensile properties of m-PP/s-G composites show greater variations as a function of cooling rate compared with the PP/G system. The Young's modulus of laminates $[\pm 45]_{3S}$ is generally much higher for m-PP/s-G than for PP/G. The low stiffness of PP/G laminates cannot be explained by a change in fiber or matrix properties, but only by a weak fiber-matrix interface that leads to inefficient stress transfer and slippage between fiber and matrix. For both composites, Young's modulus of the laminates $[\pm 45]_{3S}$ increases with lower cooling rates (more pronounced in the case of m-PP/s-G) due to the change in matrix morphology as a function of cooling rate (CR); for lower CR, the matrix structure is more spherulitic and therefore stiffer. As expected, failure strains decrease with decreasing CR, indicating that the reduction in the fraction of the amorphous phase in the matrix reduces the ductility of the composite. However, the reduction in failure stresses at low cooling rates is rather surprising as spherulitic crystalline structures are known to be strengthening entities in semi-crystalline thermoplastic polymers. Fig. 5 also shows that the reduction in laminate tensile strength is probably linked to the fact that a highly crystalline spherulitic structure reduces the importance of the amorphous phase between spherulites, which can lead to premature failure. A more important drop in tensile strains and stresses is observed at low cooling rates for m-PP/s-G composites. This drastic weakening of the laminate can be explained as a more spherulitic matrix reduces the amorphous interphase that transfers stresses between fibers and matrices and may cause initiation of failure between spherulites rather than at fiber-matrix interfaces [55].

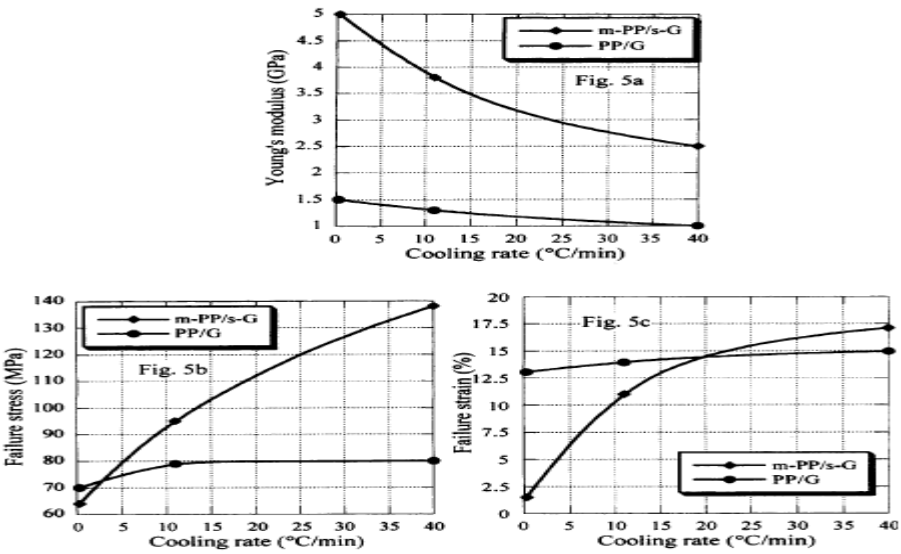

Fig. 3.74: Measured mechanical properties on ±45 tensile coupons of PP/G and m-PP/s-G composites as a function of CR [55].

3.5.2. Flexural and Impact Resistance

According to a study of a unidirectional glass fiber-reinforced PP laminate, residual stresses were found to comprise between 37% and 45% of the transverse (90°) flexural strength (26MPa). For these laminates with a semi-crystalline matrix, a higher cooling rate resulted in a lower crystallinity level as well as higher residual stresses [17,31]. In Part I, it was explained that for semi-crystalline polymers, there is a competition effect between viscoelastic relaxation of the amorphous part of the matrix and crystallization shrinkage, so it depends on the crystallization kinetics of the matrix whether a higher cooling rate results in lower residual stresses or not [5,31]. As mentioned in this composite, a higher cooling rate resulted in higher residual stresses. This resulted in lower flexural strength, including for longitudinal (0°) flexural loads [31].

In detail, Guillén and Cantwell in their study examined the effect of different cooling rates on the mechanical properties of plain composites (0°/90°) and bimaterial aluminum-composite specimens. The results showed a strong link between processing conditions and mechanical properties in fiber- and matrix-dominated loading modes. The flexural properties of plain composites and fiber-metal laminates were greater at lower cooling rates. Conversely, the tensile strength and interlaminar toughness of both types of material were higher for samples manufactured at higher cooling rates. Finally, it was demonstrated that faster cooling resulted in laminates with better impact resistance. It is believed that rapid cooling of the laminates enhanced their interlaminar fracture resistance, thereby reducing the areas damaged after impact [17]. Moreover, with respect to impact toughness, delamination due to impact has been reported to be more severe in angle-ply laminates with increasing angles, which can be attributed to interlaminar thermal residual stresses [31].

3.5.3. Compression and shear

In most polymer composite laminates, the fibers experience compressive residual stresses, which reduces the compressive properties [5,31]. Residual stresses were always found to be harmful to the transverse compressive load. As described previously, fiber waviness can be considered a defect that has formed because of residual stresses. This has been shown to affect compressive properties seriously. In a compression test, the stiffness of the composite will likely be affected by thermal stresses [31]. Furthermore, advanced fiber-reinforced thermoplastics have significantly higher interlaminar fracture toughness than untreated epoxy-based composites. This decreases their susceptibility to impact damage and enables them to be used in compression-loaded structures at higher permissible deformation levels [3].

A comparative study of the in-plane shear behavior of the AS4/PEEK thermoplastic and the T300/914 thermoset material was carried out. Tensile tests were carried out on samples of $(\pm 45)_{2S}$. It is shown that T300/914 and AS4/PEEK exhibit very similar shear behavior at the beginning of loading, with small variations of laminae orientation,θ, very few and short matrix cracks, but a very considerable loss of shear stiffness associated with the development of large plastic strains. As soon as matrix cracks appear, the damage development differs between the two materials: precise observation, on the specimen edges, of matrix cracks and interply delaminations showed that the earlier failure of T300/914 samples is mainly due to the lower shear strength of the thermoset matrix. Due to much-delayed failure, laminates with a $(\pm 45)_{2S}$ PEEK matrix (which is a thermoplastic matrix) laminates can develop more pronounced plastic behavior [56,57].

3.5.4. Modes I and II fracture toughness

Many models have been developed to predict the influence of residual stresses on mode I (interlaminar delamination) and mode II (intralaminar) fracture toughness properties [17,31,54]. Most studies have revealed that thermal residual stresses must be considered when predicting the fracture toughness properties of composite laminates in order to achieve agreement with experimental results [31,54]. The reason is that stresses significantly decrease the fracture toughness properties of composite materials [31]. For example, double cantilever beam (DCB) specimen geometry is a popular method for measuring the fracture toughness of adhesive bonds and the delamination fracture toughness of composite laminates. When adhesive joints are cured, or laminates are processed at high temperatures and then cooled to room temperature, residual stresses are inevitably present. These stresses can arise either from differential thermal shrinkage between the sample components or from chemical shrinkage of the adhesive or composite matrix resins. When a crack develops in a specimen subjected to residual stresses, these can contribute to the total amount of energy released. If the effects of residual stresses are ignored, the calculated fracture toughness will not be the true fracture toughness. Instead, it will be an apparent fracture toughness that includes a specimen property (the amount of residual stress) in the desired material property (the toughness). When such apparent toughness is used to predict the failure of adhesive joints with different levels of residual stress, these predictions will not be correct. Furthermore, the most common residual stress effect in DCB adhesive specimens is that the apparent toughness is greater than the true toughness. Thus, adhesive designs based on such non-conservative apparent toughnesses could lead to premature failure [54].

In addition, Nairn studied the effect of residual stresses on the mode I energy release rate for double cantilever beam (DCB) specimens and realized that there is a significant effect that needs to be

considered, and he proposed some experimental methods to correct for residual stresses. In order to understand the role that residual stresses play in the toughness properties of composites; Nairn hypothesized that the presence of residual stresses could contribute to the loss of toughness. Moreover, it was revealed that if both arms of the laminate DCB specimens experience symmetrical residual stresses, the effect of residual stresses on the determined mode I fracture toughness can be very large. It should be noted that the "arms" of the other two laminates in this study were not symmetrical and thus could exhibit curvature due to residual stress. In general, it was concluded that in laminate DCB samples, the residual effect disappears if both arms of the DCB sample are themselves symmetrical laminates. If the arms are not symmetrical laminates, the residual stress effect will mainly be significant [31,54].

The residual stress distribution is highly sensitive to two properties that are difficult to measure: relaxation behavior and volumetric shrinkage due to matrix crystallization. Experimental results for PEEK carbon fiber AS4 laminates showed that, based on a double cantilever beam test performed to measure performance via Mode I fracture toughness, the presence of residual stresses in cross-ply laminates reduced apparent toughness as much as 35% compared to a unidirectional baseline [58]. At free edges, in particular, predictions display that residual stresses impose a reduction in delamination strength in Mode I. In addition, it was estimated that the failure strains considering residual stresses are 73% of the failure strains when residual stresses are neglected during axial loading. The same trend was observed for the mixed mode, I/II failure strains [31].

Huang et al. stated that their fracture toughness is measured over a temperature range from -50°C to 175°C and is found to be temperature dependent. At low temperatures, the intralaminar critical matrix cracking strain (mode II) of UD and cross-ply IM7 carbon fiber K3B (thermoplastic polyimide) laminates was quite low due to high thermal residual stresses. At intermediate temperatures, the residual stresses decreased, and the matrix cracking strain increased [31,59]. In another case, the fracture toughness of AS4/PEEK was found to drop significantly at slow cooling rates, i.e., at higher levels of resin crystallinity. More recent work has confirmed these trends for AS4/PEEK. However, subsequent work on IM6/PEEK showed that G_{IC} which is mode one fracture toughness remains invariant for cooling rates between 50°C/min and 0.3°C/min [60].

3.5.5. Long-term mechanical properties: fatigue and creep

With respect to free-edge delamination in thermoplastic composites, it was noticed that residual thermal stresses produced a considerable reduction in the apparent fatigue delamination strain of the specimen [31]. Early tests on carbon fiber/PEEK (polyether ether ketone) suggested that the fatigue

properties of this fiber-reinforced thermoplastic were as good as those of its thermoset counterpart. However, more recent fatigue tests on a range of fiber-reinforced composites revealed that the thermoplastic-based composite exhibited the poorest long-term properties with its S-N curve being lower than that of more conventional epoxy-based laminates. In addition, it was discovered that varying the cooling rate of AS4/PEEK has a strong influence on the fatigue properties of APC2 [60]. Moreover, one paper examined the influence of thermal strains induced in PP/carbon fiber model composites after manufacturing cycles. The fiber strain was measured using micro-Raman spectroscopy. In addition, the initial residual stains- due to the manufacturing of the specimen - were measured before any creep load was applied. In general, the initial residual stress in the fiber was found to limit the magnitude of fiber strain during subsequent creep loading [61].

When composite laminates are subjected to thermal residual stresses, the viscoelasticity of the matrix can manifest itself as relaxation or creep. Creep behavior at room temperature was found to be greater for fast-cooled samples (high residual stresses) in cross-ply IM6 carbon fiber PEEK laminates, whereas, for unidirectional laminates loaded in the 90° direction, no difference in creep behavior was found. Since PEEK is a semi-crystalline thermoplastic and its rapid cooling results in lower crystallinity levels, but as stated above for unidirectional laminates loaded in the 90° direction, no difference in creep behavior was found. Therefore, it seems that the difference in creep behavior cannot be only attributed to differences in crystallinity levels. In contrast, creep damage is higher during creep loading caused by thermal residual stresses [31]. For instance, in one study, the effect of cooling rate on the mechanical properties of CF/PEEK was investigated. The influence of the cooling rate on the short- and long-term properties of the material was studied and showed that, for unidirectional samples with a dominant matrix, the cooling rate had little influence. For multidirectional laminates subjected to static and fatigue loads, panels cooled more slowly showed equivalent or better performance than specimens cooled more rapidly. It was concluded that the internal stresses induced during rapid cooling appear to be more detrimental to material performance than the changes in matrix structure observed during slow cooling [57]. However, in another research fatigue life behavior and underlying micromechanisms were investigated in two different types of unidirectional carbon-fiber-reinforced plastics loaded in tension-tension along the fiber direction. The carbon fibers (AS4) were the same in both composite systems. A thermoplastic matrix (polyetheretherketone, PEEK) and a thermoset matrix (epoxy toughened with a thermoplastic additive) were used. Macroscopic fatigue behavior was characterized by fatigue life diagrams. Surface replicas were taken intermittently during fatigue testing to monitor active fatigue damage micromechanisms. The thermoset-based composite showed greater fatigue resistance, with a few microcracks initiated at distributed fiber breaks and developing at a decelerated rate. The

thermoplastic composite showed more pronounced fatigue degradation, with a steeper fatigue curve, caused by the widespread propagation of matrix debonds and cracks. The use of a tougher and more ductile matrix results in a lower fatigue life performance, due to a more widely distributed accumulation of damage propagating at a higher rate [62].

Cantwell et al. used a series of tensile and creep tests on IM6/PEEK (polyether ether ketone) to assess the effect of varying cooling rates on its short- and long-term fracture properties. Two cooling rates of 50 °C/min and 1 °C/min were used to produce the specimens, with two different stacking sequences of $(90°)_8$ and $((+/-45°)_2)$. As the creep tests were undertaken for (90°) laminates, the creep response of specimens tested at 23, 120, and 160°C are presented in Figs 3.75, 3.76, and 3.77 respectively. In each case, the creep behavior was assessed by measuring total deformation after 10^3 s. Data obtained from tests at 23 and 120°C do not appear to be dependent on the cooling rate, with the two sets of data essentially coinciding. Distinct effects were again observed at the highest temperature, 160°C. Here, the strain measured after 10^3 s was considerably greater in the fast-cooled laminate. Consequently, tests on laminates (90°) show that below the glass transition temperature of the PEEK matrix, the tensile mechanical properties of the composite are not influenced by the matrix microstructure. Above the T_g of the matrix, however, variation in the percentage of crystallinity leads to changes in the short- and long-term properties of the composite. In this case, the slower-cooled laminate showed higher ultimate stress and better creep resistance [60].

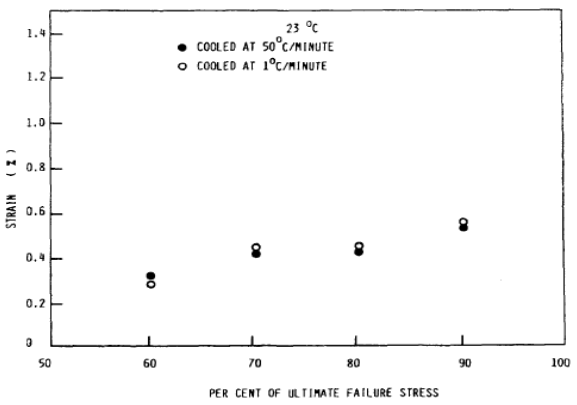

Fig. 3.75: The deformation after creep loading for 1000 s at 23°C [60].

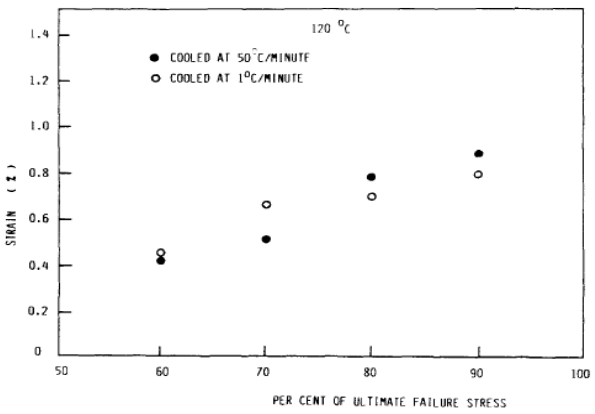

Fig. 3.76: The deformation after creep loading for 1000 s at 120°C [60].

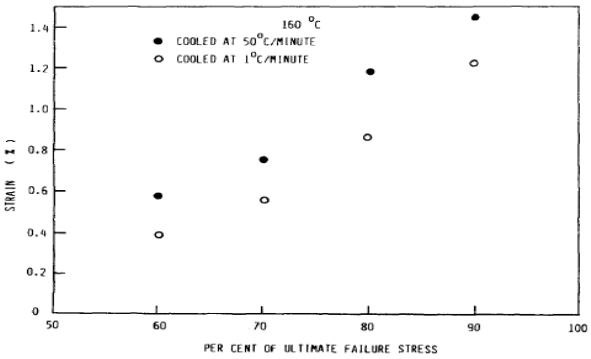

Fig. 3.77: The deformation after creep loading for 1000 s at 160°C [60].

In contrast, the results obtained from creep tests on panels (+/-45°) at 23 and 160°C are shown in Figs. 3.78 and 3.79. Here, strain after 10^4s is presented as a function of the stress level applied. At 23°C, Fig. 18, there is again a clear difference between the response of slowly cooled and fast-cooled panels. In this case, the fast-cooled laminate exhibited significantly greater strains and tended to suffer greater volume damage during loading than the 1°C/min panel. At 160°C, the response of the two laminates was again almost identical (Fig. 19), with both composites suffering significant internal damage. Consequently, in the composites (+/-45°), significant effects of cooling rate were only observed at lower temperatures. Optical micrographs carried out on these samples showed that the fast-cooled laminate exhibited significantly more internal cracking and delamination during testing. This volumetric damage is thought to result from the large thermal strains induced by the rapid cooling process. This information suggests that rapid cooling, a procedure often encouraged to control the level of crystallinity, may be more detrimental to mechanical properties than slow cooling [60].

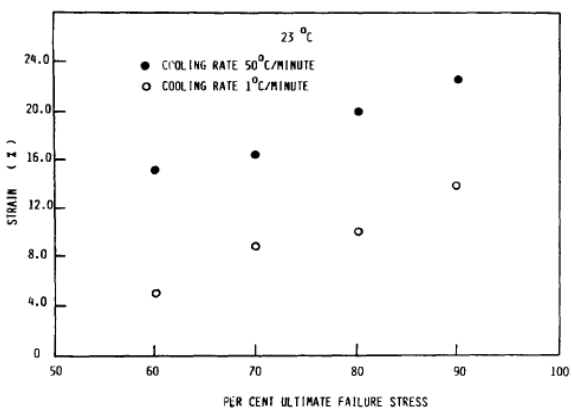

Fig. 3.78. Deformation after creep loading for 10^4 s in the (+/-45 °) laminates tested at 23°C [60].

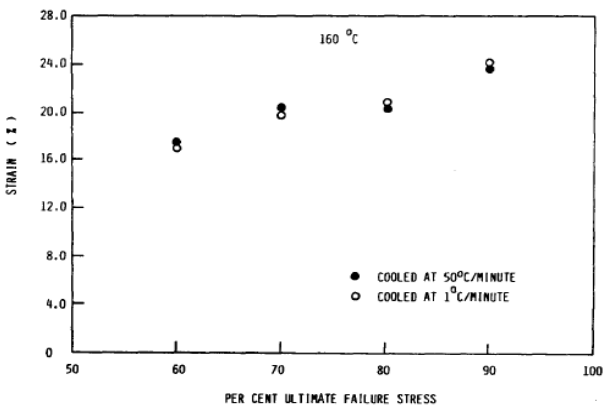

Fig. 3.79. Deformation after creep loading for 10^4s in the (+/-45 °) laminates tested at 160°C [60].

3.6. RESIDUAL STRESS EFFECTS IN COMPOSITE STRUCTURES

Until now, we have explained the effects of thermal residual stresses at a laminate. From now on, we will discuss the published literature related to the effects of residual stresses on a composite structure. In composite parts, one of the effects of residual stresses is that when machining the produced composite parts, such as drilling holes, cutting, etc., deformations can occur, because of the relaxation of residual stresses. Many experimental techniques for determining residual stresses through thickness are based on this [31,33].

Anisotropy in the shrinkage behavior of composites during cooling results in the change in shape during the cooling of a composite structure, which arises from the difference in the thermal expansion behavior of the fibers and the matrix [5,6,7,8,9,31]. For most composites, the in-plane contraction is much smaller than the out-of-plane contraction. Therefore, shrinkage on the inner plies is more restrained during cooling. As the sheet is constrained in the mold, residual stresses begin to build up during cooling. At the demolding stage, the sheet deforms instantaneously due to the relaxation of some of the residual stresses and, in the case of a subsequent cooling step, the warpage increases further [31]. The most common effect of residual stresses in composite products is the deformation of angled and curved parts (dimensional instability). The two sides of a curve mostly approach each other, resulting in a reduction of the closed angle. This change in the enclosed angle is called the "spring effect", see Fig. 3.80. In addition, since the residual stresses can distort the dimensions or shape of the processed part, it necessitates costly compensation through the use of shims when it is assembled into a structure as it is shown in Fig. 3.80 [63]. Factors that can affect the spring-in of the laminate include; tool-part interaction, thermal expansion coefficients, ply stacking sequence, symmetric/non-symmetric lay-up, fiber volume fraction, processing condition such as processing temperature. In addition, tool-part interaction or unbalanced cooling, as well as residual interlaminar stresses combined with non-symmetrical lay-up, can cause warping of the sides of angled parts or induce additional angle change. Geometrical dimensions also play a role in the spring-in of the laminate, such as enclosed angle, part thickness, and tool radius [31,64]. It has been shown that spring-in angle is mainly due to differential expansion and shrinkage behaviour in the various directions and its dependency on the tool-part interaction is little [31].

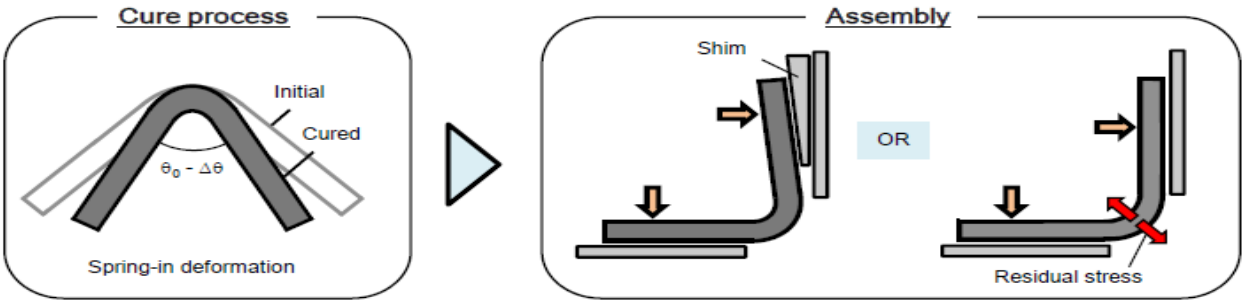

Fig. 3.80. Schematic of spring-in deformation and problems induced during assembly (i.e., either manual shimming or residual stress is necessary) [63].

Models have been developed to predict the final deformation, warpage, or spring-in angle of a product as well as the distribution of residual stresses [31,64,65]. The models are based on classical laminate theory (CLT), thermoelasticity, and viscoelastic behavior. Most studies have used finite element modelling (FEM) for further analysis [31]. The main reason for the development of these models is to predict the correct shape of the mold, in order to obtain products with the required dimensions and replace the trial-and-error based mold design [31,65].

3.6.1. Effect of residual stresses on composite structures according to their sources

As shown in the diagram in Section 5 of Chapter 1, residual stress sources can be classified as intrinsic (related to the material, lay-up, and shape of the part) or extrinsic (related to processing and tooling). Intrinsic sources generate residual stresses at the constituent level, and the effect is integrated up through the length scales. Extrinsic sources generate stresses at the boundaries of the structure, and the effect is transferred down through the length scales. Therefore, intrinsic sources act from the "inside and outwards" and extrinsic sources act from the "outside and inwards". Intrinsic sources generally have the greatest effect on fiber-matrix stresses, while extrinsic sources have the largest effect on structural stresses (Fig. 3.81). The main effects of residual stresses are strength reduction and shape distortion. Stresses at the fiber-matrix, lamina-laminate, and structural levels all affect the strength of the component, while only lamina-laminate and structural level stresses affect dimensional fidelity to any significant degree. Fig. 1 illustrates a schematic of the relationship between the source of stress, the length scale at which it acts, and the effect of that stress [52].

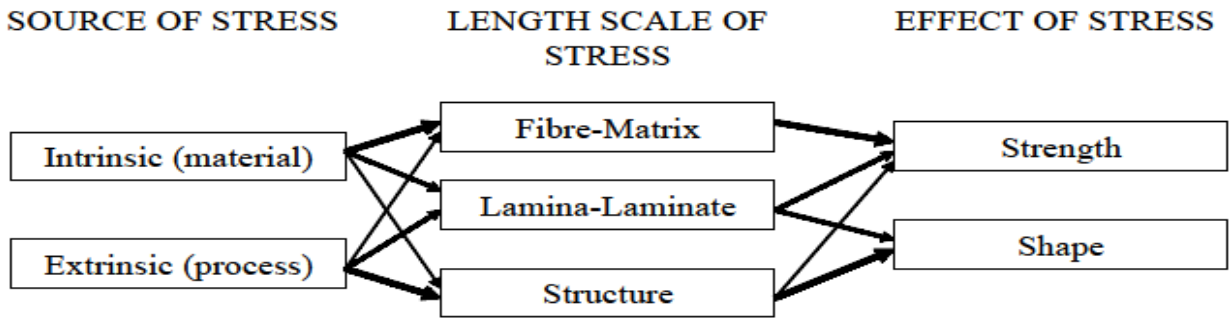

Fig. 3.81. Schematic of the relationship between stress source, length scale of stress, and the effect of residual stress. Thicker arrows indicate a stronger relationship [52].

3.6.2. Filament-wound cylinders

Other composite structures where residual stresses play an important role are filament wound or tape-layered thermoplastic composite structures (cylinders) where localized heating is applied. Products that can be obtained with this technique of production can be pressure vessels, pipes, struts, etc. [15,31]. Factors that influence the level of residual stress in these parts have been identified, such as lay-up angle, winding tension, thickness, mandrel temperature, mandrel/ compound CTE mismatch, annealing, use of aliner, and material properties. Different stress distributions through the thickness of the cylinder can be achieved, which can be attributed to temperature profiles during processing [31]. The effects of residual stresses in filament-wound composites include a considerable decrease in the compressive properties of, for example, carbon fiber/polysulfone cylinders, layer damage, and in some cases residual stresses can be so high that they promote cracking. Another effect that can be found in wound thermoplastic cylinders is fiber waviness, which has been shown to be primarily affected by the mandrel material, not the cooling rate [31,66]. Additionally, when a section or ring of the filament wound cylinder is cut, it releases the torsion and bending moment caused by the residual thermal stresses [31].

3.7. PROPOSED MECHANISMS FOR RELIEF OF RESIDUAL STRESSES

If the effects of thermal residual stresses are significant, it will be important to learn how to minimize them. Several mechanisms have been proposed to decrease residual stresses, based on a modification of the constituent materials of the composite and the processing cycle. Overall, the careful design of the composite material by defining material properties such as fiber volume fraction, number of off-axis plies, and ply thickness is necessary to minimize or optimize thermal residual stresses depending on the desired structural behavior of the composite product [5,20,31,67]. As discussed earlier, the

temperature difference between the stress-free temperature and the service temperature is a major driving force for thermal residual stress formation [5,21,31]. Thus, a matrix with a low "stress-free temperature" is proposed to minimize residual stresses [31,68]. If this is not desirable or possible, a matrix with a low glass transition temperature can be applied to the fiber-matrix interface to lower the stress-free temperature, or more specifically, an amorphous interphase with a glass transition temperature below the crystallization temperature of a semi-crystalline matrix will be applied [31,68,69]. The explanation is that the most likely situation where a low Tg interphase could be useful is in composites with high melting point, semicrystalline, and thermoplastic matrices. It is well known that semi-crystalline thermoplastics can exhibit very large volume changes when the melt cools to room temperature. If all these volume changes result in a build-up of thermal stresses, the matrix will undergo very high thermal stresses or crack. Typically, much of the volume change during cooling takes place at high temperatures during crystallization. The optimal interphase would therefore be an amorphous thermoplastic with a Tg just below the crystallization temperature of the semi-crystalline matrix. This composite would avoid the build-up of thermal stresses during the largest changes in matrix volume and would have good high-temperature properties [69]. In addition, it has been proposed to control the residual stresses by applying a thin compliant layer (of pure polymer, for example) between the different plies. Such a layer relieves residual stresses in individual plies and grows impact strength, but results in a slight decrease in interlaminar shear strength. In addition to the mentioned solutions, the use of a more resilient and tougher matrix has been considered to decrease the microcracking behavior. The incorporation of glass fibers in a carbon fiber composite has also been considered a good solution to relieve residual stresses. For example, in a hybrid composite, a failure strain enhancement was observed when glass and carbon fibers were mixed [31,67].

Another approach to decrease residual stresses is to control the shrinkage behavior of the matrix during cooling from the processing temperature to reduce the fiber-matrix mismatch [31,68]. Furthermore, adding of mineral fillers such as silica in a matrix generally reduce the coefficient of thermal expansion considerably, thereby reducing thermal residual stress [31]. The production of nanocomposites, which have been shown to be suitable for use as a matrix for composite materials, is a development of the last 15 years [31,70]. Nanocomposites have the potential to improve matrix-dominated flexural and compressive strength by increasing matrix modulus. The advantage of using nanocomposites instead of other polymers to improve the properties of composite fibers is that properties can be improved without changing processing conditions [70]. For each lay-up, the optimal processing cycle which gives the lowest residual stresses and maximizes the mechanical properties, is different [31]. Moreover, according to the considerable time-dependent relaxation that occurs

during the cooling process, residual thermal stresses are highly dependent on temperature history. It was proved that by considering the viscoelastic behavior, it is possible to find optimal cooling paths to achieve the lowest possible residual stresses [31,71]. Depending on the crystallization kinetics of the matrix, it has been proposed that rapid cooling to the crystallization temperature, followed by slow cooling to the room temperature (RT), reduces the residual stresses in the semicrystalline composites [2,31]. It is important to note that the cooling rate affects matrix morphology and that the proposed optimal cooling procedure may result in a matrix with less advantageous mechanical properties. Therefore, defining an optimal cooling procedure for a semi-crystalline matrix composite is a complex problem that must address simultaneously the evolution of matrix morphology, viscoelasticity, and residual strains [2]. After processing, annealing can also be done to reduce some stresses [5,24,31]. To reduce residual stresses near the free edges, localized heating followed by cooling under sufficient pressure has been proposed to prevent ply debonding [31]. Furthermore, it was discovered that in wound composite cylinders increasing the CET mandrel/composite mismatch was expected to increase the magnitude of residual stresses and the severity of waviness while increasing the tow tension was expected to decrease the magnitude of residual stresses and the severity of waviness [31,66]. Considering thermal residual stresses have also been found suitable for advantageous use. The reason is that several papers propose the prediction of deformed shapes of non-symmetrical laminates by taking into account residual stresses, in order to give them the necessary shape for a certain application [5,31].

GENERAL CONCLUSION

In conclusion, residual stresses play a significant role in the performance and failure of materials. Whether originating from manufacturing processes or accumulated over the life of the material, these stresses must not be overlooked at the design stage. Failure to consider residual stresses can have detrimental consequences, particularly when the material is exposed to cyclic loading or corrosive environments.

With advances in high-temperature thermoplastic resins and processing techniques such as thermoplastic filament winding or tape laying with in-situ consolidation, the presence of temperature gradients during processing has become more apparent. It has become imperative to accurately predict and measure the process-induced residual stresses.

This study has identified key factors influencing residual stress levels and reviewed various experimental techniques for measuring them. While it is challenging to eliminate processing-induced

stresses entirely, understanding their accumulation enables them to be reduced through appropriate process control and part design. Moreover, by estimating their magnitude, their influence on tool part design can be taken into account, facilitating the manufacture of parts with precise dimensions and net shape.

In addition, this research has also focused on investigating the effects of thermal residual stresses and exploring potential mechanisms for stress relief. By gaining insights into these mechanisms, it becomes possible to develop strategies for stress mitigation and enhanced material performance.

Overall, the findings of this thesis highlight the criticality of considering residual stresses in thermoplastic matrix composite design and processing. By addressing residual stresses through appropriate design, process control, and understanding their impact on the material's performance, the reliability and longevity of engineered components can be significantly improved.

REFERENCES:

[1] Li, M. C., Wu, J. J., Loos, A. C., & Morton, J. (1997). A plane-strain finite element model for process-induced residual stresses in a graphite/PEEK composite. Journal of Composite Materials, 31(3), 212-243.

[2] Nielsen, A. S., & Pyrz, R. (1998). The effect of cooling rate on thermal residual strains in carbon/polypropylene microcomposites. Science and engineering of composite materials, 7(1-2), 1-22.

[3] Unger, W. J., & Hansen, J. S. (1998). A method to predict the effect of thermal residual stresses on the free-edge delamination behavior of fibre reinforced composite laminates. Journal of composite materials, 32(5), 431-459.

[4] Manson, J. A. E., & Seferis, J. C. (1992). Process simulated laminate (PSL): a methodology to internal stress characterization in advanced composite materials. Journal of composite materials, 26(3), 405-431.

[5] Parlevliet, P. P., Bersee, H. E., & Beukers, A. (2006). Residual stresses in thermoplastic composites—A study of the literature—Part I: Formation of residual stresses. Composites Part A: Applied Science and Manufacturing, 37(11), 1847-1857.

[6] Crasto, A. S., Kim, R. Y., & Russell, J. D. (2002). In situ monitoring of residual strain development during composite cure. Polymer composites, 23(3), 454-463.

[71] Wagner, H. D., & Nairn, J. A. (1997). Residual thermal stresses in three concentric transversely isotropic cylinders: application to thermoplastic-matrix composites containing a transcrystalline interphase. Composites Science and Technology, 57(9-10), 1289-1302.

[8] Jeronimidis, G., & Parkyn, A. T. (1988). Residual stresses in carbon fibre-thermoplastic matrix laminates. Journal of Composite Materials, 22(5), 401-415.

[9] Ersoy, N., & Vardar, O. (2000). Measurement of residual stresses in layered composites by compliance method. Journal of Composite Materials, 34(7), 575-598.

[10] Sonmez, F. O., Hahn, H. T., & Akbulut, M. (2002). Analysis of process-induced residual stresses in tape placement. Journal of Thermoplastic Composite Materials, 15(6), 525-544.

[11] Mantell, S. C., & Springer, G. S. (1992). Manufacturing process models for thermoplastic composites. Journal of composite materials, 26(16), 2348-2377.

[12] Dhakal, H. N., & Ismail, S. O. (2021). Design, manufacturing processes and their effects on bio-composite properties. Sustainable Composites for Lightweight Applications; Dhakal, HM, Ismail, SO, Eds, 121-177.

[13] El Bayssari, A. M. (2022). Study and comprehension of the residual stresses and strains state in thermoplastic composite materials manufactured by tape placement (Doctoral dissertation, Nantes Université).

[14] Belnoue, J. P. H., Mesogitis, T., Nixon-Pearson, O. J., Kratz, J., Ivanov, D. S., Partridge, I. K., ... & Hallett, S. R. (2017). Understanding and predicting defect formation in automated fibre placement pre-preg laminates. Composites Part A: Applied Science and Manufacturing, 102, 196-206.

[15] Schmitt, R., & Witte, A. (2012). Control of a thermoplastic tape winding process with optical in-line metrology. Proceedings in Manufacturing Systems, 7(3).

[16] Sorensen, Larissa, Thomas Gmür, and John Botsis. "Residual strain development in an AS4/PPS thermoplastic composite measured using fibre Bragg grating sensors." Composites Part A: Applied Science and Manufacturing 37.2 (2006): 270-281.

[17] Guillen, J. F., & Cantwell, W. J. (2002). The influence of cooling rate on the fracture properties of a thermoplastic-based fibre-metal laminate. Journal of reinforced plastics and composites, 21(8), 749-772.

[18] Barnes, J. A., & Byerly, G. E. (1994). The formation of residual stresses in laminated thermoplastic composites. Composites Science and Technology, 51(4), 479-494.

[19] Youssef, Y., & Denault, J. (1998). Thermoformed glass fiber reinforced polypropylene: microstructure, mechanical properties and residual stresses. Polymer composites, 19(3), 301-309.

[20] Wang, S., Kowalik, D. P., & Chung, D. D. L. (2004). Self-sensing attained in carbon-fiber–polymer-matrix structural composites by using the interlaminar interface as a sensor. Smart materials and structures, 13(3), 570.

[21] Kim, K. S., Hahn, H. T., & Croman, R. B. (1989). The effect of cooling rate on residual stress in a thermoplastic composite. Journal of composites technology & research, 11(2), 47-52.

[22] Karami, G., & Garnich, M. (2005). Micromechanical study of thermoelastic behavior of composites with periodic fiber waviness. Composites Part B: Engineering, 36(3), 241-248.

[23] Lawrence, W. E., Månson, J. A., Seferis, J. C., Gillespie Jr, J. W., & Pipes, R. B. (1991). Prediction of residual stress in continuous fiber semicrystalline thermoplastic composites: a kinetic-viscoelastic approach. In ASC Conf., 5th Techn. Conf. (No. CONF, p. 401).

[24] Unger, W. J., & Hansen, J. S. (1993). The effect of cooling rate and annealing on residual stress development in graphite fibre reinforced PEEK laminates. Journal of Composite Materials, 27(2), 108-137.

[25] Wang, C., & Sun, C. T. (1997). Thermoelastic behavior of PEEK thermoplastic composite during cooling from forming temperatures. Journal of composite materials, 31(22), 2230-2248.

[26] Parambil, N. K., Chen, B. R., Deitzel, J. M., & Gillespie Jr, J. W. (2022). A methodology for predicting processing induced thermal residual stress in thermoplastic composite at the microscale. Composites Part B: Engineering, 231, 109562.

[27] Di Landro, L., & Pegoraro, M. A. R. I. O. (1996). Evaluation of residual stresses and adhesion in polymer composites. Composites Part A: Applied Science and Manufacturing, 27(9), 847-853.

[28] Li, X., Wang, J., Li, S., & Ding, A. (2020). Cure-induced temperature gradient in laminated composite plate: Numerical simulation and experimental measurement. Composite Structures, 253, 112822.

[29] Tsukada, T., Minakuchi, S., & Takeda, N. (2019). Identification of process-induced residual stress/strain distribution in thick thermoplastic composites based on in situ strain monitoring using optical fiber sensors. Journal of Composite Materials, 53(24), 3445-3458.

[30] Lawrence, W. E., Manson, J. A., & Seferis, J. C. (1990). Thermal and morphological skin-core effects in processing of thermoplastic composites. Composites, 21(6), 475-480.

[31] Parlevliet, P. P., Bersee, H. E., & Beukers, A. (2007). Residual stresses in thermoplastic composites–a study of the literature. Part III: Effects of thermal residual stresses. Composites Part A: Applied Science and Manufacturing, 38(6), 1581-1596.

[32] Kim, Y. K., & Daniel, I. M. (2002). Cure cycle effect on composite structures manufactured by resin transfer molding. Journal of composite materials, 36(14), 1725-1743.

[33] Parlevliet, P. P., Bersee, H. E., & Beukers, A. (2007). Residual stresses in thermoplastic composites—A study of the literature—Part II: Experimental techniques. Composites Part A: Applied Science and Manufacturing, 38(3), 651-665.

[34] Nielsen, A. S., & Pyrz, R. (2002). A novel approach to measure local strains in polymer matrix systems using polarised Raman microscopy. Composites science and technology, 62(16), 2219-2227.

[35] Pawlak, A., Zinck, P., Galeski, A., & Gerard, J. F. (2001, May). Photoelastic studies of residual stresses around fillers embedded in an epoxy matrix. In Macromolecular Symposia (Vol. 169, No. 1, pp. 197-210). Weinheim: WILEY-VCH Verlag GmbH.

[36] Chung, D. D. L. (2001). Continuous carbon fiber polymer-matrix composites and their joints, studied by electrical measurements. Polymer composites, 22(2), 250-270.

[37] Lai, L., Carman, G., Chiou, S., Kukuchek, P., & Echternach, D. (1995). Processing monitoring of carbon/phenolic composites using smart sensors. Smart Materials and Structures, 4(2), 118.

[38] Meske, R., & Schnack, E. (2003). Particular adaptation of X-ray diffraction to fiber reinforced composites. Mechanics of materials, 35(1-2), 19-34.

[39] Han, B., Post, D., & Ifju, P. (2001). Moiré interferometry for engineering mechanics: current practices and future developments. The Journal of Strain Analysis for Engineering Design, 36(1), 101-117.

[40] Cowley, K. D., & Beaumont, P. W. (1997). The measurement and prediction of residual stresses in carbon-fibre/polymer composites. Composites Science and Technology, 57(11), 1445-1455.

[41] Jeronimidis, G., & Parkyn, A. T. (1988). Residual stresses in carbon fibre-thermoplastic matrix laminates. Journal of Composite Materials, 22(5), 401-415.

[42] Hyer, M. W. (1981). Some observations on the cured shape of thin unsymmetric laminates. Journal of composite materials, 15(2), 175-194.

[43] Youssef, Y., & Denault, J. (1998). Thermoformed glass fiber reinforced polypropylene: microstructure, mechanical properties and residual stresses. Polymer composites, 19(3), 301-309.

[44] Péron, Mael, et al. "Measurement and prediction of residual strains and stresses during the cooling of a glass fibre reinforced PA66 matrix composite." Composites Part A: Applied Science and Manufacturing 137 (2020): 106039.

[45] American Society for Testing and Materials. (2020). Standard Test Method for Determining Residual Stresses by the Hole-drilling Strain-gage Method. ASTM International.

[46] D'Amore, A., Caprino, G., Nicolais, L., & Marino, G. (1999). Long-term behaviour of PEI and PEI-based composites subjected to physical aging. Composites Science and Technology, 59(13), 1993-2003.

[47] Parvatareddy, H., Wang, J. Z., Dillard, D. A., Ward, T. C., & Rogalski, A. E. (1995). Environmental aging of high-performance polymeric composites: Effects on durability. Composites Science and Technology, 53(4), 399-409.

[48] Mukherjee, S., Ananth, C. R., & Chandra, N. (1997). Effect of residual stresses on the interfacial fracture behavior of metal-matrix composites. Composites science and technology, 57(11), 1501-1512.

[49] Hsiao, H. M., & Daniel, I. M. (1996). Effect of fiber waviness on stiffness and strength reduction of unidirectional composites under compressive loading. Composites science and technology, 56(5), 581-593.

[50] Papadopoulos, D. S., & Bowles, K. J. (1990, January). Use of unbalanced laminates as a screening method for microcracking. In International SAMPE Symposium (No. NASA-TM-102517).

[51] García, I. G., Mantič, V., & Blázquez, A. (2018). The effect of residual thermal stresses on transverse cracking in cross-ply laminates: an application of the coupled criterion of the finite fracture mechanics. International Journal of Fracture, 211, 61-74.

[52] Fernlund, G., Poursartip, A., Twigg, G., & Albert, C. (2003). Residual stress, spring-in and warpage in autoclaved composite parts. Southfield, MI: Society of Manufacturing Engineers.

[53] Liu, X., Yan, B., Ren, F., Zhu, C., He, Y., & Xin, C. (2021). Isothermal crystallisation ATP process for thermoplastic composites with semi-crystalline matrices using automated tape placement machine. Composites Part B: Engineering, 227, 109381.

[54] Nairn, J. A. (2000). Energy release rate analysis for adhesive and laminate double cantilever beam specimens emphasizing the effect of residual stresses. International Journal of Adhesion and Adhesives, 20(1), 59-70.

[55] Youssef, Y., & Denault, J. (1998). Thermoformed glass fiber reinforced polypropylene: microstructure, mechanical properties and residual stresses. Polymer composites, 19(3), 301-309.

[56] Lafarie-Frenot, M. C., & Touchard, F. (1994). Comparative in-plane shear behaviour of long-carbon-fibre composites with thermoset or thermoplastic matrix. Composites science and technology, 52(3), 417-425.

[57] El Kadi, H., & Denault, J. (2001). Effects of processing conditions on the mechanical behavior of carbon-fiber-reinforced PEEK. Journal of Thermoplastic Composite Materials, 14(1), 34-53.

[58] Gillespie Jr, J. W., & Chapman, T. J. (1993). The influence of residual stresses on mode i interlaminar fracture of thermoplastic composites. Journal of Thermoplastic Composite Materials, 6(2), 160-174.

[59] Huang, X., Gillespie Jr, J. W., & Eduljee, R. F. (1997). Effect of temperature on the transverse cracking behavior of cross-ply composite laminates. Composites Part B: Engineering, 28(4), 419-424.

[60] Cantwell, W. J., Davies, P., & Kausch, H. H. (1990). The effect of cooling rate on deformation and fracture in IM6/PEEK composites. Composite structures, 14(2), 151-171.

[61] Schjødt-Thomsen, J., & Pyrz, R. (1999). Influence of thermally induced strains on subsequent creep loading using micro Raman spectroscopy. In Influence of Thermally Induced Strains on Subsequent Creep Loading using Micro Raman Spectroscopy.

[62] Gamstedt, E. K., & Talreja, R. (1999). Fatigue damage mechanisms in unidirectional carbon-fibre-reinforced plastics. Journal of materials science, 34, 2535-2546.

[63] Takagaki, K., Minakuchi, S., & Takeda, N. (2017). Process-induced strain and distortion in curved composites. Part I: Development of fiber-optic strain monitoring technique and analytical methods. Composites Part A: Applied Science and Manufacturing, 103, 236-251.

[64] Jain, L. K., Hou, M., Ye, L., & Mai, Y. W. (1998). Spring-in study of the aileron rib manufactured from advanced thermoplastic composite. Composites Part A: Applied Science and Manufacturing, 29(8), 973-979.

[65] Trende, A., Åström, B. T., & Nilsson, G. (2000). Modelling of residual stresses in compression moulded glass-mat reinforced thermoplastics. Composites Part A: Applied Science and Manufacturing, 31(11), 1241-1254.

[66] Kugler, D., & Moon, T. J. (2002). The effects of Mandrel material and tow tension on defects and compressive strength of hoop-wound, on-line consolidated, composite rings. Composites Part A: Applied Science and Manufacturing, 33(6), 861-876.

[67] Khatri, S. C., & Koczak, M. J. (1996). Thick-section AS4-graphite/E-glass/PPS hybrid composites: Part I. Tensile behavior. Composites science and technology, 56(2), 181-192.

[68] Nairn, J. A., & Zoller, P. (1985). Matrix solidification and the resulting residual thermal stresses in composites. Journal of Materials Science, 20, 355-367.

[69] Nairn, J. A. (1985). Thermoelastic analysis of residual stresses in unidirectional, high-performance composites. Polymer Composites, 6(2), 123-130.

[70] Vlasveld, D. P. N., Bersee, H. E. N., & Picken, S. J. (2005). Nanocomposite matrix for increased fibre composite strength. Polymer, 46(23), 10269-10278.

[71] Lee, K., & Weitsman, Y. (1994). Optimal cool down in nonlinear thermoviscoelasticity with application to graphite/PEEK (APC-2) laminates.